

DL

The 25th Annual Fall Field Frolic
Department of Geological Sciences Field Trip
California State University, Northridge
Friday August 17 to Wednesday August 22, 2007

Accreted Terranes of the Klamath Mountains, S. Oregon and N. California

(Fearless) Trip Leaders: D. Yule, E. Miranda, and D. Liggett

Our primary focus will be to explore the composite accretionary triad of (1) the Rogue River island arc, (2) the Josephine inter-arc basin ophiolite, and (3) the Rattlesnake Creek remnant arc:

Itinerary:

Friday – Depart at 10 a.m., "dead-head" north on I-5, overnight at RV Park in Ashland, Oregon

Saturday – en route to Onion Camp; Greyback pluton, Rattlesnake Creek terrane, Cretaceous onlap sequence, Onion Camp complex, Fiddler Mountain complex

Sunday - Pearsoll Peak hike; spectacular views and amazing geology including the Rogue Fm island arc volcanic rocks, ophiolite mélange zone, and dunitite/harzburgite of the Josephine ophiolite

Monday – Morning en route to Rogue River with stops to view Briggs Creek amphibolite, Illinois River plutonic complex; afternoon raft trip on Rogue River,

Galice to Graves Creek to view outcrops of Galice and Rogue Fm

Tuesday – en route to Jedidiah Smith Redwoods State Park, CA, with stops to view Preston Peak thrust and Josephine ophiolite

Wednesday – Return to CSUN via Hwy 101, possible stop to view blueschist outcrops near Laytonville, CA

FIELD GUIDE

GEOLOGIC AND TECTONIC EVOLUTION OF A MIDDLE TO LATE JURASSIC MARGINAL OCEAN BASIN, NORTHERN KLAMATH MOUNTAINS PROVINCE

J. Douglas Yule¹, Calvin G. Barnes², Gregory D. Harper³, Arthur W. Snoke⁴,
and Jason B. Saleeby¹

¹ Division of Geological and Planetary Sciences, California Institute of Technology,
170-25, Pasadena, California, 91125.

² Department of Geosciences, Texas Tech University, Lubbock, TX 79409

³ Department of Geological Science, SUNY-Albany, Albany, NY 12222

⁴ Department of Geology and Geophysics, University of Wyoming, Laramie, WY 82071

INTRODUCTION

The northern Klamath Mountains of the Oregon-California border region expose rocks of an ancient, accreted marginal ocean basin system, informally referred to here as the Josephine marginal basin. This basin opened along the western edge of North America in the Middle and Late Jurassic and subsequently closed as it accreted to the continental margin by approximately 150 Ma (Snoke, 1977; Saleeby, et al., 1982; and Harper and Wright, 1984; Saleeby and Harper, 1995; Harper, et al., 1995). The principal purpose of this geologic field trip to the northern Klamath Mountains is to examine the oceanic island arc and ophiolite sequences which occur in the region, and to observe the deformational features preserved in these rocks. Specific objectives of the trip are: 1) to characterize the geology, geochemistry, and geochronology of the various lithotectonic components of the Josephine marginal basin, including the active arc complex, the inter-arc basin ophiolite, and the remnant arc complex; and 2) to constrain the timing and duration of the deformational and magmatic episodes in the province. In addition, accretion-related deformation, subsequent uplift, and erosion have produced natural cross-section views and provide a unique opportunity to directly observe the structural framework and features of marginal ocean basin lithosphere.

The field trip is designed to take three full days. Approximately one day each is devoted to investigating the geology of the remnant arc, the inter-arc basin ophiolite, and the active arc complexes, in that order. A detailed road log describes each STOP. Additional travel notes and descriptions of points of geological interest are also provided to aid in following our route from one stop to the next. Alternative STOPS are included in case of road closures due to snow at higher elevations, or if time permits. Numerous place and road names are used in the guide for location purposes; many of these names are excluded from the Figures to retain clarity of the geologic data. Therefore, if you use this guide after the scheduled field excursion, we strongly recommend that you supplement it with the U.S. Geological Survey 1:24,000 topographic sheets of the region, with U.S. Forest Service road maps, or with **Northern California and Oregon Atlas and Gazetteer** maps, published by the DeLorme Mapping Company, P.O. Box 298, Freeport Maine, 04032.

GEOLOGIC FRAMEWORK

The Klamath Mountains consist of a series of fault-bounded tectonostratigraphic terranes whose stratigraphic records span >400 m.y. from the Cambrian to the Late

Jurassic. The province was assembled through the progressive accretion, from west to east, of a series of island arc, marginal basin, and subduction complex assemblages, most of which appear to have developed in relative proximity to the continental margin of North America (e.g., Burchfiel and Davis, 1981; Davis and others, 1978; Harper and Wright, 1984; Wright and Fahan, 1988; Wright and Wyld, 1994). The terranes of the province occur in four concentric lithic belts bounded by eastward dipping faults (Figure 1). Pre- and post-accretion plutons occur in each belt. Most of these plutons, >75% by area, range in age from ~170 Ma to ~135 Ma. The westernmost belt, known as the western Jurassic belt (WJB), is overridden on the east by the western Paleozoic and Triassic belt (TrPz) and underthrust on the west by the Dothan Formation (Franciscan complex in California). We will visit exposures in both the WJB and the TrPz on this trip (Figure 2).

ROCK UNITS

Western Paleozoic and Triassic belt. The TrPz contains rocks which formed part of the remnant arc in the Josephine marginal ocean basin. The belt is a composite of fault-bounded terranes which were juxtaposed in the Middle Jurassic (Irwin, 1972; Wright and Fahan, 1988). This trip will visit exposures in the Rattlesnake Creek and western Hayfork terranes (RCT and WHT, respectively) and the Grayback pluton (Table 1 and Figures 2 and 3).

The RCT consists of a serpentinite matrix melange unit intruded by arc plutons and overlain by volcanic-sedimentary strata of a primitive arc complex (Wright and Wyld, 1994). In northern California, the RCT rocks are intruded by a heterogeneous mafic complex of the Preston Peak ophiolite (Snook, 1977). The WHT structurally overlies the RCT and consists of arc volcanoclastic rocks and contemporaneous intrusive complexes. The RCT and other terranes of the TrPz are intruded by plutons similar in age and composition to the WHT. The older Klamath terranes thus appear to have comprised the basement of the western Hayfork arc. A suite of slightly younger plutons, including the Wooley Creek, Grayback, Thompson Ridge, Ashland, and Wimer plutons, intrude rocks of both terranes. These plutons occur inboard of contemporaneous volcanic and plutonic rocks exposed in the WJB suggesting that these TrPz plutons were generated in a back-arc setting (Barnes et al., 1995).

Western Jurassic belt. The WJB contains rocks which formed parts of the active arc and inter-arc basin in the Josephine marginal ocean basin. Pre-150 Ma rock units of the belt can be divided into two main groups: 1) a subgreenschist to greenschist facies, stratified overlap sequence of volcanic and sedimentary rocks, and 2) an assortment of variably deformed, subgreenschist to amphibolite facies rocktypes which formed the substratum to the layered series (Table 1 and Figures 2 and 3). Units of the overlap assemblage include the arc volcanic and sedimentary rocks of the Rogue Formation (Garcia, 1979; 1982), hemipelagic and flysch strata of Galice Formation (Pessagno and Blome, 1990), and poly lithologic breccia and megabreccia of the Lems Ridge and Fiddler Mountain olistostrome sequences (Harper et al., 1994; Ohr, 1987; Yule, in preparation). The composite basement complex consists of the Josephine ophiolite (Harper, 1984; Dick, 1976), the Briggs Creek amphibolite (BCA) (Coleman and Lanphere, 1993), the metamorphic rocktypes of the Chetco complex (Hotz, 1971), and the Onion Camp complex (OCC) (Yule, 1995). The OCC and at least part of the BCA are correlative with the RCT on the basis of distinct lithologic similarities, similar fossil and radiometric ages, and clear geochemical correlations (Yule et al., 1994; Yule, 1995).

The basement rocktypes of the WJB are intruded by the Illinois River plutonic complex, the plutonic root of the active arc and the intrusive equivalent of the Rogue Formation (Garcia, 1982). Scattered post-150 Ma mafic to intermediate dikes and small plutonic bodies occur throughout the WJB, but are most common in the California/Oregon border region.

GEOLOGIC HISTORY

Oldest of Easternmost (on this trip)

Remnant arc

Westernmost Klamath Belt
Arc = (1) (2) arc basin

The rock units studied on this trip span ~70 m.y. of geologic time, from 200 to 130 Ma (Late Triassic to Early Cretaceous). This history can be divided into the following four primary episodes: 1) Triassic to Early Jurassic primitive arc magmatism, 2) Middle Jurassic thrusting, terrane assembly, and calc-alkaline arc magmatism, 3) Middle Jurassic to Late Jurassic rifting accompanied by contemporaneous tholeiitic to calc-alkaline arc magmatism and tholeiitic inter-arc basin ophiolite generation, and 4) Late Jurassic to Early Cretaceous thrusting and regional deformation associated with the Nevadan orogeny. The first and second episodes are separated by an ~20 m.y. hiatus. However, the latter three cases are not entirely distinct from each other, and certain aspects of each episode overlap and are temporally and spatially variable along the trend of the province.

Triassic to Early Jurassic. Rocktypes of the RCT and OCC are the only rocktypes seen on this trip which have experienced the Triassic to Early Jurassic history (Figures 2 and 3). This history is best known in the southern Klamath Mountains where the RCT consists of a pre-200 m.y. serpentinite matrix mélangé unit intruded by 207-193 Ma quartz diorite intrusions (Wright and Wyld, 1994), and overlain by Late Triassic to Early Jurassic stratified volcanic and sedimentary units (Wright and Wyld, 1994; Irwin et al., 1982).

Blocks in the mélangé basement include metachert, limestone, pillow basalt, greenstone, amphibolite, a variety of mafic plutonic rocks, and peridotite, all suspended in a matrix of sheared serpentinite. Mafic rocks in the mélangé exhibit trace and REE signatures distinctive of normal to enriched mid-ocean ridge basalt (N-MORB to E-MORB) and within plate basalts (WPB) (Wright and Wyld, 1994). The cover sequence consists of a lower marine volcanic sequence with primitive island arc tholeiite trace element characteristics and an upper, clinopyroxene-phyric volcanic sequence with more evolved, calc-alkaline geochemistries. Both volcanic units interlayer with metachert, metaargillite, and coarse epiclastic rocks with detrital grains probably derived from Paleozoic rocks of western North America (Wyld and Wright, 1993; Wright and Wyld, 1994). The geochemical character of the early Mesozoic plutons are indistinguishable from the calc-alkaline volcanic sequence (Wright and Wyld, 1994).

Farther to the north along its trend, the RCT exhibits the same general structural, stratigraphic, and geochemical relationships (e.g. Norman, 1984; Gorman, 1985; and Gray, 1985), with the following notable exceptions. In the central Klamaths, the rocktypes generally occur at higher metamorphic grade, reaching into the upper amphibolite to granulite(?) facies (Donato et al., 1996; Donato, 1987). In addition, the cover sequence is not recognized in some areas and the mélangé has a block-on-block rather than a block-in-matrix character (Peterson, 1982; Donato, 1987; Barnes et al., 1993). Finally, the RCT in the Marble Mountains and equivalent rocktypes exposed in the WJB (OCC) consist of coherent amphibolite/peridotite bodies which have been complexly folded (Figure 3; Donato, 1987; Yule, 1995).

Middle Jurassic. The Middle Jurassic history is recorded by rocks of the RCT, the WHT, and other terranes of the TrPz (Figures 2 and 3). Following an ~20 m.y. hiatus, this interval marks the re-establishment of an oceanic island arc complex above an east-dipping subduction zone along the western margin of North America. Arc volcanic rocks associated with this arc range in age from 177-167 Ma and are restricted to the western Hayfork terrane. Related calc-alkaline plutonic bodies intrude the WHT and other terranes of the TrPz and range in age from 175-159 Ma (Wright and Fahan, 1988). The younger of these plutons are contemporaneous with arc magmatism in the WJB. See the discussion of possible tectonic settings, below.

The TrPz intrusions occur as two distinct types. Pre- and post- 169 Ma plutons are truncated by or cross-cut, respectively, the terrane-bounding thrust faults of the TrPz (Wright and Fahan, 1988). These data establish a distinctly pre-Nevadan Middle Jurassic age for thrusting and terrane assembly in the Klamath Mountains, with deformation ongoing at 169 Ma and over by at least 161 Ma (Wright and Fahan, 1988). Metamorphic hornblende ages from RCT amphibolites range in age from ~175-165 Ma (Saleeby et al.,

1982; D. Yule, in preparation; and G. Harper, unpublished data), and are interpreted to record cooling below amphibolite facies conditions following intraoceanic thrusting, probably related to the assembly of the TrPz.

Middle to Late Jurassic. Rifting associated with the formation of the Josephine basin occurred soon after, or overlapping with, the assembly of the TrPz and western Hayfork arc magmatism. Ages obtained from the Josephine and related ophiolite sequences range from 162-166 Ma (Saleeby and Harper, 1993; Saleeby, 1984), thus ocean ridge spreading centers were established locally by at least 166 Ma. These data support the interpretation by Snoke (1977) that the Preston Peak ophiolite represents the rift-edge facies of the Josephine basin, and thus records the early phase of ophiolite magmatism in that region (>164 Ma). The greenschist facies China Peak mafic dike complex, which occurs as part of the Condrey Mountain schist (Figure 2), may record an older age for Josephine-related spreading at ~172 Ma (U-Pb zircon; Saleeby and Harper, 1993). However, others have argued that the similarity in age of the dikes and the western Hayfork volcanic rocks suggests that these dikes are arc rather than ophiolite related (e.g., Helper, 1986; Helper, et al, 1989). Regardless of these competing views, the 166 Ma age represents a minimum age for ophiolite genesis, particularly because some period of time is required to rift apart pre-existing oceanic lithosphere and form ocean spreading centers.

Arc magmatism in the Josephine marginal basin is recorded by the Rogue Formation and the related IRPC. Radiometric ages for these units span 160-154 Ma (Figure 3). The Rogue arc was constructed upon a composite basement terrane comprised of rocktypes correlative with the Josephine ophiolite and the RCT (Figure 3). As mentioned above, contemporaneous plutons of the TrPz occur inboard (present coordinates) of the Josephine ophiolite. Hemipelagic sediments of the Galice Formation overlap the ophiolite and interfinger with the Rogue Formation. These strata are overlain by flysch deposits which contain detritus that is partially derived from the western North American craton and the older terranes of the Klamath Mountains (Miller and Saleeby, 1995). The Josephine basin thus formed in proximity to the continental margin.

Late Jurassic to Early Cretaceous. The tectonic imbrication of the Josephine basin and its subcretion beneath the older terranes of the Klamath Mountains occurred during this time. The oldest radiometric ages related to Nevadan deformation in the region come from the BCA body (156-158 Ma; Figure 3), and probably record cooling of the Rogue arc and its wallrocks as it was extinguished during the initial phases of thrusting. Basin collapse was probably complete by ~150 Ma when a variety of small plutons and dikes intruded the Preston Peak fault (Figures 2 and 3) and overprinted Nevadan metamorphic fabrics (Harper et al., 1994). The youngest strata involved in the deformation are the Kimmeridgian Galice flysch. However, metamorphism and local deformation continued until ~135 Ma when rapid exhumation of the region occurred and was closely followed by the nonconformable onlap of Lower Cretaceous strata (Harper and Saleeby, 1994). Continuation of the Nevadan orogeny until ~135 Ma is consistent with recent geochronologic studies from the Sierran foothills (Saleeby et al., 1989; and Tobisch et al., 1989).

The characteristic Nevadan structure in the cover rocks of the WJB is a slaty cleavage. Strain associated with the cleavage appears to increase eastward with proximity to the Orleans/Preston Peak fault (Cashman, 1988), and to increase in metamorphic grade from north to south (Harper et al, 1988). F1 folds associated with the slaty cleavage have hinges that vary greatly in orientation, whereas the stretching direction within the slaty cleavage plunges uniformly to the SSE (Jones, 1988). Bedding is generally subparallel to cleavage, and much of the bedding is overturned as a result of tight to isoclinal folding (Snoke, 1977; Harper, 1980; Jones, 1988; Yule, 1995). The Josephine ophiolite shows little or no penetrative deformation at latitudes of Gasquet and north, but pillow lavas, breccias, and sheeted dikes become progressively more deformed to the south as metamorphic grade increases (Harper et al, 1988).

TECTONIC MODEL

The favored model for the tectonic evolution of the WJB was first proposed by Snoke in 1977 (Figure 4), and later revised by Saleeby et al. (1982) and Harper and Wright (1984). This model proposes that the Middle Jurassic western Hayfork arc and its basement terrane (RCT) rifted apart to form an active arc, inter-arc basin, and remnant arc triad in a marginal ocean basin situated above an east-dipping subduction zone (Figure 4). The discovery of correlative remnant arc basement rocktypes on opposite sides of the Josephine spreading centers provides unequivocal evidence that the model is valid (Yule et al., 1992; D. Yule, in preparation). However, the original geometry of the basin is still debated and is complicated by the tectonic disruption of the basin during its 157-150 Ma subcretion beneath the older Klamath terranes (Nevadan deformation).

Constraints regarding the geometry of the basin are as follows. Spreading directions are inferred to have been oriented parallel to the continental margin, north-south in present coordinates (Figure 4), on the basis of structural and faunal data (Harper and Wright, 1984; Pessagno and Blome, 1990; Alexander and Harper, 1992). The Rogue arc and the WH remnant arc are separated by the Preston Peak-Orleans fault, the roof thrust of the WJB. A minimum dip (westward) displacement on the fault is 40 km based on its outcrop pattern but is estimated to be >100 km based on gravity data (Jachens et al., 1986). The amount of lateral displacement is unconstrained at this time and may conceivably exceed the dip displacement.

The current debate centers on the relative position of the Rogue arc to the western Hayfork remnant arc. Both regions expose contemporaneous plutons, the circa 160 Ma plutons of the Rogue arc (WJB) and the Wooley Creek plutonic belt (TrPz; Irwin, 1985), that form parallel, north-south trending magmatic belts in present coordinates. One interpretation suggests that the Rogue belt formed as a classic, subduction related arc and the plutons of the Wooley Creek belt were emplaced in an extensional environment inboard of the back-arc Josephine basin (Figure 5; Hacker et al. 1995; and Barnes et al., 1995). This scenario is consistent with the Wooley Creek belt representing the western edge of diffuse magmatism that extends as far east as western Utah. However, this view cannot reconcile the spreading geometry of the Josephine basin which suggests that the Rogue arc and its rifted TrPz basement should occur far to the north. Also, it is implicit in this interpretation that motion across the Preston Peak Orleans was mostly west-directed.

An alternative interpretation (Yule, 1995) suggests that the Josephine ophiolite is an intra-arc ophiolite separating the northern Rogue arc from the southern Wooley Creek belt, with both belts part of the same subduction-related arc (Figure 6). This view reconciles the north-south directed spreading in the Josephine basin and the offset of the remnant arc fragments (TrPz). Notice that spreading ridges of the Josephine ophiolite also occur in the "arc" setting, and may help to explain the observed arc geochemical signatures in some Josephine rocktypes (G. Harper, unpublished data). Finally, this interpretation requires that the Josephine basin was tectonically collapsed by highly left-oblique shortening. If the lateral:dip offsets exceeded 2:1, then the Preston Peak-Orleans fault may have experienced >200 km of north-directed displacement. This is consistent with the large-scale, left-lateral displacements along the western North American margin during the Late Jurassic, i.e., displacements across the proposed Mojave-Sonora megashear at ~155-150 Ma (Anderson and Silver, 1974). The Preston Peak-Orleans thrust and the WJB may thus represent the deformational belt that formed as cratonal North America accelerated northward in the Late Jurassic.

FIRST DAY

The first day will visit exposures in the "remnant" arc complex of the Josephine marginal basin. STOPS include river and roadcut exposures in the WHT and RCT located in the Applegate Reservoir area (Figure 7), and a road metal quarry in the Grayback pluton. Mileages are measured to the nearest tenth of a mile starting from the intersection of U.S. Hwy 199 and Oregon State Hwy 238, located on the south side of Grants Pass. The first

mileage listed is for the distance between road log entries, and the second mileage listed (in parentheses) is for the cumulative day's mileage.

0.0 (0.0) The first few miles of the trip travel through the ~139 Ma (U-Pb zircon) Grants Pass pluton (Harper et al., 1994), a dioritic through granitic pluton which intrudes the Preston Peak/Orleans fault. The pluton weathers more readily than the surrounding country rocks and forms the valley in which the city of Grants Pass and surrounding communities occur. The pluton margin and contact aureole within the TrPz occur a few miles to the south of Grants Pass near the town of Murphy. Continue southeast from here along the alluviated Applegate River valley. The hillslopes in this region are underlain by rocks of the Applegate Group (Donato et al., 1996; Wells et al., 1949) and probably consist of both RCT and WHT lithologies.

23.2 24.2 (24.2) Turn right at the intersection of Oregon State Hwy 238 and Hamilton Road.

✓ 0.9 (25.1) Turn right at the intersection of Hamilton Road and Cantrall Road (road to Tallowbox Mountain Lookout).

28.2 4.3 (29.4) **STOP 1.** Roadcuts on the southern flank of Negro Ben Mountain expose interlayered fine to medium greenish-gray volcanogenic meta-sandstone and grayish-brown meta-argillite of the western Hayfork terrane. Partial Bouma sequences can be seen. The sandstones range from lithic arenite to lithic wacke. They contain grains of plagioclase + volcanic rock fragments ± augite ± hornblende. These units are commonly interbedded with conglomeratic deposits in which the cobbles are typically plagioclase + augite ± hornblende-phyric basalt to andesite. Dacitic and dioritic cobbles are rare. Metamorphism is generally weak, with partial albitization of plagioclase and partial to complete replacement of primary augite and hornblende by actinolite.

Elsewhere in the Applegate Reservoir area, arenitic units contain rare detrital quartz. Also, in addition to the metasedimentary rocks observed on this trip, sparse basaltic lavas and hyaloclastite breccias (with relict olivine) are present, as are grayish green fine-grained meta-ash deposits that retain relict shards.

Lavas and cobbles from the western Hayfork terrane are typically calc-alkaline and display trace element abundances (low TiO₂, P₂O₅, Nb, and Ta; light rare earth element enrichment; Figures 8 and 9) characteristic of arc magmas (Barnes et al., 1995 and in review; Donato et al., 1996). These features are consistent with previous interpretations of the origin of the WHT as the principal representative of the Middle Jurassic arc in the Klamath Mountains. However, the fact that most of the WHT is clastic and that the abundance of lavas and pyroclastic deposits is low suggests that the exposed parts of the WHT were derived from an arc in which volcanic activity was waning and erosional degradation was predominant (e.g., Marsaglia & Ingersoll (1992)).

32.4 4.3 (33.7) Return to Hamilton Road. Turn right.

33.4 1.2 (34.9) Turn right at intersection of Hamilton Road with Applegate Road.

9.5 (44.4) **Optional STOP** to look at meta-argillite unit of the Hayfork arc exposed along the banks of the Applegate River. These outcrops may be submerged during periods of high runoff.

46.0 3.8 (48.2) Turn left on Squaw Creek Road and proceed across the Applegate Reservoir Dam. Fresh roadcuts of Hayfork meta-andesite occur on the west side of Applegate Road, located ~0.1 - 0.2 miles below the dam. Bedding strikes northeast and dips steeply to the southeast, sub-parallel to the outcrop face.

Stop 2

western Hayfork terrane

0.5 (48.7) **STOP 2.** Park where the road turns toward the east. The steep outcrop on the northeastern side of the road exposes interbedded volcanogenic meta-sandstone and meta-argillite similar to that at STOP 1. Several andesitic dikes (>3 meters wide) cut obliquely across the interbedded metasedimentary rocks. In this locality, some of the meta-arenites contain unaltered olive hornblende. Elsewhere, for example near Bolan Lake, olive to reddish brown hornblende is preserved. Microprobe analyses of these amphiboles (C. Barnes, unpubl. data) indicate that they range from magnesio-hornblende through pargasite to ferroan pargasitic hornblende. They commonly show normal zoning (to more silica- and Fe-rich rims) and are interpreted to be primary igneous amphibole. ⁴⁰Ar/³⁹Ar dating of hornblende from meta-arenite collected from this exposure yielded a plateau age of 173.3 ± 1.3 Ma and hornblende from a crosscutting dike gave a ⁴⁰Ar/³⁹Ar plateau age of 156.3 ± 1.3 Ma (Donato et al., 1996). Hornblende separated from an arenite collected in the Bolan Lake area yielded a ⁴⁰Ar/³⁹Ar plateau age of 172.3 ± 1.0 Ma (Donato et al., 1996).

0.5 (49.2) Return to Applegate Road and turn left.

50.0

2.0 (51.2) **STOP 3.** Metaserpentinite of the Rattlesnake Creek terrane. The serpentinite is an irregular shaped body that exhibits a shallowly dipping gneissic foliation. This and other small serpentinite bodies, generally <2 km², are a distinctive feature of the RCT in Oregon. Similar serpentinite bodies occur in arc basement terrane of the WJB and occur at STOPS 17 and 18 (DAY 3). Here, as in the WJB, the serpentinite bodies are associated with massive to pillowed metabasalts and bedded chert, Fe- and Mn-rich siliceous metasediments (ironstone), marble (some outcrops bear Norian conodonts), finely laminated gneissic, schistose, and semi-schistose metavolcanic and metasedimentary rocks.

Metamorphic grade ranges from approximately middle greenschist to uppermost amphibolite or granulite(?). From the Applegate Lake area westward to the Grayback and Thompson Ridge plutons, metabasic rocks range from amphibolite-facies greenstone to amphibole schist and ultramafic rocks. The relict peak metamorphic assemblage is olivine + enstatite + tremolite (Donato et al., 1996). Blackwall is common, which indicates hydrothermal exchange between metaserpentinite and mélangé blocks during and after metamorphism. West of the Bolan Lake area, metabasic rocks contain the greenschist facies assemblage albite + chlorite + quartz ± actinolite and argillitic samples contain rare relict andalusite, which indicates metamorphic pressure less than about 4 kb. One of the striking features of these low-grade RCT rocks is a "shattered" appearance. In thin section, samples typically show abundant brittle fractures with negligible offset and veining is widespread. This type of deformation is generally absent in the overlying western Hayfork rocks.

Collectively, these rock associations probably represent a serpentinite matrix mélangé that was subsequently deformed and metamorphosed. In the California Klamath Mountains, the RCT mélangé is locally overlain by coherent, interbedded metasedimentary and metavolcanic strata (Wright & Wyld, 1994; Gray, 1985). Greenstone blocks in the RCT mélangé show both MORB (common) and IAB (uncommon) compositions (Figures 8 and 10). Similar rocks probably underlie a large area between Bolan Lake (Barnes et al., 1995 and in review) and Cave Junction; however, detailed mapping will be necessary to confirm this idea.

0.7 (51.9) Massive metabasalt is exposed in a degraded roadcut opposite "Copper Ramp" boat access to Applegate Reservoir.

~1.2 Turn left at stop sign and continue driving on Applegate Road.

1.3 (54.4) Approximately 1/8 to 1/4 mile after the pavement ends, make a 180° right hand turn and proceed down the hill to the Applegate River.

0.2 (54.6) **STOP 4.** Metasediments of the RCT (Marble Mountains terrane) are exposed beneath the bridge over the Applegate River. The rocks here exhibit a gneissic foliation, an intersection lineation, and tight to isoclinal folds. Similar lithologies and deformational features occur in basement rocks of the Rogue River arc complex (DAY 3).

Blake et al. [1982] named high-grade ophiolitic mélangé in the Marble Mountains area of California the "Marble Mountains terrane". This unit, as well as the high-grade rocks at this locality have been shown to be equivalent to the RCT. In the Marble Mountains, metamorphic grade reaches staurolite zone conditions and in the headwaters of the Applegate River, Lieberman & Rice, (1986) and Grover (1984) described metamorphic assemblages consistent with granulite facies conditions of 700° to 800°C and 7-8 kb.

Use caution when examining these outcrops, they are very slippery when wet! A less treacherous alternative occurs along the shore of the Applegate Reservoir. To get to this outcrop, drive 0.2 mile back to the Applegate Road, turn left and drive 0.4 miles and turn right on Manzanita Creek road. The outcrop lies approximately 100 meters ahead on the west side of the road (toward the lake). This outcrop exposes a deformed metadiorite (158 ± 1 Ma, Ar/Ar hornblende, M. Donato, personal communication) intruding calcareous quartzites. Numerous tight to isoclinal folds are visible in the quartzite. This locality can be underwater when the lake level is at a maximum.

75.2 ~25.0 (80.0) Return to Applegate Road and drive north to the village of Applegate via Carberry and Thompson Creek roads. Turn left on S.H. 238 in Applegate and proceed to Provolt.

79.2 ~4.5 (84.5) Turn left (south) at intersection of Williams Hwy and S.H. 238.

6.4 (90.9) Bear right onto Cedar Flat Road in the center of Williams.

0.6 (91.5) Bear left at fork in Cedar Flat Road.

86.2 2.4 (93.9) Turn left (south) onto Caves Camp Road and proceed toward Little Sugarloaf Peak.

7.4 (101.3) Bear left on a spur road which leads to **STOP 5.**

0.8 (102.1) **STOP 5.** Fresh gabbro and norite of the 160 Ma (U-Pb zircon) main stage of the Grayback pluton are exposed in a road metal quarry on the northern flank of Little Sugarloaf Peak. The view to the north is to the lowlands of the Williams-Provolt area, which is underlain by the northern part of the pluton and has been preferentially weathered and eroded relative to the surrounding wall rocks.

Rock types at this locality vary from hornblende melagabbro to norite and hornblende norite. In many samples it is easy to distinguish among deep green augite, brown orthopyroxene, and black hornblende. Sparse clusters of orthopyroxene suggest that olivine was a primary phase (elsewhere in the pluton, olivine (~Fo75) is present). Plagioclase in these rocks displays sharply-bounded calcic cores (> An80) and intermediate rims (~An50). In some melanocratic samples, calcic plagioclase is poikilitic (and therefore not relict).

The Grayback pluton is the largest of a chain of five plutons that intrude rocks of the RCT and WHT (Figure 2). This line of plutons strikes NNE and extends from the 162 Ma

(U-Pb zircon) Thompson Ridge pluton in the south, through the Sucker Creek pluton, the Grayback pluton, an unnamed pluton, and the ~160 Ma (U-Pb zircon) Wimer pluton. Dense swarms of dikes are present between the Thompson Ridge and Sucker Creek bodies and between the Sucker Creek and Grayback plutons (e.g., Figure 11). Tomlinson (1991) and Donato et al. (1996) showed that the Thompson Creek pluton and adjacent dikes intruded a high-angle fault that separated low-grade WHT rocks on the west from high-grade RCT rocks on the east.

These plutons range in composition from gabbro to granite, with gabbro through mafic tonalite the predominant compositions. The Grayback pluton (Barnes et al., 1995b) is the best example of this variability. The main stage of the Grayback pluton consists of medium to coarse grained gabbro through tonalite (Figure 11). It is cut by late stage granodioritic and tonalitic dikes, many of which are composite or mingled dikes with basaltic and intermediate enclaves. One granodioritic dike yielded a U-Pb age (zircon) of ~156 Ma. Within the main stage, numerous examples of equigranular mafic dikes and coarse-grained gabbroic to pyroxenitic pods display mutual cross-cutting relationships with medium-granited "host" plutonic rocks. These features suggest that the Grayback pluton received numerous injections of mafic, predominantly liquid, basaltic magma and of crystal mushes that represent cumulates derived by fractional crystallization at other levels. Evolution of the magmas at deeper crustal levels is supported by initial $^{87}\text{Sr}/^{86}\text{Sr}$ and $\delta^{18}\text{O}$ values, which indicate assimilation of metasedimentary crustal rocks below the level of emplacement (Barnes et al., 1992).

Within the main stage, samples with both calc-alkaline and tholeiitic magma lineages are present (Figure 12). Tholeiitic compositions are most common as mafic dikes, but are also present in samples of the "host" pluton. These rocks are enriched in Al_2O_3 and Sr and depleted in Ba and Zr; they are typical of fractionated high-aluminum tholeiite. Calc-alkaline rocks span the compositional range from gabbro to granodiorite. Mass-balance calculations show that this compositional suite can be produced by fractional crystallization with minor crustal assimilation. Many gabbroic samples and all melagabbroic and pyroxenitic samples represent partial cumulates formed during this process (Figure 13).

Detailed studies of late-stage hybrid dikes [Johnson, 1991] showed how magma mixing among basaltic and tonalitic magmas was also an important process during main-stage activity (Barnes et al., 1995b). Basalt-granite mixing also occurred during late-stage activity, but was apparently rare during the main stage (during which granodioritic magmas were formed by fractional crystallization).

Figure 13 attempts to show how this complex set of processes resulted in the range of rocks observed, with trends for fractional crystallization and two mixing curves. The consequences of these models are: (1) at least two and probably three mafic end members were present in the Grayback system, calc-alkaline and tholeiitic basalt; probably two distinct calc-alkaline basaltic end members were present. (2) At least two felsic end members were present, granodioritic magmas formed by fractional crystallization of calc-alkaline basalts and tonalitic magmas formed by crustal melting. (3) Much of the magmatic evolution was at deeper crustal levels, where the tholeiitic magmas differentiated, some fractional crystallization and crustal assimilation occurred, and the late-stage tonalitic magmas were produced. (4) Mantle source rocks for the basaltic magmas were compositionally variable. It is noteworthy that similar variability of basaltic compositions is observed within the High Cascade arc and within the back-arc region of the Basin and Range Province of Oregon.

THE END OF THE FIRST DAY (unless time and enthusiasm inspire visit(s) to the following Optional STOPS).

Optional STOP A. From STOP 5, return to Caves Camp Road and turn left (south). Drive 4.6 miles to a roadcut and creek exposure of foliated diorite of the Grayback pluton.

Optional STOP B. From STOP 5, return to Caves Camp Road and turn left (south). Drive 15.6 miles to the intersection of USFS 4611 and SH 46. Turn left and proceed approximately 7.5 miles to the Oregon Caves National Monument. The Caves occur in marble of the RCT in the contact aureole of the Grayback pluton.

Optional STOP C. At the intersection of USFS 4611 and SH 46 turn right and proceed 11.7 miles to U.S. Hwy 199. Turn left onto U.S. Hwy 199 and proceed 6.6 miles to the intersection with Waldo Road. Turn left (east) and drive 0.6 miles and park at the bridge over the West Fork Illinois River. The rounded hill northeast of the bridge, known as Indian Hill, is underlain by Cretaceous (~130 Ma) sediments (Hornbrook Formation). These strata lie unconformably upon the Galice Formation and are faulted against the Applegate Group (RCT). Thus, they place a minimum age for Nevadan deformation of the Galice Formation deposits. Layering in this unit dips north $\sim 15^\circ$ to 30° , an indication of post-Nevadan tilting. The basal gravels are exposed directly beneath the bridge and include primarily of cobbles and boulders of Galice Formation. These fluvial deposits contain red beds (paleosols). The overlying strata are fossiliferous massive marine sandstones.

SECOND DAY

Mileages start from Patrick Creek Lodge. DAY 2 is designed to spend the morning examining roadside exposures of the Preston Peak thrust fault and associated rocktypes in the hanging wall of the fault (Figures 2, 14 and 15), and the afternoon studying river polished exposures in the 162-165 Ma Josephine ophiolite sequence (Figures 2 and 16; Harper, 1984; Harper et al., 1994). The Preston Peak fault is a major terrane bounding fault which underthrusts WJB inter-arc basin rocks beneath the remnant arc terrane of the TrPz. The Josephine ophiolite is the largest and most complete ophiolite sequence exposed in western North America and is interpreted to have formed in a suprasubduction zone tectonic setting in an inter-arc basin separating the remnant and active arcs (Harper 1984). Note that some of the afternoon STOPS are also described in Harper (1989).

0.0 (0.0) Turn left (east) from the Patrick Creek Lodge entrance onto U.S. Hwy 199.

8.1 (8.1) Turn right (south) onto Knopti Creek Road.

6.0 (14.1) Bear right at fork in the road.

2.6 (16.7) **STOP 6.** Park just beyond mile post 9 (note that distances between mile posts along Knopti Creek Road are inaccurate). Walk back to mile post 9 where the Preston Peak fault is exposed. At this locality, the hanging wall consists of serpentinitized ultramafic rocks (part of a serpentinite-matrix mélangé at the base of the Preston Peak ophiolite), and greenschist-facies rocks inferred to be part of the Late Jurassic Galice Formation from the footwall. Along the fault zone, serpentine slip fibers trend northward and indicate top to the north sense of shear. The inferred Galice rocks, immediately west of the fault contact, consist of mafic and felsic metatuff, pebbly metamudstone, and slaty black argillite. A metamorphosed(?), white quartz keratophyre intrusion, dated by U-Pb zircon at ~ 150 Ma (sample PP582, Saleeby et al., 1982), has intruded this rock sequence. In turn these keratophyric rocks and the Galice(?) rocks are intruded by a suite of mafic dikes. Farther north along the Knopti Creek Road, more typical Galice rocks including semischistose metagraywacke and slaty mudstone form the footwall of the Preston Peak fault.

The name "Preston Peak fault" was coined for a reverse fault that forms the boundary between a hanging-wall block composed of the Preston Peak ophiolite and a footwall block

of Late Jurassic Galice Formation (Snoke, 1977). This tectonic boundary was originally recognized and mapped by Hershey (1911). On his Del Norte County geologic map, he called it the "Orleans fault," considering it to be correlative with a fault just east of the village of Orleans far to the south on the Klamath River. Snoke (1977) abandoned the name "Orleans fault" and referred to this boundary as the "Preston Peak thrust," because he argued that at the time of his analysis that the fault near Orleans had not been conclusively shown to be the same as the fault in the Preston Peak area. Subsequently, a geological and geophysical study by Jachens et al. (1986) used the term "Orleans fault" as a regional thrust fault that separated rocks of the western Paleozoic and Triassic belt from rocks of the western Jurassic belt. However, on his recent geologic map of the Klamath Mountains, Irwin (1994) used the term "Preston Peak fault," and the name "Orleans fault" does not appear on the map. The fault near the village of Orleans appears to be a tectonic boundary between oceanic-arc metavolcanic rocks of the western Hayfork terrane and western Jurassic belt, whereas the Preston Peak fault is interpreted as a tectonic boundary between the ophiolitic Rattlesnake Creek terrane (Preston Peak ophiolite and related rocks) and the western Jurassic belt. Detailed, serial regional cross-sections are necessary to truly establish the exact geometric relationships between these various tectonic boundaries, and thus the name "Preston Peak fault" is retained in this article.

The age of the Preston Peak fault is clearly post-Kimmeridgian, because the Galice Formation which forms the footwall block of the fault is firmly established as middle Oxfordian to late Kimmeridgian based on the pelecypod *Buchia concentrica* (Sowerby) (Imlay, 1980). The minimum age of displacement along the Preston Peak fault is much more uncertain, because in the type area of the fault, no conclusive field relationships have been discovered that provide an upper boundary for the movement history (Snoke, 1977). However, to the north along the strike of the Preston Peak fault, several field relationships suggest a complex, polyphase movement history or perhaps subsequent overprinting by later tectonic events. The Grants Pass pluton (dated at ~139 Ma, Harper and others, 1994) intrudes the fault zone, and thus provides a clear upper limit for the movement history for the fault, at least in that immediate area of the Oregon Klamath Mountains. However, near the California-Oregon border (northeast of O'Brien, Oregon, see Optional STOP C), Early(?) Cretaceous rocks (Hornbrook Formation) are immediately west of a fault that forms the boundary between ophiolitic mélangé and the western Jurassic belt (Shenon, 1933; Nilsen, 1984; Irwin, 1994). Irwin (1994) shows the fault bounding the Cretaceous rocks as thrust fault, whereas the generalized geologic map in Harper and others (1994) indicates that this fault cuts the Preston Peak fault and thus may not be related to Late Jurassic contraction.

In summary, the Preston Peak fault is part of a regional thrust system that developed in the Late Jurassic during the collapse of the Josephine inter-arc marginal basin beneath the Preston Peak ophiolite (Rattlesnake Creek terrane) and an originally overlying remnant arc system (now partly preserved as the western Hayfork terrane).

0.8 (17.5) Amphibolite block in serpentinite-matrix mélangé. A composite dike with a fine-grained margin of microporphyritic metabasalt and a core of metagabbro is intruded into the amphibolite. Such crosscutting mafic rocks could be feeder dikes to the overlying mafic complex of the Preston Peak ophiolite.

0.3 (17.8) **STOP 7.** Metadiabase block in serpentinite-matrix mélangé. Metadiabasic rocks comprise the bulk of the multiphase mafic complex of the Preston Peak ophiolite. These metadiabasic rocks occur as intermingled sills and dikes indicating a piecemeal growth history, perhaps related to rifting associated with the initial opening of the Josephine back-arc basin (Saleeby et al., 1982).

0.3 (18.1) **STOP 8.** Slaty argillite and basaltic breccia block within serpentinite-matrix mélangé. Are these rocks a piece of the footwall block for the Preston

Peak fault (i.e., rocks of the Galice Formation) mechanically mixed into the upper plate during development of the basal serpentinite-matrix mélangé? Or, are they part of the original stratigraphy of the upper part of the Preston Peak ophiolite (e.g., metavolcanic rocks and subordinate siliceous argillite of Broken Rib Mountain) incorporated into the serpentinite-matrix mélangé? These rocks are very similar in appearance to deposits in the Lems Ridge and Fiddler Mountain olistostrome sequences (see STOP 15).

0.4 (18.5) Hairpin turn, with roadcut in serpentinitized peridotite cut by a rodingite dike.

0.6 (19.1) Quarry in serpentinitized peridotite with abundant shallowly inclined serpentine fibers.

0.3 (19.4) **STOP 9.** Composite block of amphibolite and peridotite (Snock and Whitney, 1979) within serpentinite-matrix mélangé. On Haystack Mountain to the north, the contact between amphibolite and mylonitic lherzolite is well-exposed and concordant with high-temperature, metamorphic foliation in both the amphibolite and peridotite (Figure 14; Snock, 1977; Cannat and Boudier, 1985). Foliations and lineations in both rock types are parallel. Cannat and Boudier (1985) argued that the basal peridotite and underlying amphibolite sole were deformed together under amphibolite-facies conditions during intraoceanic thrusting, thus prior to the development of the mafic complex of the Preston ophiolite and the lower temperature faulting associated with the Preston Peak fault (Snock, 1977). A K-Ar (hornblende) age from this amphibolite block yielded a date of 165 ± 3 Ma (sample PP580, Saleeby et al., 1982); this date is interpreted as a minimum age for the amphibolite-facies metamorphism manifested near the base of the Preston Peak ophiolite.

A similar amphibolite and peridotite contact occurs at STOP 18 (DAY 3).

11.3 (30.7) Return to U.S. Hwy 199. Turn left and proceed to **STOP 10**.

6.9 (37.8) **STOP 10** (Stop 2 of Harper, 1989). Park in a clearing on the left (east) side of Hwy 199 and take a path down to the Middle Fork Smith River. The trail meets the river at the top of the radiolarian-bearing, Smith River section described in Pessagno and Blome, 1990. Walk down river through radiolarian argillites and a few thick graywacke beds of the basal Galice Formation flysch which grade down section into the hemipelagic sequence of the Galice Formation. Farther down the depositional contact with pillow lavas of the 162 Ma Josephine ophiolite is exposed. The lavas immediately beneath the depositional are lobate pillows. To view more lavas, climb up the embankment to U.S. 199, walk down the road to a position across the river from the mouth of Little Jones Creek (CAUTION!, Hwy 199 has no shoulder), and climb down to the river. Here, massive lava progresses upsection into isolated pillow breccia and pillow lava.

Numerous syn-Nevadan 146-151 Ma hornblende-bearing, calc-alkaline sills and dikes cut all of the units exposed at this STOP. Nevadan deformational features in the Galice Formation include: 1) slaty cleavage subparallel to slaty cleavage, 2) flattened pebbles at the base of turbidite beds, 3) boudinage of sills, and 4) fibrous extension and mixed mode veins.

1.2 (39.0) Patrick Creek Lodge and the confluence of Patrick Creek and the Middle Fork Smith River. Here, a north-trending fault with normal separation is truncated by a northeast-trending fault exhibiting right lateral separation (Figure 16). To the south, this fault has thinned and omitted the crustal section of the ophiolite. This fault may represent an oceanic normal fault that developed as extension outpaced ophiolite crust generation at the spreading center (Alexander and Harper, 1992). However, the evidence is equivocal

Day 5 Stop 2 - 1

Day 5
me

and cannot preclude that the offset occurred during out of sequence faulting of Nevadan age.

West from Patrick Creek to the village of Gasquet, the highway crosses a large, peridotite-cored anticline.

10.2 (49.2) **STOP 11** (Stop 4 of Harper, 1989). Sheeted dike-gabbro transition. This large river outcrop was the subject of a very detailed study on the sheeted mafic dike complex, including its structural evolution, hydrothermal alteration history, and Sr and O isotopic signatures (Alexander et al., 1993). This locality is situated in the hinge area of a gently SSE plunging synform (Figure 14), such that the oceanic structures occur in outcrop close their original orientation. Here, sheeted dikes dip 40° south, illustrating the $\sim 50^{\circ}$ of tilting about a horizontal axis that has affected the crustal sequence throughout the Josephine ophiolite (Harper, 1982; Alexander and Harper, 1992). At this locality, a late-stage, subvertical dike cuts the sheeted dikes suggesting that the tilting occurred at the spreading ridge axis. The late-stage dike is chemically identical to the uppermost pillow lavas viewed at STOP 10, which are distinctive because of their highly fractionated and MORB-like chemistry (Coulton et al., 1995). The dikes and oceanic normal faults strike E-W, suggesting N-S directed spreading in present coordinates. Paleomagnetic evidence suggests that the region may have rotated clockwise by an uncertain amount during the Tertiary (Smith and Harper, in review).

Day 5
stop 4

2.6 (51.8) **STOP 12** (Stop 5 of Harper et al., 1989). Park at a gravel turnout and walk down a road to a gravel bar on the Smith River. Large slide blocks of plagiogranite with enclaves of diabase occur here. Walk upstream to a layered gabbro. Here, igneous layering dips steeply to the north. These exposures also occur in the hinge area of the large syncline suggesting that the tilting occurred at the spreading ridge. A thick cataclasite, locally cut by fibrous Nevadan extension veins, occurs at the south end of the outcrop and separates the layered gabbro with very few dikes from the sheeted dike-gabbro transition. This low-angle fault is interpreted by Alexander and Harper (1992) as a large low-angle oceanic fault with evidence for top to the south normal displacement. The cataclasite is well indurated and exhibits a regional metamorphic overprint, indicating that the cataclasis is pre-Nevadan in age.

Day 5
stop 5

2.0 (53.8) Turn left (south) onto South Fork road, cross the bridge over the North Fork Smith River and proceed to STOP 13.

0.3 (54.1) **Stop 13**. Turn right into a parking lot before reaching the bridge over the South Fork Smith River. Walk about 100 meters to view harzburgite tectonite exposures on the north bank of the South Fork Smith River. The rock commonly appears massive, but the mantle fabric is visible on weathered surfaces where trails of black Cr-spinel define the high temperature foliation and lineation. Banded textures are also common in the harzburgite tectonite unit where the layering is defined by variable proportions of orthopyroxene and olivine in the rock. In weathered outcrops, the pyroxene-rich bands are more resistant to weathering and give the rock a corrugated appearance. In thin section, olivine and orthopyroxene are highly strained and partially recrystallized, indicative of ductile deformation at very high temperatures in the upper mantle.

END OF THE SECOND DAY

THIRD DAY

STOPS for DAY 3 are in the central Illinois River drainage area, northwest of Cave Junction, Oregon. The objective for DAY 3 is to examine the geologic features of the active arc complex of the Josephine marginal basin and its basement lithologies (Figure

17). Basement rocktypes of the Onion Camp complex (OCC) bear a striking resemblance to RCT lithologies seen on DAY 1 and in the morning of DAY 2.

The northern part of the WJB was previously interpreted as an imbricate, fault-bounded stack of four subterranean units (Blake et al., 1985). Their designation is abandoned by Yule (1995) and D. Yule (in preparation) because field and structural data support an alternative structural interpretation. Based on these data (Figure 18), the northern WJB is best characterized as a fold belt with attenuated and truncated limbs (Figure 17). The characteristic Nevadan slaty cleavage strikes NNE and dips moderately to the SE, parallel to the axial planes of F1 folds (Figures 18c, d, g). The predominant orientation of faults and serpentine shears parallels the regional foliation. F1 and late metamorphic F2 folds are tight to isoclinal and trend NNE to SSW with a shallow plunge (Figures 18e, f). Hinges of these folds are rarely observed in the field due to shearing at a low angle to the axial surface. F3 folds are open folds which plunge moderately to the east (Figures 18e, g). Structures in the OCC (Figures 18a, b) are randomly oriented, reflecting their more complicated structural history and the dispersal of Middle Jurassic structures by Nevadan folds.

These data explain the outcrop patterns shown on Figure 17. The overall NE-SW trend of the WJB is controlled by the F1-F2 folds and the regional NE-SW strike of the foliation. F3 folds "crenulate" these overall NE-SW trends. The simplified geologic map (Figure 17) can be thought of as a natural cross section of a complexly folded and faulted, largely intact fragment of an oceanic arc and its basement terrane. A generalized cross section view is shown in Figure 19. The deepest structural level occurs on the SW, where the Josephine peridotite is exposed, and suggests that the rock units are gently plunging toward the northeast.

0.0 (0.0) Patrick Creek Lodge entrance and U.S. Hwy 199.

32.0 (32.0) Turn left on USFS 4201, a logging and access road leading to the eastern border of the Kalmiopsis Wilderness Area.

0.5 (32.5) The Illinois River Valley fault, here buried by Quaternary alluvium separates the Josephine peridotite on the west from the Galice Formation on the east. North of the road the fault dips moderately to the west ($\sim 30-45^\circ$) beneath Eight Dollar Mountain (Ramp, 1986). However, this shallow dip is not characteristic of the fault along most of its trace. To the south and north of Eight Dollar Mountain, shear fabrics in the fault zone generally dip $>70^\circ$ and the trace of the fault is linear with respect to topography. Fault-bounded masses of greenstone and gabbro locally occur along the trace of the fault and suggest that the ophiolite was disrupted and attenuated by movement along the fault. Uplifted alluvial terraces on the west side suggest that the fault has experienced Quaternary offset.

0.5 (33.0) USFS Boundary.

1.9 (34.9) Bridge across the Illinois River. Partially cemented, elevated alluvial deposits occur in roadcut exposures 100-200 meters beyond the bridge (on the west side of the river). These outcrops primarily consist of gravel and cobble size clasts of Josephine peridotite with subordinate amounts of Galice Formation clasts, often partially weathered to clay minerals. Some deposits have been extensively worked for gold. One of these workings, an excavation in the basal alluvial deposits, is visible in the roadcut at the end of the pavement.

3.5 (38.4) **STOP 14.** Park at a turnout on the east side of the road. Roadcut exposures of Josephine peridotite occur on the west side of the road. These rocks are

Day 3
Stop 1

identical to those seen at STOP 13 and represent the northern extension of the Josephine peridotite body.

Across the valley to the east, note the sharp vegetation change on the west flank of Eight Dollar Mountain. Also note that this feature dips southward and is thus not strictly related to elevation induced climatic changes. This vegetation break marks a boundary between sheared, serpentinized peridotite (>75% serpentine minerals) of the lower, grass covered slopes and blocky peridotite (<50% serpentine minerals) of the upper, forested slopes. The serpentinized peridotite always occupies a position between the Josephine peridotite massif and the greenschist and amphibolite facies crustal rocks of the Onion Camp complex.

Though the nature of the boundary has not been studied in detail, indirect evidence suggests that it separates two distinctly different generations of depleted mantle peridotite, one >175 Ma and the other ~162 Ma associated with the Josephine ophiolite (D. Yule, in preparation). The boundary may represent an ancient, mantle lithosphere/aesthenosphere transition zone which subsequently transformed, as spreading occurred at ~162 Ma, into a contact between "remnant" arc and Josephine inter-arc basin mantle lithosphere. This multi-stage history of the Josephine/RCT peridotite mass supports the polyphase, suprasubduction zone evolution of the Klamath terranes (e.g., Burchfiel and Davis, 1975, 1981; Harper and Wright, 1984; Miller and Saleeby, 1995; Saleeby and Harper, 1994; Snoke, 1977). Granted this history, the Josephine/RCT peridotite body may be the first documented example of a composite peridotite mass. It would be interesting to examine other Cordilleran-type peridotites to see whether they exhibit similar polygenetic histories.

2.1 (40.5) High angle cross-fault separating Onion Camp complex rocktypes and Josephine peridotite.

0.8 (41.3) Recrystallized red chert outcrop, characteristic of the metabasalt-chert unit of the Onion Camp complex.

0.9 (42.2) **Optional STOP D.** Heterogeneous mafic intrusive complex exhibiting characteristic hydrothermal alteration and brittle fragmentation textures. These rocktypes are very similar to the mafic intrusive complex of the Preston Peak region (STOP 7; also see Snoke, 1977).

0.2 (42.4) Roadcut with shallowly dipping dacite dike (150 Ma, U-Pb zircon) cutting foliated metavolcanic and metasedimentary rocktypes of the Onion Camp complex.

0.3 (42.7) Headscarp of a recent landslide on the east side of the road (mass wasting at work!).

2.7 (45.4) **STOP 15.** Park on the left shoulder across from the roadcut exposures of slaty meta-argillite and polyolithologic, ophiolite clast breccia of the Fiddler Mountain olistostrome complex. Walk over to the subvertical exposures of slaty argillite and siliceous argillite. At this locality, the slaty rock cleavage is subvertical or steeply inclined to the SE. Secondary structures include conjugate sets of kink bands. Though not present at this STOP, bedded sequences of white to gray chert layers are often interbedded with the meta-argillite unit and provide the only available age data for the complex. Chert beds collected ~2.5 km to the west yield poorly constrained Late Jurassic (possible Kimmeridgian?) radiolaria (M. Silk, unpublished data). However, stratigraphic relations suggest that the cherts and related olistostrome deposits are older. Specifically, they occupy a position at the base of the cover sequence, the same stratigraphic level as the Callovian-Oxfordian hemipelagic strata of the Galice Formation (Pessagno and Blome, 1990).

Day 3
STOP 15

Walk up the road to the west end of the metasedimentary outcrops and view the conformable, depositional contact with breccia deposits. In contrast to the highly strained argillite, the breccia unit is essentially nondeformed, probably due to rheologic differences between the two rocktypes. Here, the breccia deposits are massive. Outcrops ~1 km to the west are stratified, finer-grained sand and conglomerate. Small offset faults with normal separation locally cut these layers.

The breccias are distinctly poly lithologic, a feature that is most evident when the outcrop is wet. The dominant clast lithologies are aphyric to phyric green to gray metabasalt, fine- to medium- grained metadiabase, and medium- to coarse-grained gabbro. Secondary clast lithologies include chert, argillite, serpentinite, serpentinized peridotite, and rare occurrences of quartzite, chlorite schist, phyllonite, and amphibolite. The matrix materials consist of clay- to sand-size grains derived from the same material. Clast lithologies are identical to rocktypes of the Josephine ophiolite sequence and Onion Camp complex. However, the ophiolitic clasts predominate suggesting that the Josephine ophiolite was the primary source terrane. Distinctive deformation and alteration textures exhibited by the clasts also match those of the host lithologies. Specifically, many clasts display the cataclastic texture, hydrothermal veins, and static alteration common in the ophiolitic bedrock lithologies.

The olistostrome also includes "megabreccia" deposits, with clasts >100 m in size, which comprise ~50% of the Fiddler Mountain unit. Hydrothermally altered and fragmented gabbro and diabase are the most common megabreccia clast type. Poor exposure in the area makes it difficult to determine whether these blocks are clast or matrix supported because most outcrop dimensions are smaller than the megabreccia blocks themselves. As a result, the unit at first glance appears to be a heterogeneous intrusive complex except for the occurrence of the interbedded finer-grained facies.

Similar deposits to those of the Fiddler Mountain olistostrome complex occur at various localities throughout the Klamath Mountains and California Coast Ranges where they interfinger with the basal strata of the Galice Formation and the Great Valley sequence (e.g., the Lems Ridge olistostrome, Ohr, 1987; the Devil's Elbow ophiolite section, Wyld and Wright, 1988; Coast Range ophiolite near Paskenta, CA, Blake and others, 1987; the Preston Peak ophiolite, Snoke, 1977). These units are also closely associated with the RCT and the Josephine ophiolite and suggest that the Josephine and northern Coast Range marginal ocean basins formed as older oceanic arc terranes rifted apart. These basins, prior to their overlap by Galice Formation and Great Valley sequence strata, must have contained localized areas of considerable topographic relief. The Lau Basin located in the SW Pacific may represent a modern analog where basin and range bathymetry, seafloor spreading centers, and remnant arc rift-fragments occur within an inter-arc basin (Hawkins, 1995).

2.4 (47.8) Bear right at intersection (toward Onion Camp).

0.2 (48.0) Bear right at intersection (away from Onion Camp).

0.1 (48.1) **STOP 16.** Park and enter a road metal quarry exposing massive and pillow(?) metabasalt of the Onion Camp complex. The regional SE dipping foliation is weakly developed in these rocks and occurs as an anastomosing rock cleavage. These rocks are completely recrystallized to the greenschist facies mineral assemblage epidote+chlorite+ albite+ calcite+titanite± actinolite± quartz. Fe-oxide and pyrite are secondary. Prehnite, quartz+prehnite and quartz+calcite veins occur in most outcrops. Small pieces of red chert occur as float on the hillslopes surrounding the quarry (see optional STOP E, described below). These and rocktypes occur as a serpentinite matrix and block on block mélange. Other associated rocktypes in the mélange include: 1) a heterogeneous mafic intrusive unit, 2) finely laminated and highly strained metavolcanic and metasedimentary rocks, 3) scarce basalt breccia with relict clinopyroxene rich clasts, 4) amphibolite gneiss and shists, and 5) a matrix of sheared serpentinite lenses.

Day 3
Step 2b

Day 3
Step 3a

Metabasalt samples from this and other locations in the OCC were analyzed for major, trace, and REE analysis (Yule et al., 1993; Yule, 1995). The data help to correlate the OCC metabasaltic rocks with similar units in the RCT. Both RCT and OCC mafic rocks range in composition from 46% to 55% SiO₂ and display a wide range of FeO/MgO values and generally high TiO₂ concentrations (Wyld and Wright, 1988; Wright and Wyld, 1994; Barnes et al., 1995; Yule et al., 1993; Yule, 1995). The OCC trace and REE data span the spectrum from N-MORB to E-MORB to alkaline WPB, most similar to the lower melange metabasalts of the type RCT (Wright and Wyld, 1994).

0.2 (48.3) Turn left (north) toward Whetstone Butte.

0.5 (48.8) **STOP 17.** Bear left (west) at all forks in the road and park upon reaching the end of the road, at a logging platform in a late 1980's clear cut. The roadbed here consists of polished, black serpentinite.

The objectives of this STOP are to examine OCC serpentinitized peridotite, volcanogenic turbidites of the Rogue Formation, and the nature of the boundary between both units (Figures 17 and 19). Plan to spend approximately 2 hours away from the vehicles during a hike to view outcrops located on the ridgecrest. If the weather is clear, the ridgeline provides a nearly full panorama of the region with views overlooking all rocktypes of the Josephine marginal basin. It also provides a vantage point from which to view regional scale Nevadan structures (Figure 17).

Hike up to the ridgeline along a contact separating peridotite from metabasalt and chert. This contact is a remobilized mélangé contact in the OCC. Upon reaching the ridgeline join a trail and proceed west, examining the outcrop along the way. The ridgeline exposures provide a striking contrast to the Josephine peridotite (STOPS 13 and 14). The OCC peridotite is often completely serpentinitized and cut by numerous dikes. Dike lithologies include websterite and gabbro pegmatite, plagiogranite, diabase, aphanitic basalt, and acicular hornblende-phyric diorite. Some dikes are bordered by antigorite, a high-temperature serpentine. Clinopyroxene crystals in the websterite and gabbro dikes reach 50 cm in length but are now largely replaced by fibrous amphibole (uralite). Generally the dikes are rarely continuous for more than 10 meters occurring as boudins in sheared serpentinite. In addition, dike orientations are random, reflecting a multi-phase history of intrusion and folding.

Two plagiogranite dikes collected here yielded concordant U-Pb zircon ages of 175 Ma and place a minimum age on the OCC peridotite. These dikes are essentially unaltered, suggesting that serpentinitization of the OCC ultramafic rocks occurred prior to dike emplacement. This suggests that the OCC is at least Early Jurassic in age, consistent with well documented Triassic to Early Jurassic age of the RCT in the southern Klamath Mountains (Irwin et al., 1982; Wright and Wyld, 1994). Leave the trail where it bends north toward Whetstone Butte and continue to hike west toward a small peak located at the west end of the ridge. Hike to the top of the peak, crossing a nonconformity between OCC peridotite and volcanogenic turbidites of the Rogue Formation. The Rogue turbidites strike parallel to the contact and dip 45°-50° to the NNE, beneath the OCC peridotite. The west face of the hill has excellent exposures of partial Bouma sequence beds which indicate the strata are overturned. To the west of this locality, upright layers overlie the OCC peridotite, thus defining a tight, overturned syncline. The Rogue Formation/OCC nonconformity thus represents the depositional onlap of distal arc volcanogenic turbidites upon a fragment of the remnant arc basement, the RCT. This contact can be traced for over 50 km to the northeast, parallel to the regional strike of the belt (Figure 17). In places it is clear that the contact is faulted along a moderately SE-dipping structure. However, where studied, bedding in the footwall always intersects the fault at < 30°, consistent with a west-vergent, fault propagation fold geometry. The Rogue/OCC contact is therefore interpreted as a sometimes faulted-modified, depositional contact.

- Day 3
Step 3b
- 0.5 (49.3) Return to fork in the road and turn left (east).
- 0.4 (49.7) **Optional STOP E.** Bedded red chert at this locality has yielded Late Triassic conodonts (Roure and DeWever, 1983) and possible Late Triassic and Early Jurassic radiolaria (Yule et al., 1992; M. Silk, unpublished data).
- 15.7 (65.4) Return to U.S. Hwy 199. Turn left (north).
- 7.7 (73.1) Turn left (west) on Swede Basin Road, USFS Road 25.
- 1.9 (75.0) Roadcut exposures and grassy slopes are underlain by sheared serpentinite of the Illinois River Valley Fault. Shear foliations in the serpentinite are subvertical. Slaty argillite and siltstone of the Galice Formation occurs on both sides of the fault. The road switches back across the fault 0.6-0.7 miles farther up the road.
- 3.0 (78.0) Galice contact with deformed volcanic rocks and Josephine peridotite.
- 0.4 (78.4) Josephine ophiolite mafic dikes, massive and cumulate textured gabbro.
- 0.5 (78.9) Sheared contact between serpentinitized peridotite (RCT or Josephine?) and crustal rocks. Slivers of cumulate textured gabbro occur along the shear zone.
- 0.8 (79.7) Fault contact with the Onion Camp complex.
- 1.0 (80.7) At Four Corners, turn left onto Spaulding Mill Road, USFS Road 2524. The saddle at Four Corners marks the faulted limb of the regional fault propagation fold described at STOP 17.
- 0.9 (81.6) Bear left at fork, USFS Road 015.
- 0.1 (81.7) Fault contact between serpentinite of the OCC and Galice Formation metasedimentary strata.
- 1.2 (82.9) **STOP 18.** This STOP will examine exposures of the complexly folded, composite amphibolite/serpentinite belt of the OCC. Park opposite a steep roadcut exposing amphibolite gneiss and hornblende schist.
- Amphibolitic rocks of the OCC consist of distinctly foliated rocks with subordinate massive metagabbro and metadiabase. Field, petrographic, and age relations indicate that these rocks are the higher grade equivalents of the greenschist grade OCC crustal rocks.
- The typical amphibolite consists of hornblende and plagioclase with subordinate epidote, titanite, and opaque oxides (mostly ilmenite). Retrograde alteration is common and consists of the following vein and static alteration minerals: chlorite, epidote, clinozoisite, prehnite, green amphibole, white mica, and quartz (sausserite). Hornblende usually comprises 60% to 80% of the rock. Plagioclase is untwinned and ranges from albite to intermediate oligoclase. Impure quartzite (metachert) accounts for <5% of the amphibolitic rocks in outcrop, and consists of 60%-90% quartz with secondary cummingtonite, almandine, biotite, white mica, and opaque oxides.
- Texturally the amphibolitic rocks are massive or foliated. Coarser-grained varieties are gneissose and display a faint intersection lineation, while the finer-grained varieties are schistose with a well-developed intersection lineation. Alternating plagioclase-rich and hornblende-rich layers, generally <3 millimeters thick, define the gneissic layering. The deformed amphibolitic rocks display at least two styles of folding. Folds deform the

gneissic banding and include syn-metamorphic, tight to isoclinal folds with highly attenuated limbs, and post-metamorphic open, similar folds (Figure 18e).

Brown amphibole from this outcrop yielded $^{40}\text{Ar}/^{39}\text{Ar}$ plateau cooling ages of 169.6 ± 0.7 Ma; another amphibolite gneiss collected 2 km to the south yielded a slightly older hornblende age $^{40}\text{Ar}/^{39}\text{Ar}$ plateau cooling of 173 ± 0.6 Ma (Hacker et al., 1995). These data place a minimum age on the amphibolite facies metamorphism of these rocks, presumed correlative with the intraoceanic thrusting which was ongoing during this time (Cannat and Boudier, 1985; Wright and Fahan, 1988).

The amphibolite/peridotite boundary is poorly exposed at this STOP. However, outcrops nearby show that foliations and lineations in both units are parallel, similar to the relationship seen at STOP 9. The difference here is that the units occur as an intact belt rather than a block in a *mélange*. However, the similar age of the amphibolite and the nature of the amphibolite/peridotite boundary suggests that the OCC and Preston Peak amphibolite bodies may be correlative.

2.2 (85.1) Return to Four Corners. Turn left (north) on Swede Basin Road, USFS Road 25.

4.5 (89.6) Turn left (west) at intersection and continue on Swede Basin Road.

2.5 (92.1) Fault contact between the OCC and Rogue Formation (refer to text for STOP 17).

5.2 (97.3) Junction of Swede Basin Road with USFS Road 2512, turn left (west). Sam Brown Campground is on the left.

0.7 (98.0) Cross a fault separating the Rogue Formation and the Briggs Creek amphibolite. This fault, informally named the Chetco Pass fault, separates a high grade metamorphic-plutonic terrane to the west, rocks of the Illinois River plutonic complex (IRPC) and its wall rocks, e.g., the Briggs Creek amphibolite (BCA), from low grade metamorphic rocks to the east, rocks of the Rogue Formation.

1.4 (99.4) **STOP 19.** Road metal quarry with exposures of the Briggs Creek amphibolite (BCA) body. Lithologies exposed here include amphibolite gneiss, hornblende schist, and subordinate impure quartzite. Foliations strike NE-SW and dip variably to the NW and SE, and are folded about shallowly plunging, NE and SW trending syn- and post-metamorphic folds. Mineral elongation and intersection lineations trend parallel to the fold axes. Structures here and throughout the body are uniform (Figure 16e), and suggest that the unit was deformed by WNW-ESE directed compression and/or NNE/SSW directed extension.

Coleman and Lanphere (1988) argue that the BCA represents metamorphosed Josephine ophiolite crust. However, the lithologic and geochemical evidence suggest that the protolith materials consisted, at least in part, of OCC (RCT) rocktypes. Mineralogically, these units are very similar to the OCC amphibolites (STOP 18). Their geochemical signatures exhibit MORB and WPB trends (Coleman and Lanphere, 1991), similar to those of the OCC metabasalts.

$^{40}\text{Ar}/^{39}\text{Ar}$ hornblende cooling ages range from 156-158 Ma (Hacker et al., 1995; Hacker and Ernst, 1993). These ages overlap with, and are slightly older than the $^{40}\text{Ar}/^{39}\text{Ar}$ hornblende ages obtained from the Illinois River plutonic complex (IRPC, STOP 20). These age data combined with field and structural data from the Illinois River plutonic complex (see below) indicate that the BCA was deformed and metamorphosed in a wide dynamothermal aureole surrounding the intrusive complex.

0-4.5 (103.9) The road crosses the BCA/Chrome Ridge peridotite (CRP) contact several times in the 1.8 miles from STOP 19. From 1.8-4.5 miles, the road passes through relatively unaltered harzburgite and dunite tectonite of the CRP body, a probable northern equivalent of the Josephine peridotite mass. 4.5 miles from STOP 19 the road crosses the boundary between the IRPC and the CRP.

2.2 (106.1) **STOP 20.** Park where convenient and examine the roadcut exposure of a tonalite-granodiorite dike cutting the norite/olivine gabbro. The IRPC is identical and similar in composition to the Grayback pluton (STOP 5). The tonalite unit has yielded concordant to slightly discordant U-Pb zircon apparent ages of 157 ± 1 Ma from several localities along the Illinois River. Hornblende diorite and biotite-hornblende quartz diorite associated with the gabbro/norite unit yield concordant 160 Ma U-Pb zircon apparent ages. Hornblende cooling ages obtained from the margin of the pluton and from dikes intruding the wallrocks yield $^{40}\text{Ar}/^{39}\text{Ar}$ plateaus at 155-156 Ma, in general agreement with Dick (1976) and Hotz (1971).

This outcrop is part of a mafic to intermediate plutonic complex, referred to here informally as the Illinois River plutonic complex (IRPC). Previous workers named these rocks the Illinois River gabbro (Jorgenson, 1970) and the Illinois River batholith (Garcia, 1979; 1982). This distinction is made because the plutonic complex neither consists entirely of gabbro nor contains multiple plutonic bodies as the term batholith implies. Hotz (1971) included these rocks in the Chetco complex, a unit including plutonic rocks, metagabbro, amphibolite schist, gneiss, and metaperidotite. However, this designation is abandoned here to emphasize the distinction between the IRPC and its wallrocks, such as the BCA, CRP, and Rum Creek metagabbro (Hotz, 1971).

The IRPC is reversely zoned with massive norite, hornblende gabbro and diorite, and sparse biotite-hornblende quartz diorite surrounding a core region consisting of coarsely crystalline, layered troctolite, norite, and hornblende gabbro. Except for a late stage hornblende pegmatoid sill at the south end of the intrusion, rocks of the IRPC have been recrystallized to some degree. The most common recrystallization textures are granoblastic textures with sub-grain development, undulose extinction, and bent twinning lamellae. The original igneous textures, indicated by relict and pseudomorph features, were cumulate in the core and xenomorphic- to hypidiomorphic-granular at the margin of the complex. Compositional layering in the core rocks is defined by varying proportions and sizes of mafic and felsic minerals. Cumulus phases were ortho- and clinopyroxene, olivine, spinel, and anorthite with post-cumulus overgrowth by clinopyroxene, hornblende, and labradorite. Kelpyitic rims are common surrounding spinel and olivine. Normally zoned plagioclase is rare in the cumulus rocks, but common in the marginal gabbros and diorites with typical cores of An₇₀₋₉₅ and rims of An₅₀₋₇₅. Approximate modal mineralogies are shown in Table 2.

The rocks of the plutonic complex are relatively unstrained at the core with ductile strain increasing progressively toward the margins. Typically, rocks at the margin are L>>S tectonites and exhibit a variable foliation orientation with a consistent moderate to shallow, NE-SW trending elongation lineation. The general structure of the IRPC is that of an asymmetric dome, gently plunging to the NNE and SSW and steeply plunging to the WNW and ESE. Linear features of the plutonic complex are thus parallel to structures in the wallrocks (e.g., the BCA, STOP 19, Figure 16e) illustrating the pre- to syn-deformational emplacement of the IRPC.

END OF DAY AND END OF TRIP.

References

- Alexander, R.J. and Harper, G.D., 1992, The Josephine ophiolite, an ancient analog for oceanic lithosphere formed at intermediate-spreading ridges, in *Ophiolites and Their Modern Oceanic Analogues*, edited by B. Parsons and P. Browning, pp. 3-38, Blackwell Scientific Publ., Oxford.
- Alexander, R.J., Harper, G.D., and Bowman, J.R., 1993, Oceanic faulting and fault-controlled subseafloor hydrothermal alteration in the sheeted dike complex of the Josephine ophiolite, *Jour. Geophys. Res.*, v.98, p. 9731-9759.
- Barnes, C.G., Petersen, S.W., Kistler, R.W., Prestvik, T., and Sundvoll, B., 1992, Tectonic implications of isotopic variation among Jurassic and Early Cretaceous plutons, Klamath Mountains, *Geol. Soc. Amer. Bull.*, v.104, 117-126.
- Barnes, C.G., Donato, M.M., and Tomlinson, S.L., 1993, Correlation of the Applegate Group in the Oregon Klamath Mountains with terranes of the western Paleozoic and Triassic belt in California: *Geol. Soc. Am. Abstr. with Prog.*, v. 25, p. 6.
- Barnes C.G., K. Johnson, M.A. Barnes, T. Prestvik, R.W. Kistler, and B. Sundvoll, 1995, The Grayback pluton: Magmatism in a Jurassic back-arc environment, Klamath Mountains, Oregon, *J. Petrology*, 36, 397-416.
- Blake M.C., Jr., D.G. Howell, and D.L. Jones, 1982, Preliminary tectonostratigraphic terrane map of California, *U.S. Geol. Surv. Open File Rep.* 82-593.
- Blake, M.C., Jr., D.C. Engebretson, A.S. Jayko, and D. L. Jones, 1985, Tectonostratigraphic terranes in southwest Oregon, in: *Tectonostratigraphic Terranes of the Circum-Pacific Region*, Earth Sci. Ser., edited by D.G. Howell, pp. 147-157, Circum-Pacific Council for Energy and Mineral Resources, Houston, Texas.
- Burchfiel, B.C., and Davis, G.A., 1981, Triassic and Jurassic tectonic evolution of the Klamath Mountains-Sierra Nevada geologic terrane, in Ernst, W.G., ed., *The geotectonic development of California (Rubey Volume 1)*: Englewood Cliffs, New Jersey, Prentice-Hall, p. 50-70.
- Cannat, M., and Boudier, F., 1985, Structural study of intra-oceanic thrusting in the Klamath Mountains, northern California: implications on accretionary geometry: *Tectonics*, v. 4, p. 435-452.
- Cashman, S.M., 1988, Finite-strain patterns of Nevadan deformation, western Klamath Mountains, California, *Geology*, v. 16, p.839-843.
- Coleman, R.G., and Lanphere, M.A., 1991, The Briggs Creek amphibolite, Klamath Mountains, Oregon: Its origin and dispersal, *N. Z. J. Geol. Geophys.*, 34, 271-284.
- Coulton, A.J., Harper, G.D., and O'Hanley, D.S., 1995, Oceanic versus emplacement-age serpentinization in the Josephine ophiolite: Implications for the nature of the Moho at intermediate and slow spreading ridges, *Jour. Geophys. Res.*, v. 100, p. 22,245-22,260.
- Davis, G.S., Monger, J.W.H., and Burchfiel, B.C., 1978, Mesozoic construction of the Cordilleran "collage," central British Columbia to central California, in Howell, D.G., and McDougall, K. A., eds., *Mesozoic paleogeography of the western United States, Pacific coast paleogeography symposium 1*: Los Angeles, California, Pacific Section, *Society of Economic Paleontologists and Mineralogists*, p. 1-32.
- Dick, H.J.B., 1976, The origin and emplacement of the Josephine Peridotite of southwestern Oregon, Ph.D. dissertation, Yale University, 409p.

- Donato, M.M., 1987, Evolution of an ophiolitic tectonic melange, Marble Mountains, northern California Klamath Mountains: *Geol. Soc. Am. Bull.*, v. 98, p. 448-464.
- Donato, M.M., Barnes, C.G., and Tomlinson, S.L., 1996, The Enigmatic Applegate group of southwestern Oregon: age, correlation, and tectonic affinity, *Oregon Geology*, in press.
- Garcia, M.O., 1979, Petrology of the Rogue and Galice formations, Klamath Mountains, Oregon: Identification of a Jurassic island-arc sequence, *Jour. Geol.*, **87**, 29-41.
- Garcia, M.O., 1982, Petrology of the Rogue River island-arc complex, southwest Oregon, *Amer. Jour. Sci.*, **282**, 783-807.
- Gorman, C.M., 1985, Geology, geochemistry and geochronology of the Rattlesnake Creek terrane, west-central Klamath Mountains, California, M.S. thesis, Salt Lake City, University of Utah, 111p.
- Gray, G.G., 1985, Structural, geochronologic and depositional history of the western Klamath Mountains, California and Oregon: Implications for the early to middle Mesozoic tectonic evolution of the western North American Cordillera, Ph.D. dissertation, 161 p., Univ. of Texas, Austin.
- Grover, T.W., 1984, Progressive metamorphism west of the Condrey Mountain dome, north-central Klamath Mountains, northern California, M.S. thesis, 129 pp., Univ. of Oregon, Eugene.
- Hacker, B.R., Donato, M.M., Barnes, C.G., McWilliams, M.O., and W.G. Ernst, 1995, Timescales of orogeny: Jurassic construction of the Klamath Mountains, *Tectonics*, v. 14, 677-703.
- Harper, G.D., 1980, The Josephine ophiolite-remains of a late Jurassic marginal basin in northwestern California, *Geology*, **8**, 333-337.
- Harper, G.D., 1982, Evidence for large-scale rotations at spreading centers from the Josephine ophiolite: *Tectonophysics*, v. 82, p. 25-44.
- Harper, G.D., 1983, A depositional contact between the Galice Formation and a Late Jurassic ophiolite in northwestern California and southwestern Oregon: *Oregon Geology*, v. 45, p.3-9.
- Harper, G.D., 1984, The Josephine ophiolite, *Geol. Soc. Amer. Bull.* **95**, 1009-1026.
- Harper, G.D., 1989, Field Guide to the Josephine ophiolite and coeval island arc complex, Oregon-California, in *Geologic Evolution of the Northernmost Coast Ranges and Western Klamath Mountains, California*, K.R. Aalto and G.D. Harper, eds., *28th Geol. Cong. Field Trip Guidebook T308*, p. 2-21, Am. Geophys. Union, Washington, D.C.
- Harper, G.D., and Wright, J.E., 1984, Middle to Late Jurassic tectonic evolution of the Klamath Mountains, California-Oregon, *Tectonics* **3**, 759-772.
- Harper, G.D., Bowman, J.R., and Kuhns, R., 1988, A field, chemical and stable isotope study of subseafloor metamorphism of the Josephine ophiolite, California-Oregon, *J. Geophys. Res.* **93**, 4625-4656.
- Harper, G.D., Saleeby, J.B., and Heizler, M., 1994, Formation and emplacement of the Josephine ophiolite, and the age of the Nevadan orogeny in the Klamath Mountains, California-Oregon: U/Pb zircon and $^{40}\text{Ar}/^{39}\text{Ar}$ geochronology, *J. Geophys. Res.*, **99**, 4293-4321.
- Hawkins, J.W., Evolution of the Lau Basin; insights from ODP Leg 135, *in*, Active margins and marginal basins of the western Pacific, B. Taylor, J. Natland, eds., University of Hawaii, Honolulu, Hawaii, Geophysical Monograph, **88**, p. 125-173.

- Helper, M.A., Deformation and high P/T metamorphism in the central part of the Condrey Mountain window, north-central Klamath Mountains, California and Oregon, *Geol. Soc. Am. Mem.* 164, 125-141, 1986.
- Helper, M.A., N.W. Walker, and D.W. McDowell, 1989, Early Cretaceous metamorphic ages and middle Jurassic U-Pb zircon ages for the Condrey Mountain Schist, Klamath Mountains, NW Calif. and SW Oregon, *Geol. Soc. Am. Abstr. Prog.*, 21, 92.
- Hershey, O.H., 1911, Del Norte County [California] geology: Mining and Scientific Press, v. 102, p. 468.
- Hotz, P.E., 1971a, Geology of lode gold districts in the Klamath Mountains, California and Oregon, *U.S. Geol. Survey Bull.*, 1290, 91p.
- Imlay, R.W., 1980, Jurassic paleobiogeography of the western conterminous United States in its continental setting, *U.S. Geol. Sur. Professional Paper 1062*, 134 p.
- Irwin, W.P., 1994, Geologic map of the Klamath Mountains, California and Oregon, *U.S. Geol. Survey Misc. Field Investigations I-2148*, scale 1:500,000.
- Irwin, W.P., Jones, D.L., and Blome, C.D., 1982, Map showing radiolarian localities in the western Paleozoic and Triassic belt, Klamath Mountains, California, *U.S. Geol. Survey Misc. Field Investigations, MF-1399*.
- Irwin, W.P., 1985, Age and tectonics of plutonic belts in accreted terranes of the Klamath Mountains, California and Oregon, in *Tectonostratigraphic terranes of the circum-Pacific region, Circum-Pacific Council for Energy and Mineral Resources, Earth Science Series*, edited by D.G. Howell, Houston, 187-199.
- Jachens, R.C., Barnes, C.G., and Donato, M.M., 1986, Subsurface configuration of the Orleans fault: implications for deformation in the western Klamath Mountains, California: *Geological Society of America Bulletin*, v. 97, p. 388-395.
- Johnson, K., 1991, Magma mixing and mingling in the Grayback pluton, Klamath Mountains, southwest Oregon, M.S. thesis, Texas Tech University, 122 p.
- Jones, F.R., 1988, Structural geology of the northern Galice Formation, western Klamath Mountains, Oregon and California, M.S. thesis, State University of New York, Albany, 211 p.
- Jorgenson, D.B., 1970, Petrology and Origin of the Illinois River Gabbro, a part of the Josephine Peridotite-Gabbro Complex, Klamath Mountains, Southwestern Oregon, Ph.D., University of California, Santa Barbara, 195 pp. Saleeby, J.B., 1984, U-Pb zircon ages from the Rogue River area, western Jurassic belt, Klamath Mountains, Oregon, *Geol. Soc. Amer. Abstr. with Prog.*, 16, 331.
- Kays, M. A., 1995, Metamorphism in the northern Klamath Mountains, Oregon, *Geol. Soc. of Am. Spec. Paper 299*, p. 173-190.
- Lieberman, J.E., and J.M. Rice, 1986, Petrology of marble and peridotite in the Seiad ultramafic complex, northern California, USA, *J. Metamorphic Geol.*, 4, 179-199.
- Marsaglia, K.M., and R.V. Ingersoll, 1992, Compositional trends in arc-related, deep-marine sand and sandstone: A reassessment of magmatic-arc provenance, *Geol. Soc. Am. Bull.* 104, 1637-1649.
- Miller, M. M., and J. B. Saleeby, 1995, U-Pb geochronology of detrital zircon from Upper Jurassic synorogenic turbidites, Galice Formation, and related rocks, western Klamath Mountains: Correlation and Klamath Mountains provenance, *Jour. of Geophys. Res.*, 100 B9, 18,045-18,058.

- Ohr, M., 1987, Geology, geochemistry and geochronology of the Lems Ridge olistostrome, Klamath Mountains, California, M.S. thesis, SUNY Albany, 278p.
- Nilsen, T.H., 1984, Stratigraphy, sedimentology, and tectonic framework of the Upper Cretaceous Hornbrook Formation, Oregon and California, in Nilsen, T.H., ed., Geology of the Upper Cretaceous Hornbrook Formation, Oregon and California: Los Angeles, California, The Pacific Section, Society of Economic Paleontologists and Mineralogists, v. 42, p. 51-88.
- Norman, E.A.S., 1984, The structure and petrology of the Summit Valley area, Klamath Mountains, California, M.S. thesis, Salt Lake City, University of Utah, 128 p.
- Pessagno, E.A., and Blome, C.D., 1990, Implications of new Jurassic stratigraphic, geochronometric, and paleolatitudinal data from the western Klamath terrane (Smith River and Rogue Valley subterranean), *Geology*, **18**, 665-668.
- Petersen, S.W., 1982, Geology and petrology around Titus ridge, north-central Klamath Mountains, California, M.S. thesis, Eugene, University of Oregon, 73 p.
- Pinto-Auso, M., and Harper, G.D., 1985, Sedimentation, metallogenesis, and tectonic origin of the basal Galice Formation overlying the Josephine ophiolite, Northwestern California, *J. Geol.*, v. 93, p. 713-725.
- Ramp, 1986 Geologic map of the northwest quarter of the Cave Junction quadrangle, Josephine County, Oregon, *Oregon Dept. Of Geol. And Mineral Industries Geol. Map Series GMS-38*, scale 1:24,000.
- Roure, F., and DeWever, P., 1983, Decouverte de radiolarites du Trias dans l'unite occidentale des Klamath, sud-ouest de l'Oregon, U.S.A.: Consequences sur l'age des peridotites de Josephine, *Comptes Rendus de l'Academie des Sciences (Paris)*, **297**, 161-164.
- Saleeby, J.B., Harper, G.D., Snoke, A.W., and Sharp, W.D., 1982, Time relations and structural-stratigraphic patterns in ophiolite accretion, west central Klamath Mountains, California, *J. Geophys. Res.* **87**, 3831-3848.
- Saleeby, J.B., Geary, E.E., Paterson, S.R., and Tobisch, O.T., 1989, Isotopic systematics of Pb/U (zircon), and $^{40}\text{Ar}/^{39}\text{Ar}$ (biotite/hornblende) from rocks of the Central Foothills terrane, Sierra Nevada, California, *Geol. Soc. Am. Bull.*, v. 101, p. 1481-1492.
- Saleeby, J.B. and G.D. Harper, 1993, Tectonic relations between the Galice Formation and the schists of Condrey Mountain, Klamath Mountains, northern California, in *Mesozoic Paleogeography of the Western United States*, vol. II, edited by G. Dunne and K. McDougall, pp.61-80, Society of Economic Paleontologists and Mineralogists, Pacific Section, Los Angeles, California.
- Shanon, P.J., 1933, Geology and ore deposits of the Takilma-Waldo district, Oregon (including the Blue Creek district): U.S. Geological Survey Bulletin 846-B, p. 141-194.
- Snoke, A.W., 1977, A thrust plate of ophiolitic rocks in the Preston Peak area, Klamath Mountains, California, *Geol. Soc. Amer. Bull.*, **88**, 1641-1659.
- Snoke, A.W., and Whitney, S.E., 1979, Relict pyroxenes from the Preston Peak ophiolite, Klamath Mountains, California: *American Mineralogist*, v. 64, p. 865-873.
- Smith, G.M., Harper, G.D., and Sun, S., 1995, Paleomagnetism of the Josephine ophiolite complex: Northwestern California, in review.
- Tobisch, O.T., Paterson, S.R., Saleeby, J.B., and Geary, E.E., 1989, Nature and timing of deformation in the Foothills terrane, central Sierran Nevada, California: Its bearing on orogenesis, *Geol. Soc. Am. Bull.*, v. 101, p. 401-413.

- Tomlinson, S.L., 1993, Tectonostratigraphy of the Bolan Lake area, Klamath Mountains, Oregon, *Unpubl. MS thesis, Texas Tech Univ.*, Lubbock, 84 pp.
- Wells, F.G., Gates, G.O., Grantham, R.M., Hotz, P.E., James, H. L., Kenneth, W.E., Neuman, J.V. Jr., Rynearson, G.A., Smith C.T., Tabor, E.C., and Tate, E.J., 1940, Preliminary geologic map of the Grants Pass quadrangle, Oregon, *Oreg. Dep. Geol. Miner. Ind. Map 5*.
- Wright, J.E., and Fahan, M.R., 1988, An expanded view of Jurassic orogenesis in the western United States Cordillera: Middle Jurassic (pre-Nevadan) regional metamorphism and thrust faulting within an active arc environment, Klamath Mountains, California, *Geol. Soc. Amer. Bull.*, **100**, 859-876.
- Wright, J. E., and S. J. Wyld, 1994, The Rattlesnake Creek terrane, Klamath Mountains, California: an early Mesozoic volcanic arc and its basement of tectonically disrupted oceanic crust, *Geol. Soc. Am. Bull.*, **106**, 1033-1056.
- Wyld, S.J., and Wright, J.E., 1988, The Devils Elbow ophiolite remnant and overlying Galice Formation: New constraints on the Middle to Late Jurassic evolution of the Klamath Mountains, California, *Geol. Soc. Amer. Bull.*, **100**, 29-44.
- Wyld, S.J., and Wright, J.E., 1993, Is the Rattlesnake Creek terrane out of place with respect to other terranes in the Klamath Mountains, CA?, *Geol. Soc. Am. Abstr. with Prog.*, v. 25, p. 169.
- Yule, J.D., Saleeby, J.B., Jones, D.L., and Silk, M., 1992, Correlation of basement terranes across the Late Jurassic Josephine inter-arc basin, southwestern Oregon and northern California, *Geol. Soc. Amer. Abs. with Programs*, **24**, 5, 93.
- Yule, J.D., and Saleeby, J.B., 1993, Highly extended oceanic lithosphere: The basement and wallrocks for the Late Jurassic Rogue-Chetco oceanic arc, Oregon Klamath Mountains, *Geol. Soc. Amer. Abs. with Programs*, v. 25, 169.
- Yule, J.D., Saleeby, J.B., and Barnes, C.G., 1994, Geochemistry of Rattlesnake Creek terrane fragments contained within the western Jurassic belt, Oregon Klamath Mountains, *Geol. Soc. Am. Abstr. with Prog.*, v. 26, p. 106-107.
- Yule, J.D., 1995, Geologic and tectonic evolution of Jurassic marginal ocean basin lithosphere, Oregon Klamath Mountains, Pasadena, California Institute of Technology, Ph.D. thesis, 309 p.
- Yule, J.D., in preparation, Geology of the central Illinois River drainage, Oregon.

LIST OF FIGURES

Figure 1. Generalized geologic map of the Klamath Mountains region showing the primary lithotectonic units of the province (modified from Irwin, 1972). See the text and Table 1 for a description of the rock units which comprise the western Jurassic belt and the western Paleozoic and Triassic belt. (WTrPz).

Figure 2. Generalized tectonostratigraphic terrane map and map explanation of the Oregon-California border region. Boxes outline the general areas of Figures 7, 14, 16, and 17 for DAYS 1, 2, and 3 of the scheduled field trip. Pluton abbreviations include: A=Ashland; BM=Bear Mountain; BK=Buckskin Peak; GB=Grayback; GP=Grants Pass; IR=Illinois River; PP=Pony Peak; RP=Russian Peak; S=Slinkard; SM=Squaw Mountain; SV=Scott Valley; TR=Thompson Ridge; VB=Vesa Bluffs; W=Wimer; and WC=Wooley Creek.

Figure 3. Diagrammatic columnar sections from the Josephine marginal ocean basin.

Figure 4. Generalized cross-section view of the Josephine marginal ocean basin at ~160 Ma (modified after Snoke, 1977; Saleeby et al., 1982; and Harper and Wright, 1984).

Figure 5. Back-arc basin tectonic setting for the Josephine basin at ~160-155 Ma, and subsequent margin perpendicular tectonic collapse of the basin and the Rogue arc beneath the older Klamath terranes at ~157-150 Ma (see text for discussion).

Figure 6. Inter-arc basin tectonic setting for the Josephine basin at ~160-155 Ma, and subsequent highly oblique tectonic collapse of the basin and the Rogue arc beneath the older Klamath terranes at ~157-150 Ma (see text for discussion).

Figure 7. Generalized geologic map of the Applegate Reservoir region, from Donato et al. (1996). STOPS 2-4 are located approximately. STOP 1 is located ~3 km north of the map, due north of Kinney Mountain. STOP 5 is located in the Grayback pluton, just west of the map area.

Figure 8. Ti, Zr, and P₂O₅ compositions of meta-volcanic and metasedimentary rocks from the WJB and TrPz (after Barnes et al. (in review)). Note fields associated with specific tectonic settings in panel E (Pearce & Cann, 1973), where field I is for island-arc tholeiite (IAT), field II is for MORB, IAT, and calc-alkaline basalts, field III is for calc-alkaline basalts, and field IV is for MORB. Note (1) similarity of metabasalts from the RCT mélangé in all parts of the province, (2) similarity of western Hayfork samples from California (labeled "Western Hayfork") with those from Oregon (labeled "Applegate Group"), (3) the arc affinity of the western Hayfork (calc-alkaline) and Rogue and Galice greenstones (calc-alkaline and IAT).

Figure 9. Spidergrams of RCT mélange samples. Note that Rb and Ba show scatter due to hydrothermal exchange during metamorphism. MORB-like patterns are predominant, but ocean-island basalt (OIB) patterns are also present.

Figure 10. Spidergrams of western Hayfork greenstone, volcanic cobbles, and meta-arenite. The prominent Nb anomaly and weaker P and Zr anomalies are consistent with an origin in a calc-alkaline arc.

Figure 11. Sample location map of southern half of the Grayback pluton (from Barnes et al. (1995b)) with symbols keyed to rock type. Note the crude zoning from predominantly norite and gabbro in the east-central area to quartz diorite and tonalite in the western and southern areas. LM is Lake Mountain, GM is Grayback Mountain. SC is the Sucker Creek pluton. Sample 2 is from the STOP 5 locality. Sample 1 is from the OPTION A locality.

Figure 12. AFM diagram for the Grayback pluton (from Barnes et al. (1995b)). The dashed curve divides the tholeiitic from the calc-alkaline compositional fields. Samples enclosed by the short-dashed line are comparable to evolved high-alumina tholeiite. Samples from late-stage hybrid dikes studied by Johnson [1991] are enclosed by long dashes (basalt-tonalite hybrids) and a solid line (basalt-granite hybrids).

Figure 13. $\text{CaO}/\text{Al}_2\text{O}_3$ versus $\text{Mg}/(\text{Mg}+\text{Fe})$ for the Grayback pluton (from Barnes et al. (1995b)). Computed trend for fractional crystallization (fc) shows how granodioritic rocks can be derived from parental basalts. Pyroxenitic and melagabbroic compositions represent cumulates from basaltic magmas (vector 1), whereas gabbros represent cumulates from andesitic magmas. Basaltic magmas parental to the fc trend and the basalt-granite hybrids are very similar in composition. However, basaltic compositions from basalt-tonalite hybrids apparently have higher $\text{CaO}/\text{Al}_2\text{O}_3$. Neither of these basaltic compositions is a logical parent to the evolved high-alumina tholeiite group. Therefore, the Grayback pluton contained two and probably three mafic magma compositions and at least two felsic magma compositions (tonalitic and granodioritic to granitic).

Figure 14. Geologic map of the Knopti Creek Road area and environs, Preston Peak, California-Oregon 15' quadrangle. The general area of STOPS 6-9 is outlined.

Figure 15. Diagrammatic stratigraphic column for the Preston Peak ophiolite. Modified from Saleeby et al. (1982). Revised U-Pb zircon age on quartz dioritic dike from Saleeby and Harper (1993, their table 1, sample 3).

Figure 16. Geologic map and map explanation of the Josephine ophiolite and overlying Galice Formation (Harper, 1984). The ophiolite is broadly folded into an F2 anticline and syncline, and the upper part of the ophiolite is repeated four times due to reverse faulting in the northeastern part of the map area. Numbers refer to field trip stops.

Figure 17. Generalized geologic map of the central Illinois River drainage. The region is tightly folded by shallowly plunging, NE trending F1 and F2 folds (Figure 18). The

TABLE 1 (continued). LITHOLOGIC DESCRIPTION OF ROCK UNITS**Western Jurassic belt****Cover sequence**

Fiddler Mountain olistostrome - Poly lithologic, ophiolite clast megabreccia, breccia, conglomerate, and lithic arenite, interlayered with silicic argillite and Kimmeridgian(?) chert. These deposits probably represent rift-basin deposits of early Josephine age

Rogue Formation - ~157-154 Ma (U-Pb zircon, $^{40}\text{Ar}/^{39}\text{Ar}$ hornblende), interlayered arc volcanogenic rocks including: clinopyroxene-, hornblende-, and plagioclase-phyric lava, lava breccia, tuff, tuff-breccia, lithic arenite (turbidites), and silicic argillite. The unit interfingers with the basal Galice Formation hemipelagic sequences and is overlain by Oxfordian-Kimmeridgian Galice flysch.

Galice Formation - Hemipelagic grading upward into flysch strata of Latest Callovian through Kimmeridgian age. Basal hemipelagic layers overly pillow basalts of the Josephine ophiolite and interfinger with strata of the Rogue Formation and Fiddler Mountain olistostrome.

Composite oceanic crust and mantle rocks, substratum for the cover sequence

Josephine ophiolite - The complete ophiolite sequence is exposed in the Smith River area including pillow lava, sheeted mafic dikes, massive and cumulate gabbro, and mantle peridotite (tectonized harzburgite and dunite). Radiometric ages are 162 ± 1 Ma (U-Pb, zircon) and $165 \text{ Ma} \pm 3 \text{ Ma}$ ($^{40}\text{Ar}/^{39}\text{Ar}$ hornblende).

Onion Camp complex (OCC) - A complexly folded sequence of amphibolite to greenschist facies rocks correlative with the RCT.

Briggs Creek amphibolite (BCA) - Strongly deformed, amphibolite gneiss and schist, plus subordinate impure metaquartzite. Candidate protolith materials probably include both the OCC and the Josephine ophiolite. $^{40}\text{Ar}/^{39}\text{Ar}$ hornblende cooling ages range from 156-158 Ma.

Illinois River plutonic complex (IRPC) - A reversely zoned, mafic to intermediate plutonic complex

interpreted to represent the plutonic root of the Rogue volcanic arc. U-Pb zircon ages range from 160 Ma for the main phase, to 157 Ma for a late-stage tonalite-trondhjemite sill. $^{40}\text{Ar}/^{39}\text{Ar}$ hornblende cooling ages range from 155-156 Ma. Wallrocks of the plutonic complex include the Pearsoll Peak and Chrome Ridge peridotite bodies, the Rum Creek metagabbro, and the BCA.

Table 2 . Approximate range of modal mineral percentages for the primary lithologies of the Illinois River plutonic complex.

<u>Rock type</u>	<u>Quartz</u>	<u>Muscovite</u>	<u>Biotite</u>	<u>Plagioclase</u>	<u>Hornblende</u>	<u>Clinopyroxene</u>	<u>Orthopyroxene</u>	<u>Olivine</u>	<u>Accessory minerals</u>	<u>Secondary minerals</u>
Troctolite (n=4)	0%	0%	0%	55-65% An 95-100	5-27%	0%	<5% En 71	10-20% Fo 72-77	Hercynite	Orthopyroxene Hornblende Serpentine
Norite (n=23)	<5%	0%	0%	45-65% An 77-93	0-25%	<5% to 20% Fs 11-17	<5% to 25% En 58-71	0%	Magnetite	Hornblende
Hornblende gabbro and diorite (n=28)	<10%	0%	0% to <2%	40-75% An 70-95 core An 70-80 rim An 45-60	10-55%, but generally 40-55%	5-40%, but generally <10% Fs 11-17	0%	0%	Magnetite Apatite Zircon	Chlorite Hornblende Epidote
Biotite-hornblende quartz gabbro and diorite (n=12)	10-25%	0%	5-10%	45-60% core An 65-75 rim An 40-60	20-40%	<5%	0%	0%	Magnetite Apatite Zircon	Epidote Sericite Chlorite
Tonalite and trondhjemite (n=10)	25-35%	0-10%	0-15%	45-55% An 30-40	0-15%	0%	0%	0%	Garnet Apatite Zircon	Epidote Sericite Chlorite

Modal percentage values are tabulated from approximate modal estimates made for 25 samples during this study, plus more precise point counting results reported for six samples by Garcia (1982) and for 46 samples by Jorgenson (1970). Mineral compositions are taken from Jorgenson (1970). Anorthite content for plagioclase is given for nonzoned crystals unless otherwise noted.

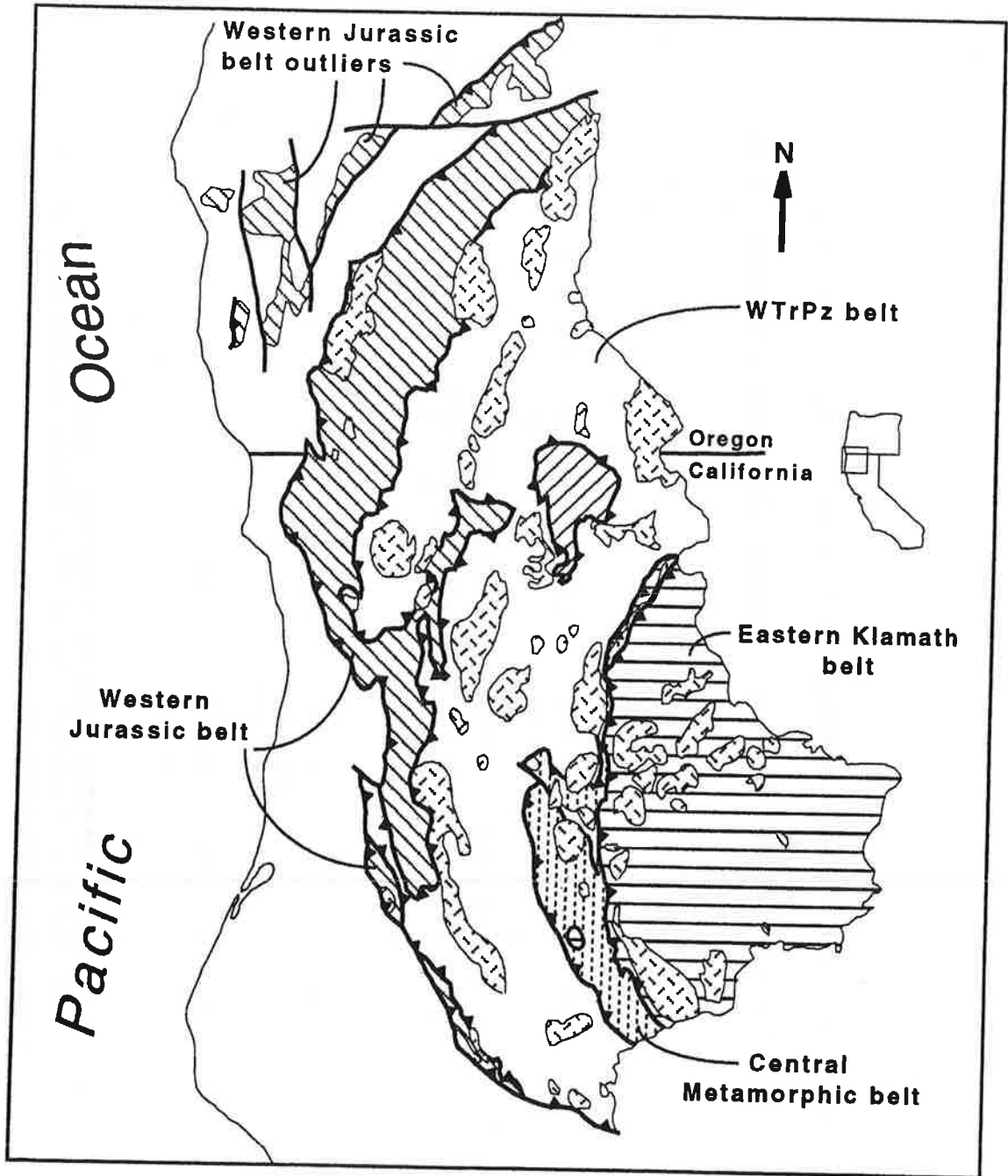


Figure 1

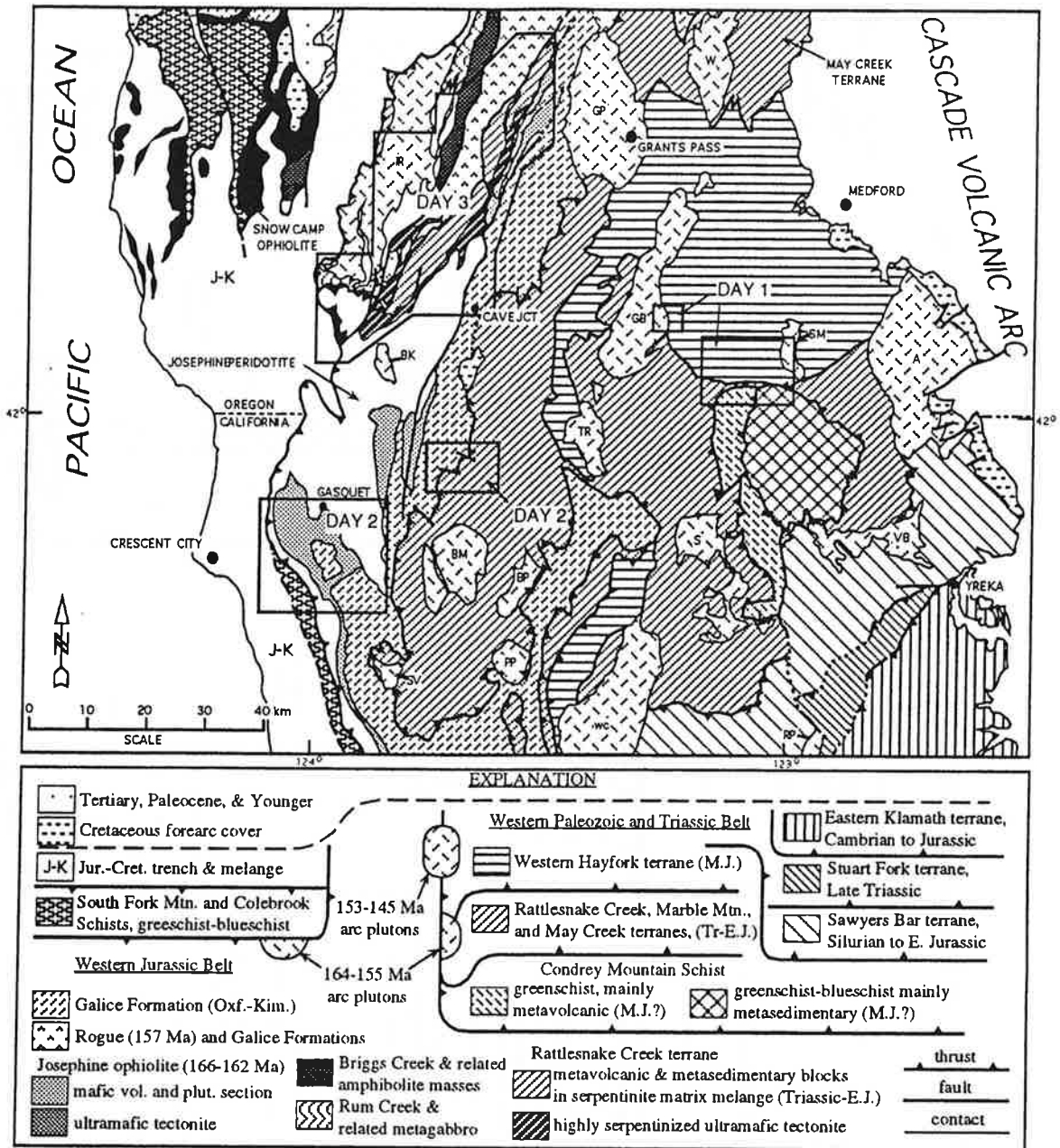


Figure 2

Diagrammatic columnar sections from the Josephine marginal ocean basin

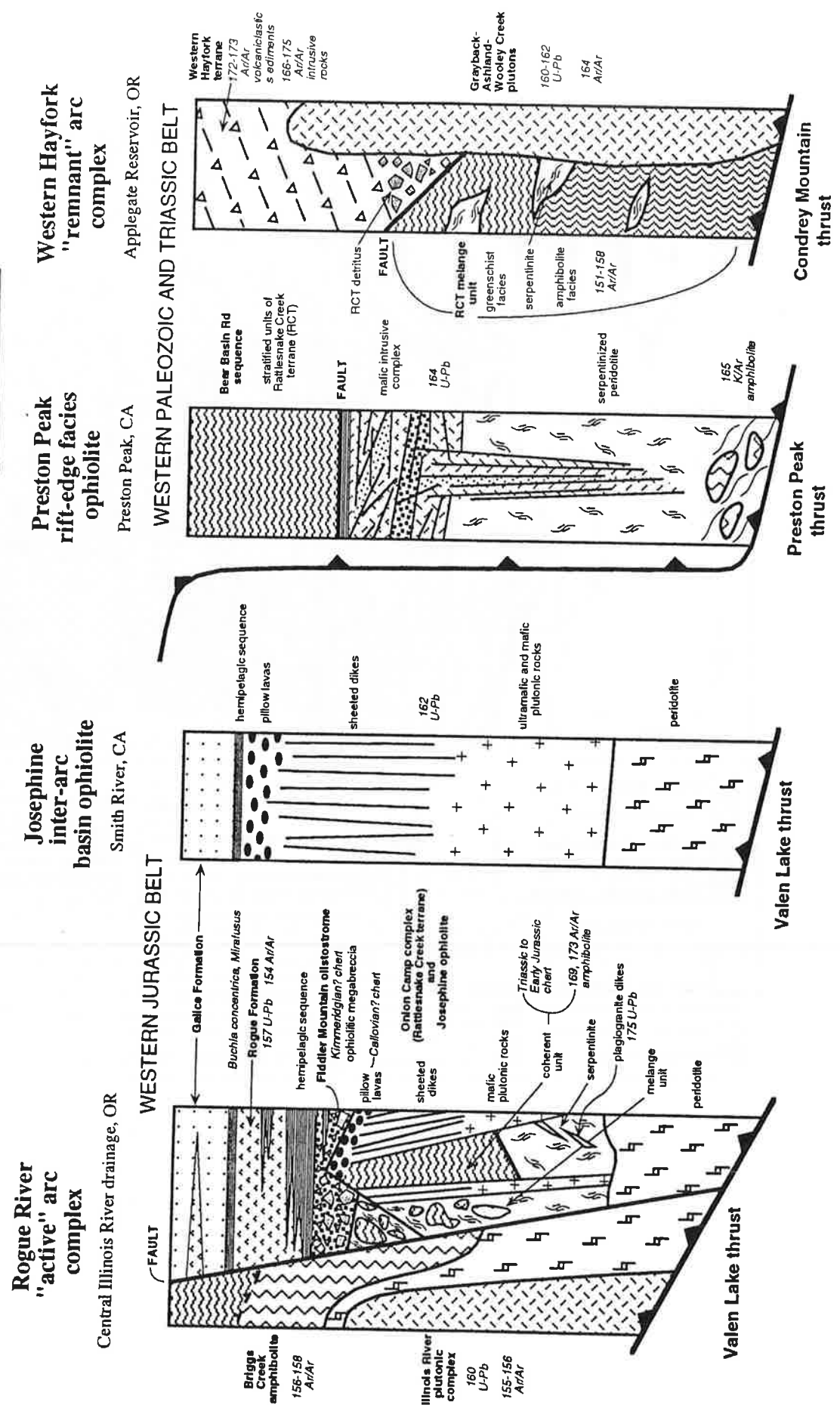


Figure 3

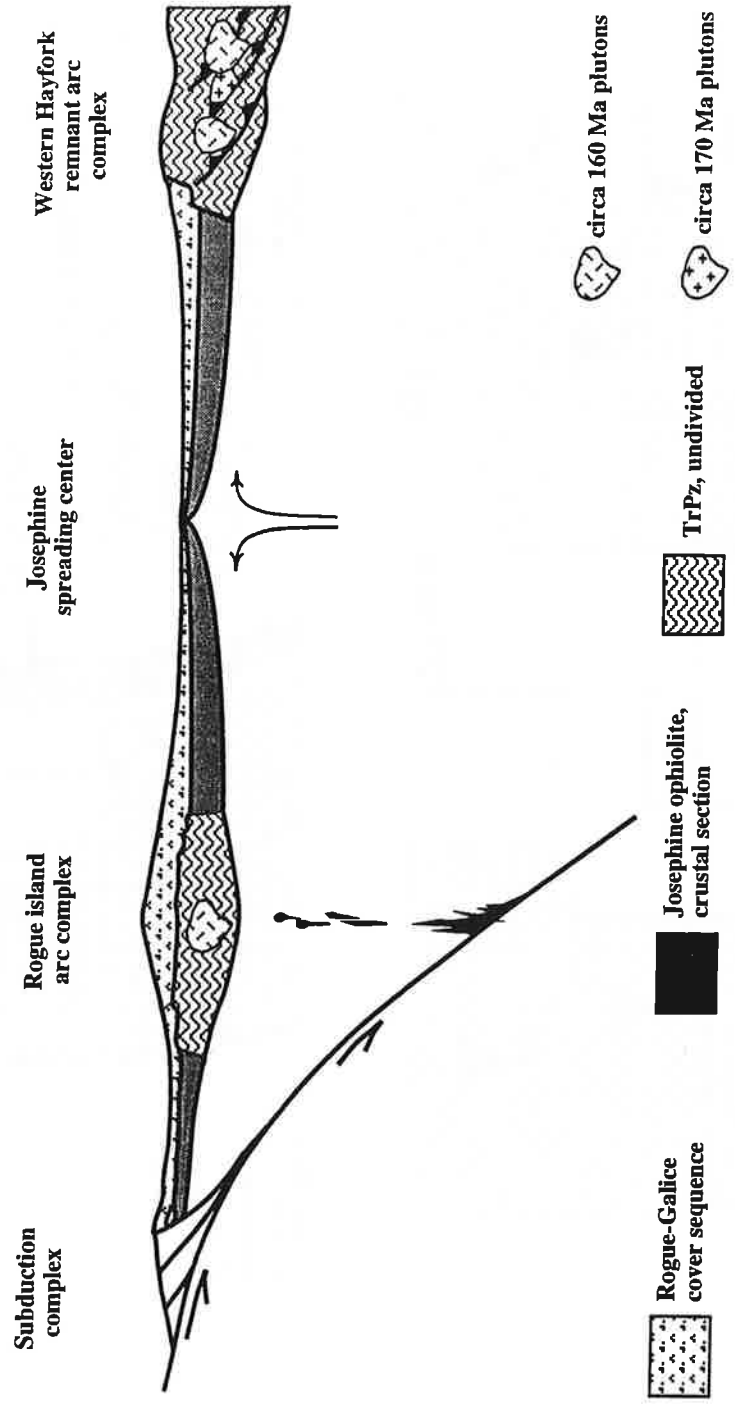


Figure 4

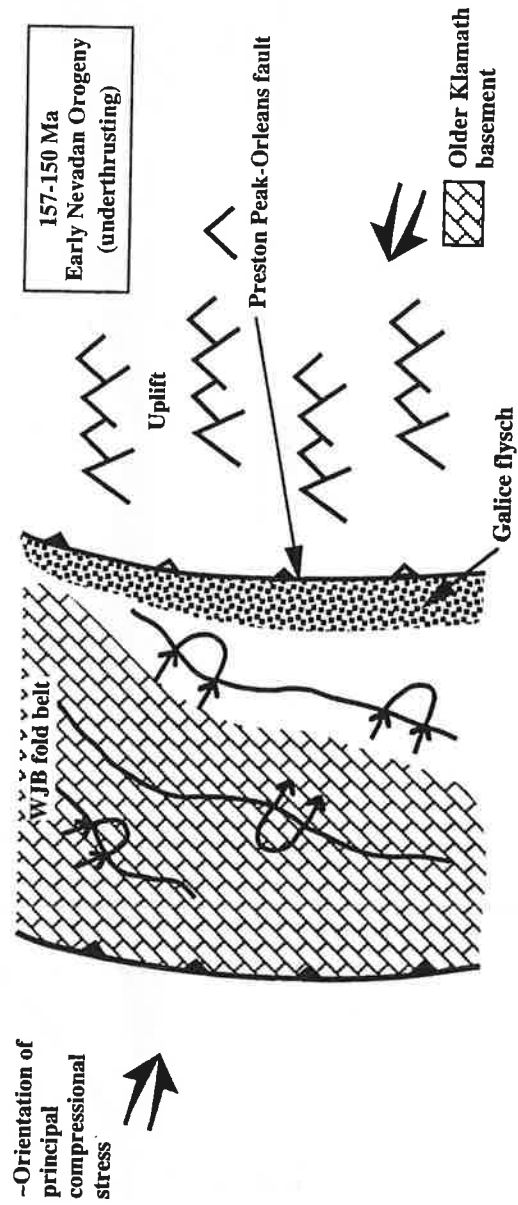
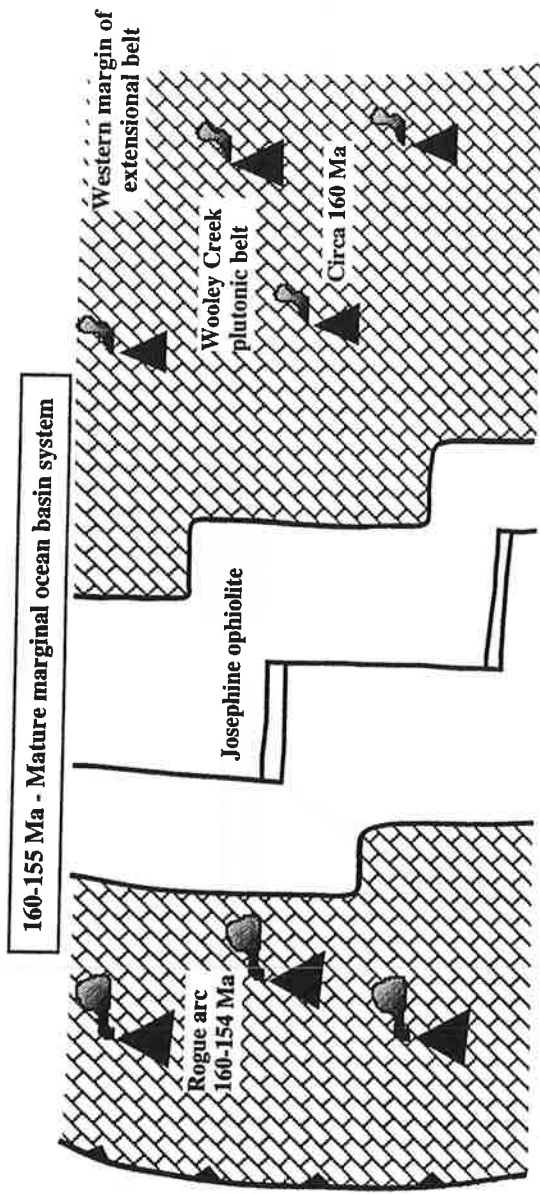


Figure 5

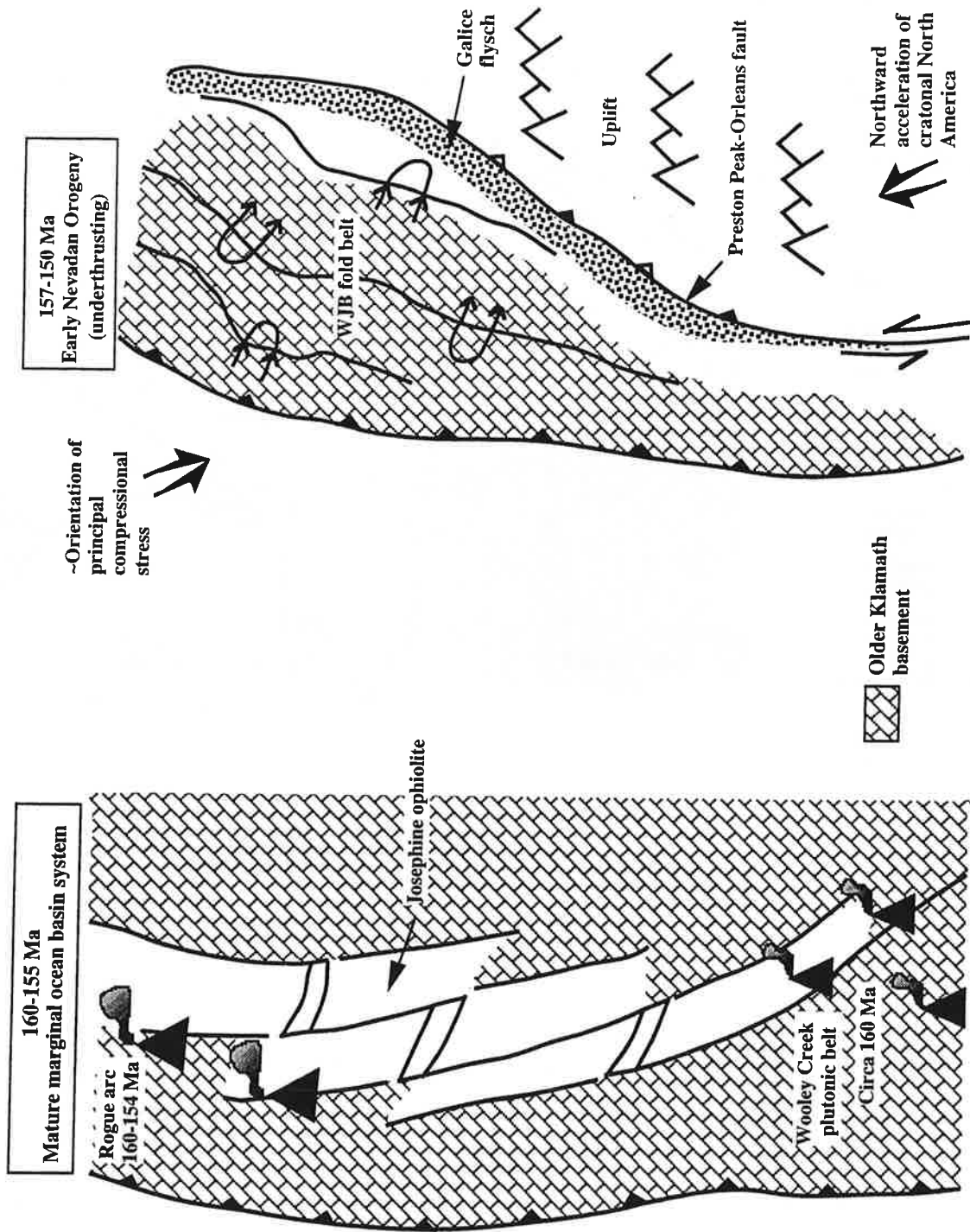



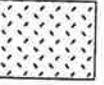
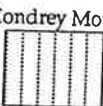

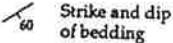
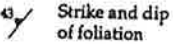
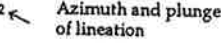



Figure 6

EXPLANATION

-  Western Hayfork terrane
-  Rattlesnake Creek terrane
-  metaserpentinite within Rattlesnake Creek terrane
-  Granitic intrusive rocks
- Condrey Mountain Schist**
-  Amphibole schist
-  Graphitic schist
-  Strike and dip of bedding
-  Strike and dip of foliation
-  Azimuth and plunge of lineation
-  $^{40}\text{Ar}/^{39}\text{Ar}$ sample locality

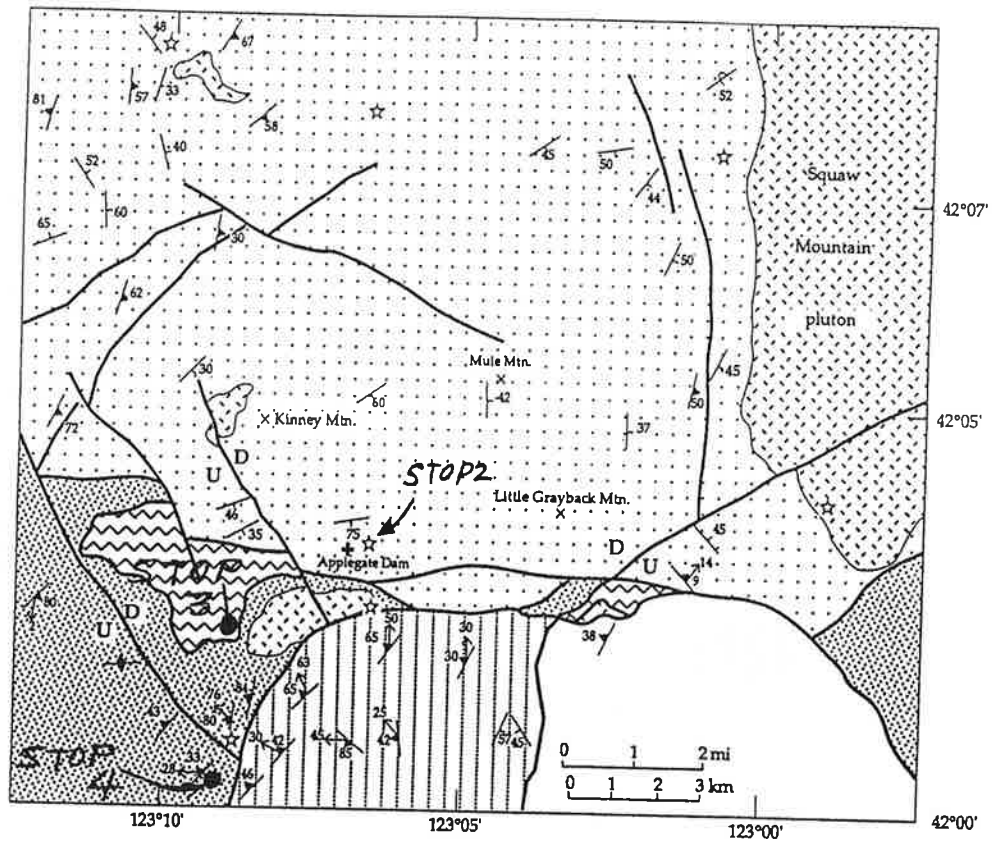


Figure 7

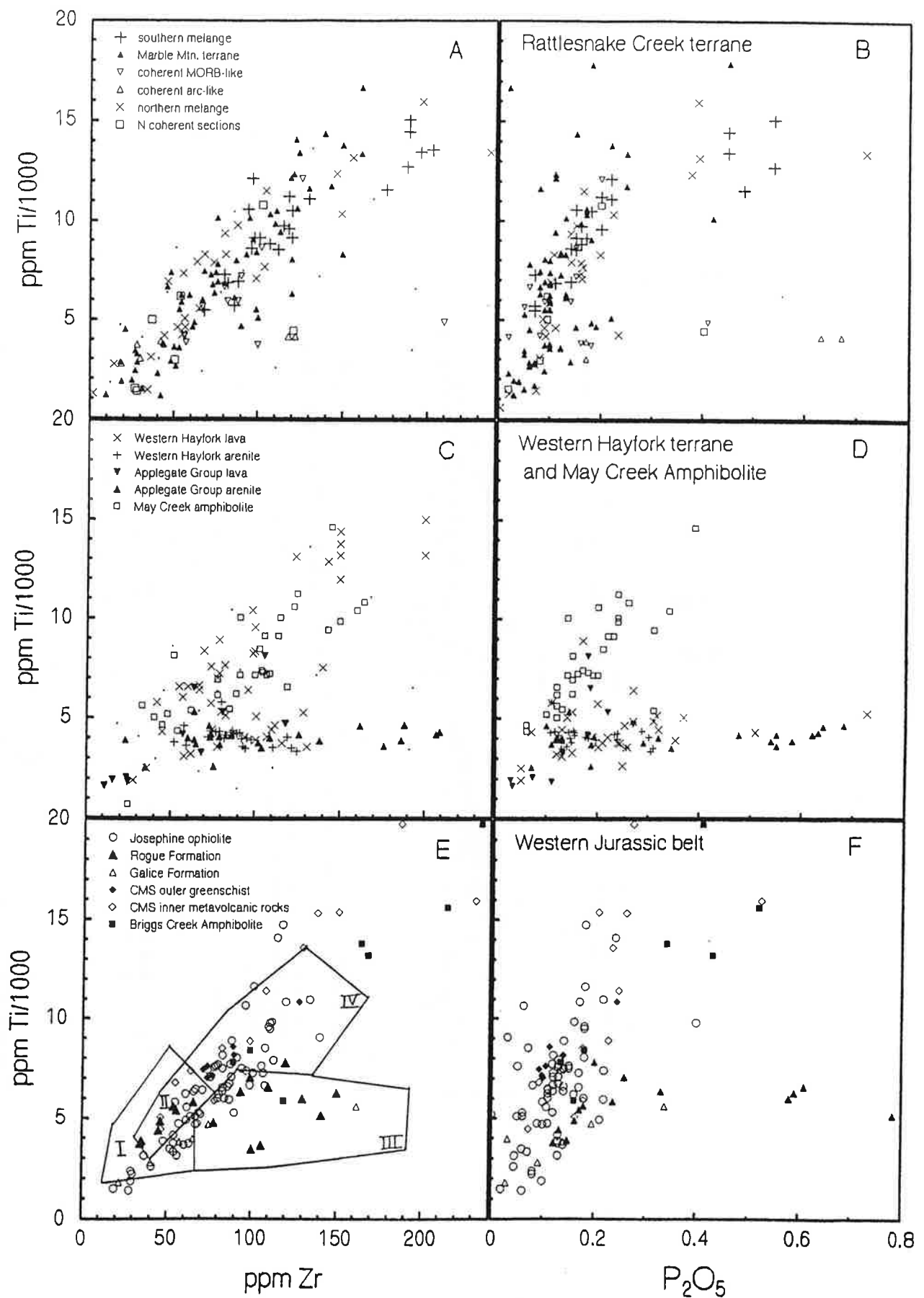


Figure 8

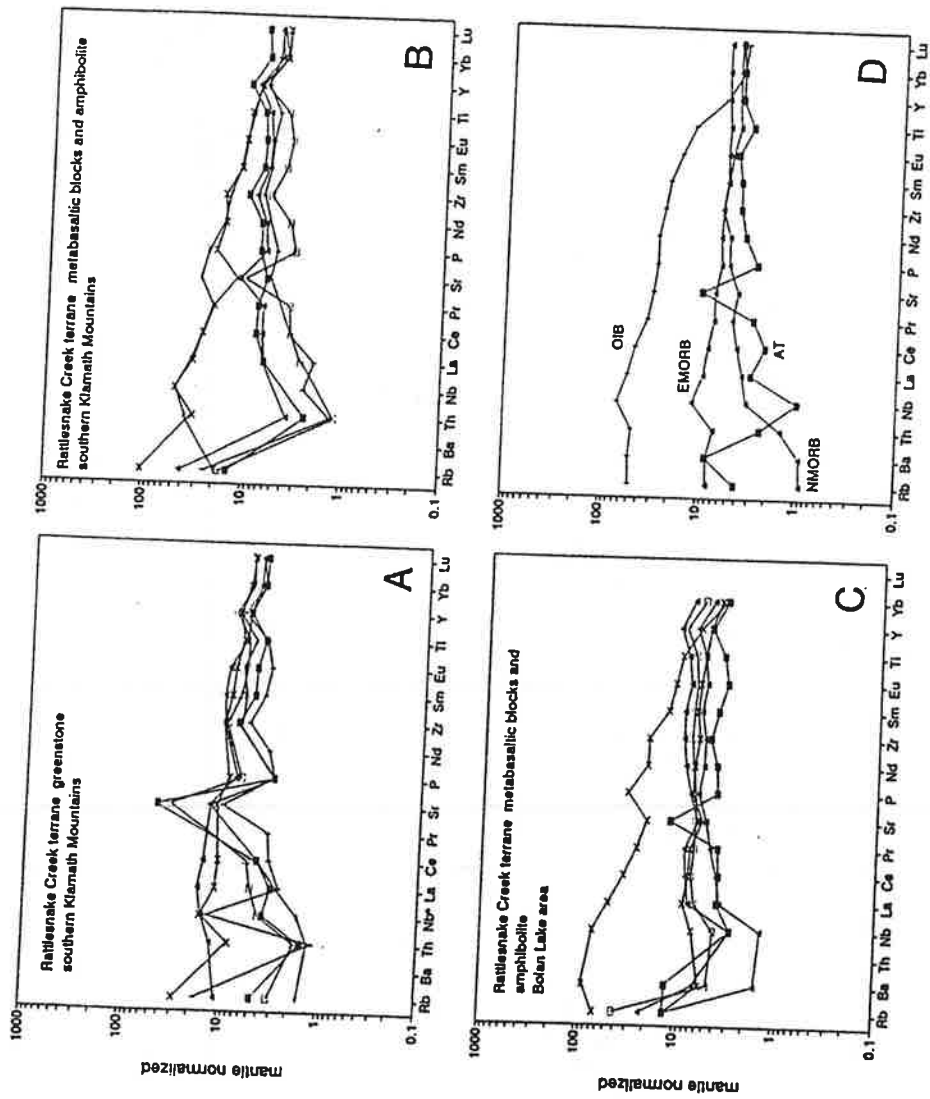


Figure 9

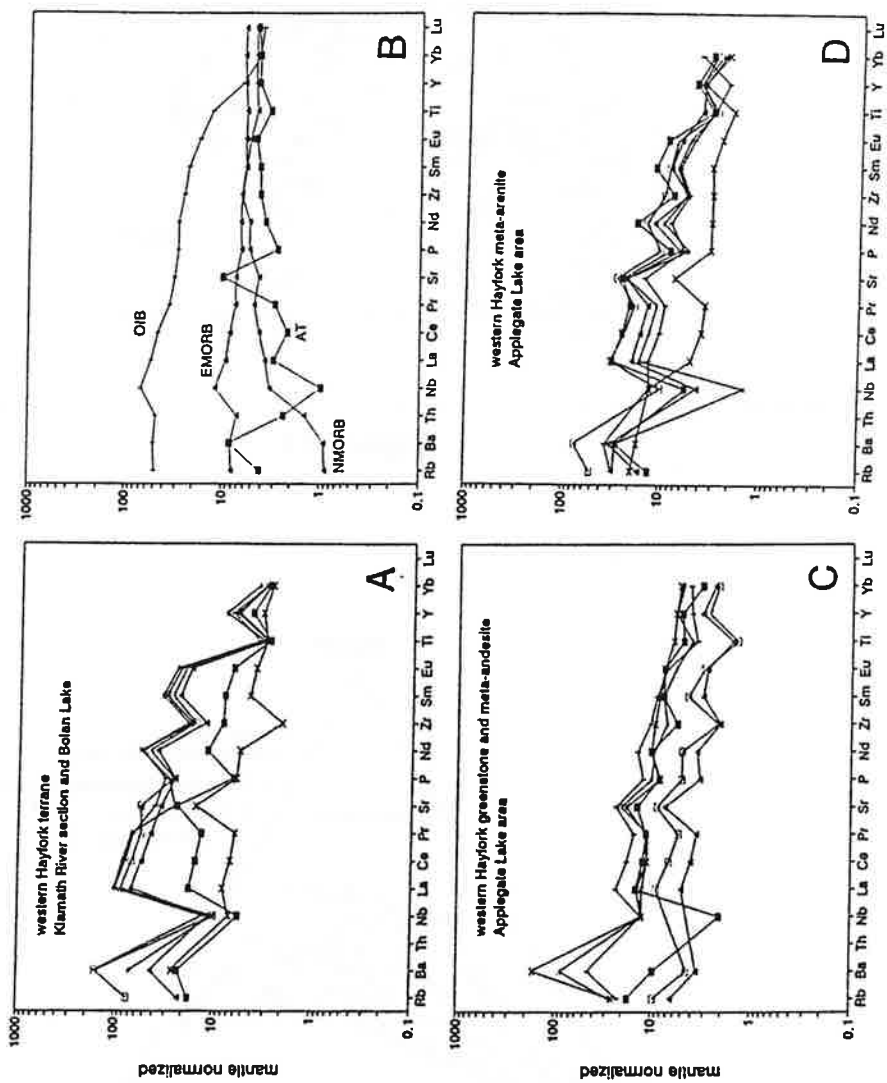


Figure 10

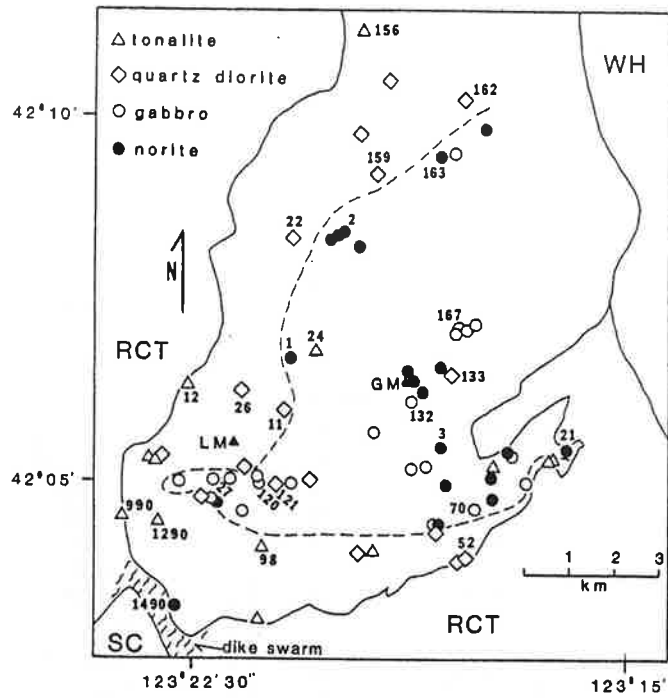


Figure 11

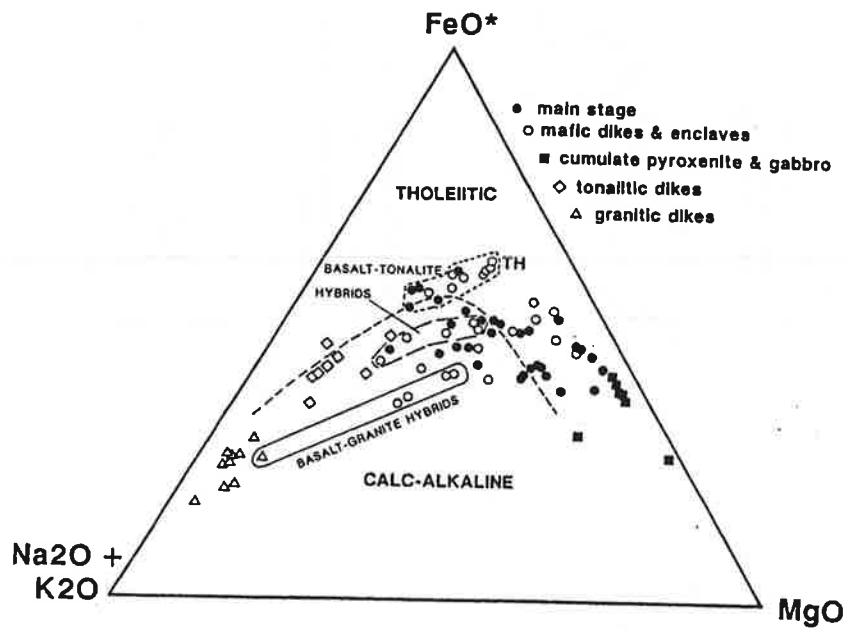


Figure 12

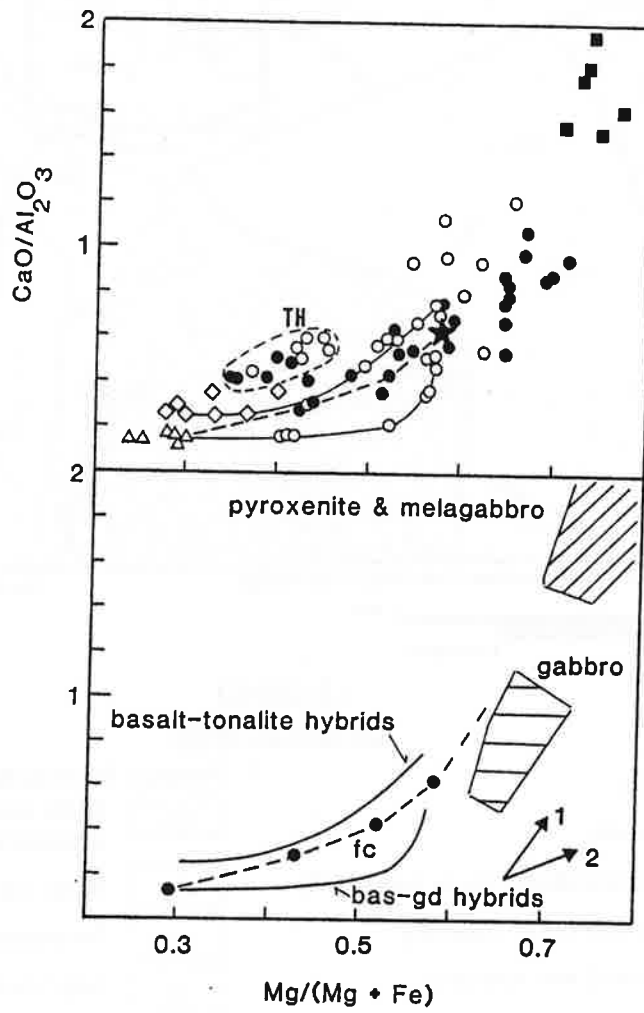
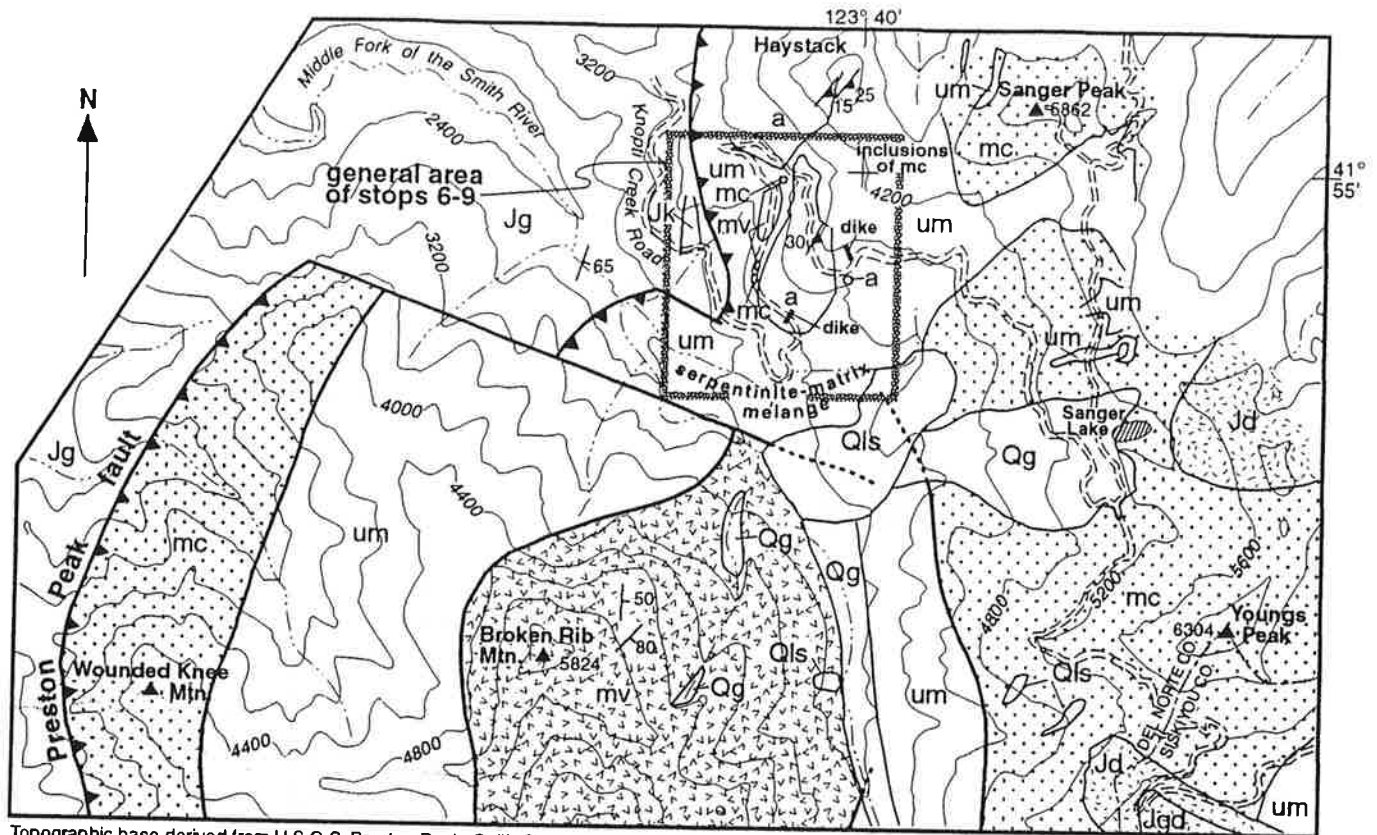
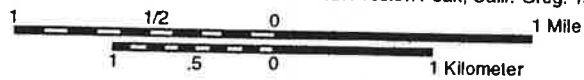


Figure 13



Topographic base derived from U.S.G.S. Preston Peak, Calif.-Oreg. 15' quadrangle

Geologic mapping by A.W. Snoke (1969-71, 74, 79)



LEGEND

Lithologic units

Qg	Glacial deposits	mv	Preston Peak ophiolite of Snoke (1977) Mafic metavolcanic rocks and minor metasedimentary rocks
Qls	Landslide deposits	mc	Mafic complex, chiefly metadiabasic rocks
Jd/Jgd	Diorite and/or granodiorite (Late Jurassic?)	um	Serpentinized ultramafic rocks
Jk	Quartz keratophyre (Late Jurassic)	a	Amphibolite and amphibolitic gneiss
Jg	Galice Formation (Late Jurassic)		

Symbols

\swarrow_{65} Strike and dip of bedding

\swarrow_{15} Strike and dip of foliation

Figure 14

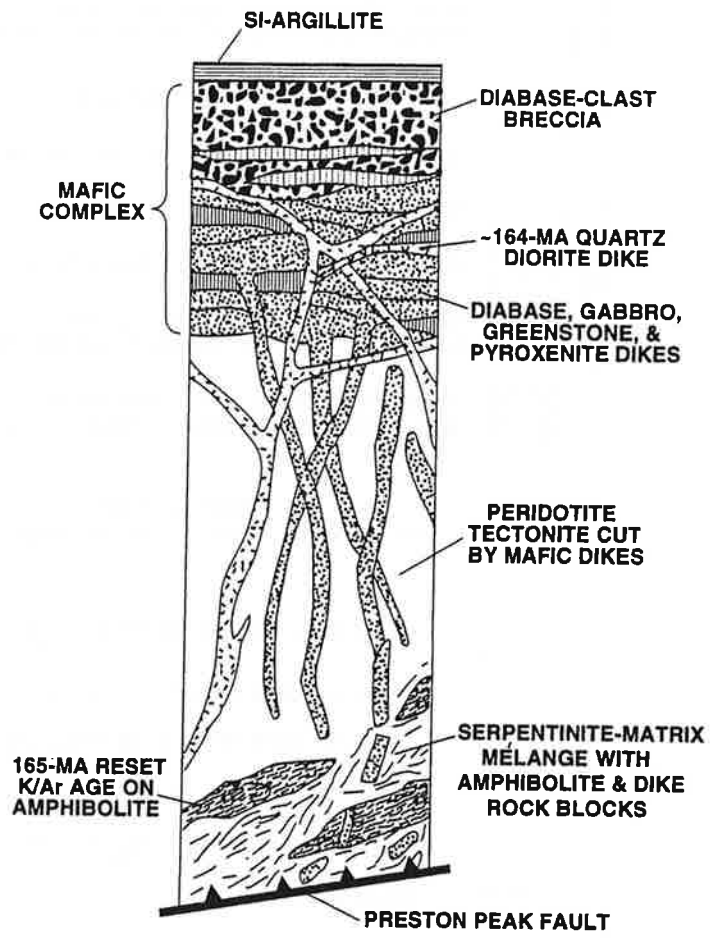


Figure 15

- Quaternary Alluvium
- Late Miocene Fluvial gravel in east, grading westward into marine facies consisting of silt, clay, and diatomite
- Late Jurassic or Cretaceous Foliated slate and metagraywacke of the Franciscan(?) complex.
- Late Jurassic 145 Ma Lower Coon Mountain pluton. Mostly ultramafic rocks with minor gabbro and diorite.
- Late Jurassic Oxnardian-Kimmeridgian Galle Formation. Slate, metagraywacke, and rare conglomerate. Basal unit is radiolarian-bearing slaty argillite (hemipelagic sequence). Conformably overlies Josephine ophiolite.

JOSEPHINE OPHIOLITE

- Pillow basalt and minor massive basalt and breccia
- Sheeted dike complex
- Gabbro, including some ultramafic rock, commonly layered
- Ultramafic cumulates. Mostly wehrlite and clinopyroxenite with some gabbro, dunite, hercynite, and orthopyroxenite.
- Mostly harzburgite with lesser dunite (Josephine Peridotite). Serpentinized and sheared near faults.

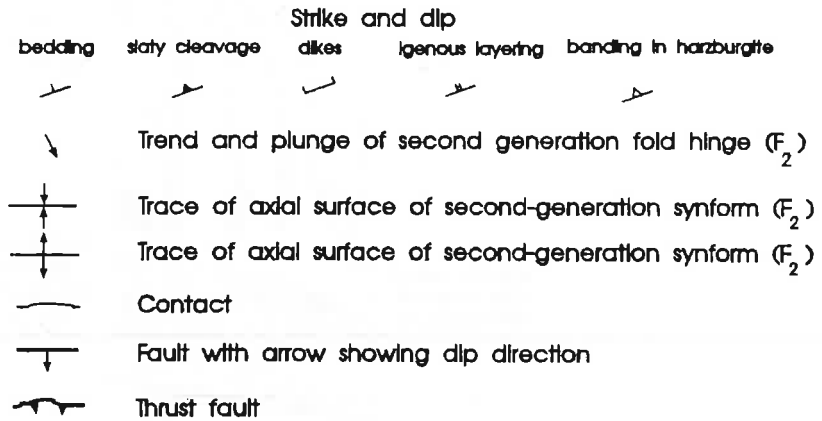


Figure 16

(Explanation)



Figure 16

EXPLANATION

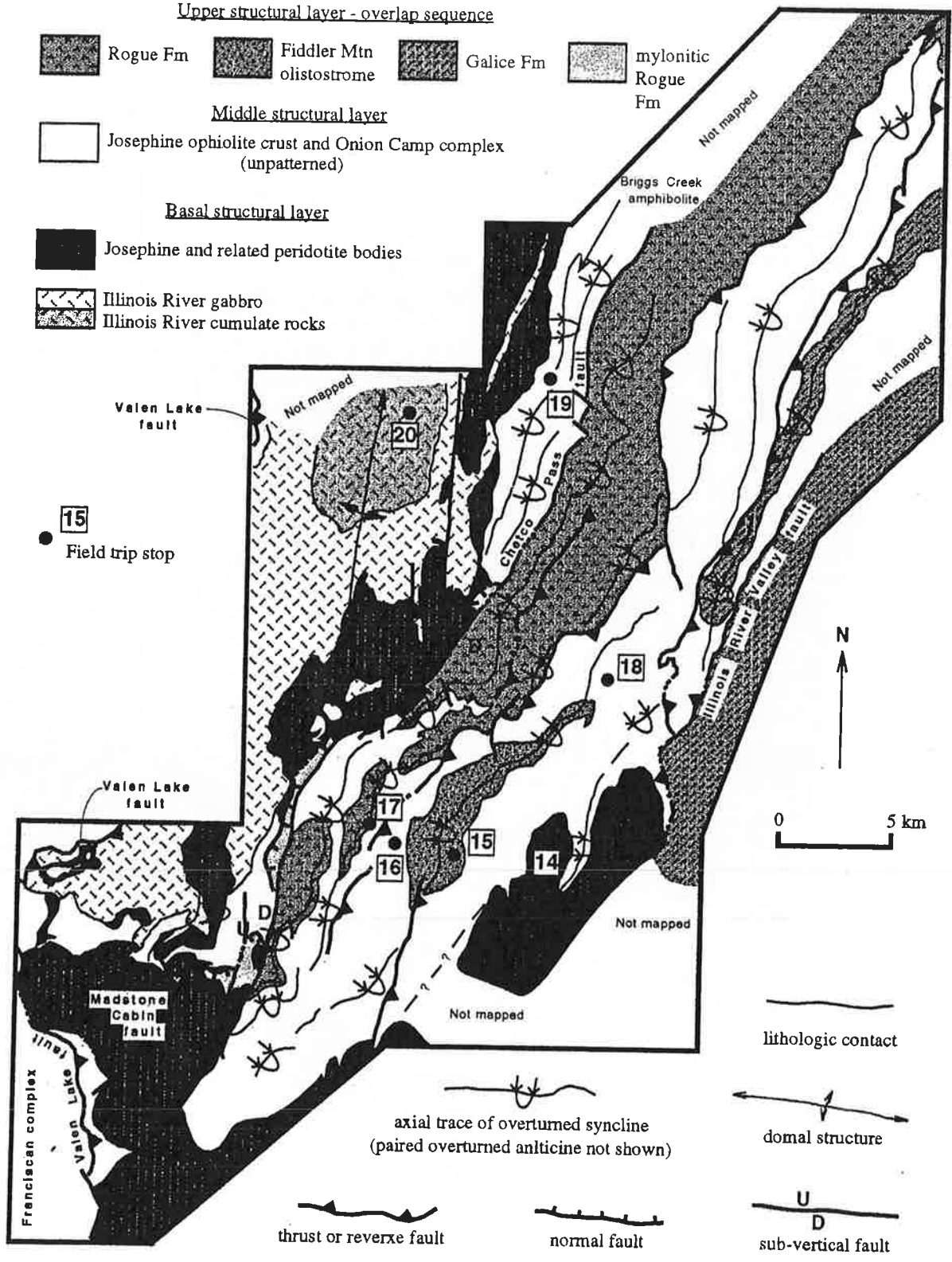


Figure 17

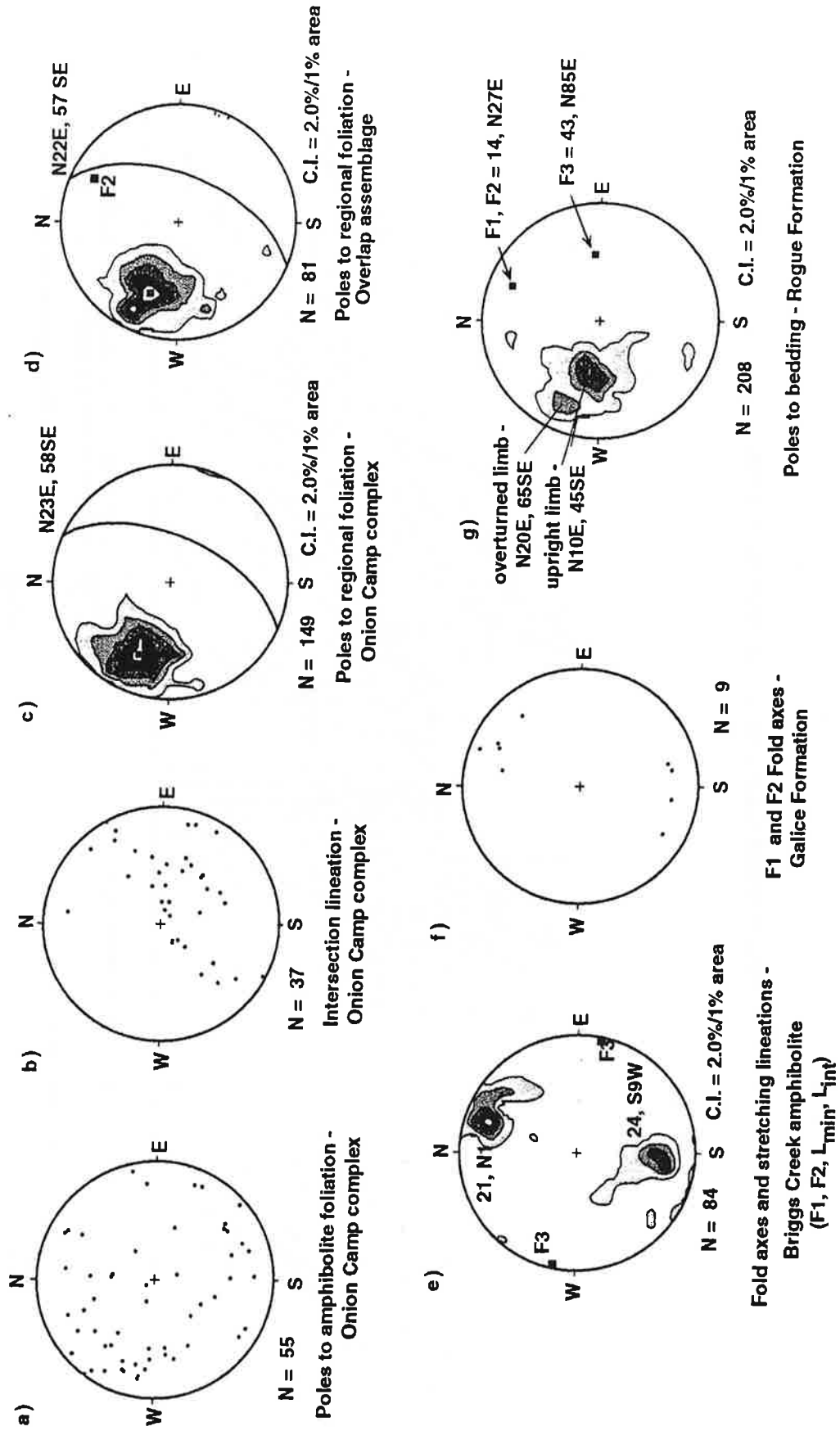


Figure 18

SIMPLIFIED GEOLOGIC CROSS SECTION

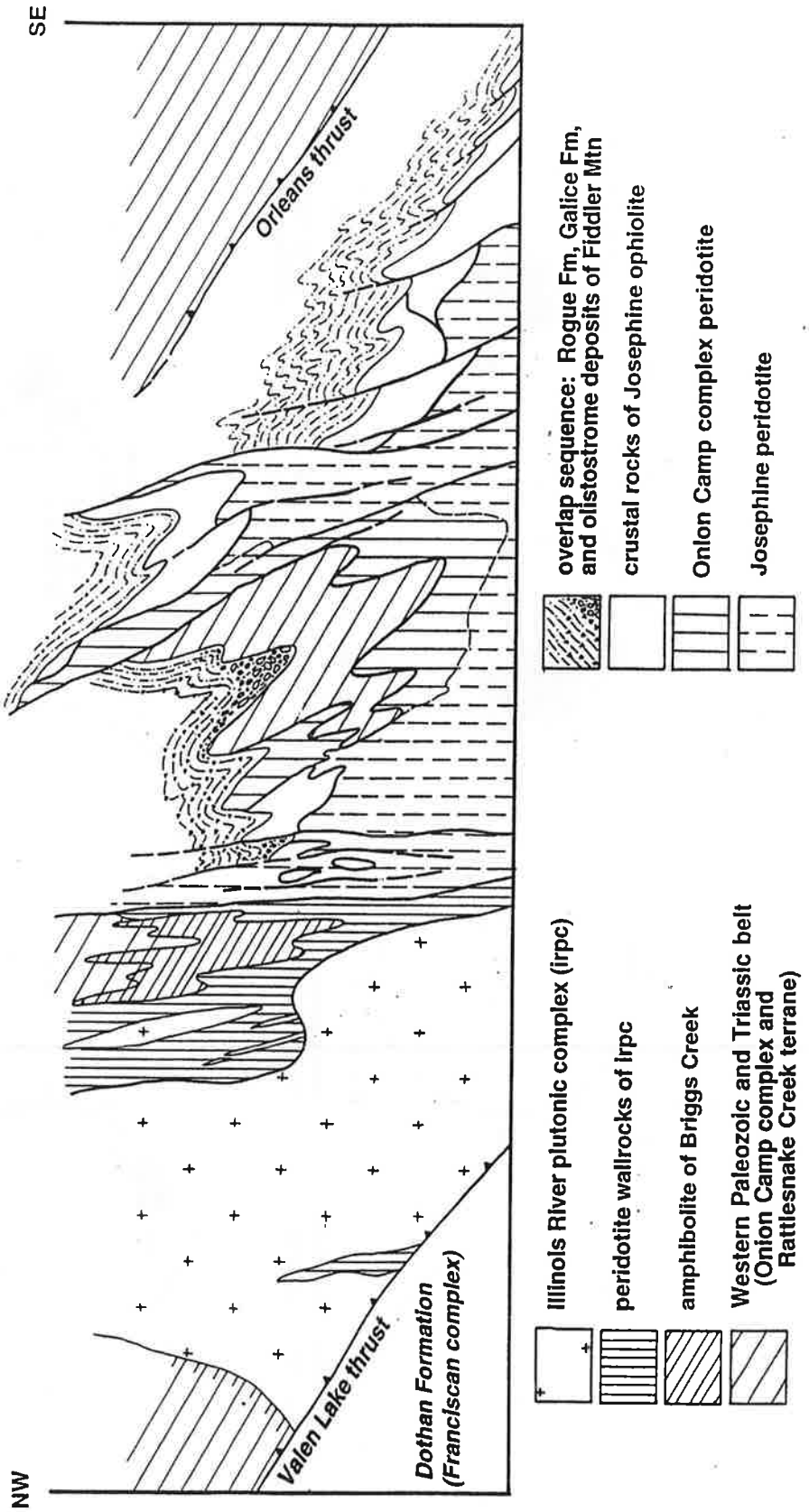


Figure 19

Geologic Evolution of the Northernmost Coast Ranges and Western Klamath Mountains, California

Galice, Oregon to Eureka, California
July 20–28, 1989

Field Trip Guidebook T308

Leaders:

K. R. Aalto G. D. Harper

Associate Leaders:

G. A. Carver S. M. Cashman
W. C. Miller III H. M. Kelsey

FIELD GUIDE TO THE JOSEPHINE OPHIOLITE AND COEVAL ISLAND ARC COMPLEX, OREGON-CALIFORNIA

Gregory D. Harper

Department of Geological Sciences, State University of New York at Albany

INTRODUCTION

The Klamath Mountains occupy the fore-arc region of the Cascade volcanic arc. They consist of east-dipping thrust sheets ranging from early Paleozoic to late Mesozoic. The terranes and thrust faults generally become younger from east to west [Irwin, 1981; Wright and Fahan, 1988]. There is no Precambrian basement present; the Klamath terranes consist of magmatic arcs, ophiolites, and accretionary prisms.

The western Klamath terrane (Fig. 1) consists of two east-dipping thrust sheets emplaced during the Late Jurassic Nevadan orogeny. The lower sheet (Fig. 2) includes the Rogue Formation and calc-alkaline plutonic rocks of the Chetco intrusive complex. The upper sheet includes the Josephine ophiolite which is in thrust contact with the Chetco intrusive complex along an amphibolite sole (Figs. 1, 2) [Dick, 1976; Cannat and Boudier, 1985]. Late Jurassic flysch of the Galice Formation conformably overlies both the Rogue Formation and the Josephine ophiolite (Fig. 2) [Harper, 1984; Wood, 1987]. The Rogue-Chetco complex and the Josephine ophiolite apparently represent a Late Jurassic island arc [Dick, 1976; Garcia, 1979] and back-arc basin [Saleeby et al., 1982; Harper and Wright, 1984]. This interpretation is based on similarities in radiometric and fossil ages (Fig. 2), overlying flysch, age of emplacement, and regional geology [Saleeby et al., 1982; Harper and Wright, 1984; Harper et al., 1986].

THE ROGUE AND GALICE FORMATIONS (ISLAND ARC COMPLEX)

On the first day of the trip, we will be rafting down the Rogue River to observe the Rogue and Galice Formations (Fig. 3). The Rogue Formation consists of a thick sequence of tuffs, breccias, and rare flows which range from mafic to silicic in composition [Garcia, 1979; Riley, 1987]. Riley [1987] subdivided the Rogue Formation into units consisting, from oldest to youngest, of (1) andesitic breccia, (2) volcanoclastic turbidites, (3) massive fine-grained tuff (Figs. 2, 3). The presence of pillow lavas, Bouma sequences, and cherty tuffs containing radiolaria and sponge spicules indicate submarine deposition [Riley, 1987]. Trace-element geochemistry of the volcanic rocks indicates that they are calc-alkaline [Garcia, 1979]. Saleeby

[1984] reports a concordant Pb/U zircon age of 157 ± 2 Ma on a tuff-breccia in the Rogue Formation (Fig. 2) and a 150 ± 2 Ma age on a felsic dike.

Kuroko-type massive sulfide deposits occur in the Rogue Formation [Koski and Derky, 1981; Wood, 1987]. We will visit one of these (Almeda Mine, Stop 3) which is exposed on the Rogue River, just below the contact between the Rogue Formation and overlying Galice Formation.

The Galice Formation consists of graywacke, slaty shale, and rare conglomerate. Bouma sequences are common and sole marks are locally present, indicating deposition by turbidity currents.

Bedding and foliation in the Rogue Formation generally dip steeply to the southeast, and the Galice Formation has a steeply dipping slaty cleavage. Tight to isoclinal folds occur in both the Rogue and Galice Formations (Fig. 3) [Kays, 1968; Riley, 1987; Park-Jones, 1988]. Folds are overturned to the west and axial planes generally strike northeast (Fig. 3). Fold hinges in the Galice plunge from $0-90^\circ$ [Kays, 1968; Harper and Park, 1986; Park-Jones, 1988]; it is uncertain whether this variation is primary or the result of post-Nevadan cross folding. Volcanic rocks east of the village of Galice (Fig. 3) were originally mapped as volcanic members in the Galice Formation [Wells and Walker, 1953]; however, at least some of these rocks are overturned and may in fact be the Rogue Formation [Park-Jones, 1988].

We will not be visiting other parts of the island arc complex. The probable plutonic roots of the arc are represented by the gabbroic Chetco intrusive complex which has yielded Late Jurassic K/Ar hornblende ages (Fig. 2). The southern part of the complex is predominantly gabbro, whereas the northern part is largely quartz diorite.

Other rocks associated with the Rogue Formation and Chetco intrusive complex include the Briggs Creek amphibolite, Rum Creek metagabbro (gneissic amphibolite), and minor peridotite (Figs. 2, 3) [Garcia, 1982]. The Briggs Creek amphibolite contains minor quartzites and has been interpreted to be metamorphosed pillow lava and chert. The association of metagabbro, peridotite, metabasalt, and metachert suggests that these rocks may represent a dismembered and regionally metamorphosed ophiolite [Coleman et al., 1976]. This interpretation is tentative, however, because of the possibility of large fault displacements, lack of structural work, and limited geochronology.

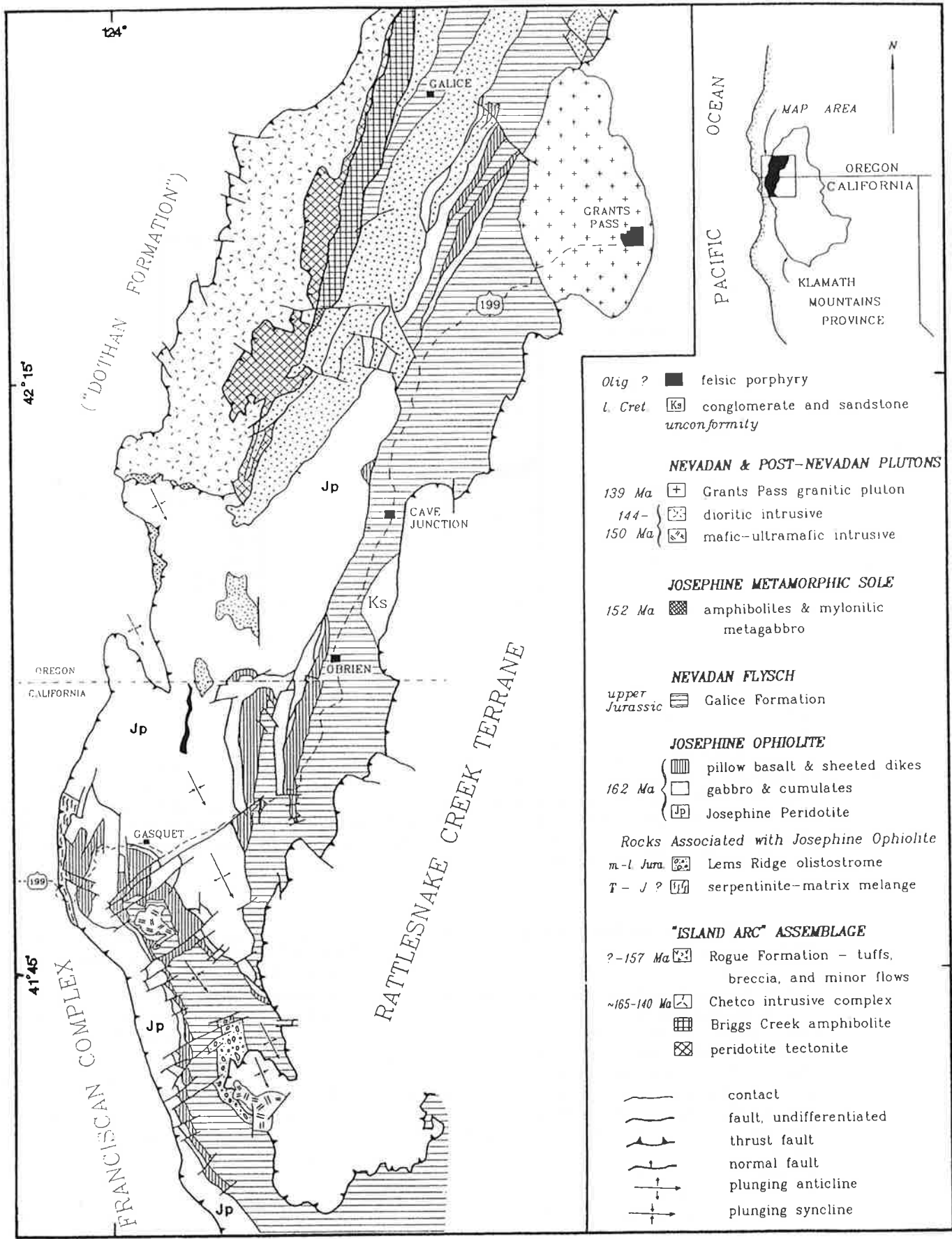


FIGURE 1 Generalized geologic map of the western Klamath terrane. Modified from Smith et al. [1982], Harper [1984], and Wagner and Saucedo [1987].

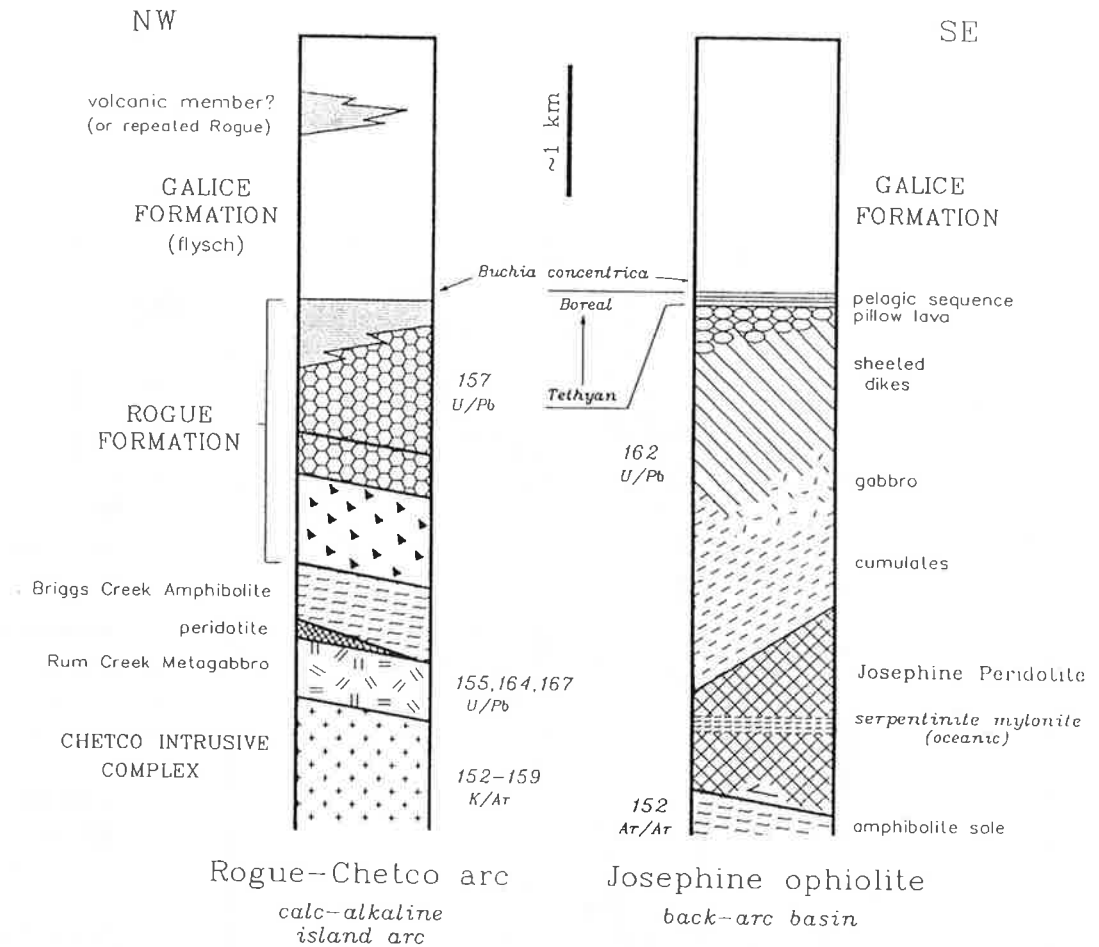


FIGURE 2 Late Jurassic island-arc complex and the Josephine ophiolite exposed along the Rogue River, Oregon, and the Smith River, California, respectively (Figs. 3 and 4) [Garcia, 1979, 1982; Riley, 1987; Park, 1987]. Symbols for the Rogue Formation are the same as those in Figure 3. The Josephine ophiolite was thrust over the island arc and thrust beneath western North America at ~150 Ma, at which time both sequences were intruded by calc-alkaline dikes and sills [Saleeby, 1984; Harper and Wright, 1984; Harper et al., 1987]. K/Ar hornblende (recalculated using standardized decay constants), Ar/Ar hornblende, and U/Pb zircon ages are from Hotz [1971] and Dick [1976], Saleeby, [1984, 1987] and Harper [unpublished data], respectively.

THE JOSEPHINE OPHIOLITE AND GALICE FORMATION

The Josephine ophiolite is one of the largest and most complete ophiolites in the world. The ophiolite and overlying metasedimentary rocks compose a >10-km-thick, east dipping thrust sheet (Figs. 2, 4). The ophiolite consists of (1) depleted peridotite (mostly harzburgite) covering >800 km² (Fig. 1), (2) gabbroic and ultramafic cumulates (Fig. 5), (3) high-level gabbro (Fig. 6), (4) sheeted dikes (Figs. 7, 8), and (4) pillow lava (Fig. 9), massive lava, and pillow breccia.

The ophiolite was originally dated at 157±2 Ma by Pb/U on zircon from two plagiogranites [Saleeby et al., 1982]. With the use of newer techniques, it was discovered that the ages were

slightly discordant. After abrasion of the zircon, one of the samples has yielded a concordant age of 162±1 [Saleeby, 1987]. In addition, a small fragment of the ophiolite exposed in the southwestern Klamath Mountains has yielded a zircon age of 164±1 Ma [Wright and Wyld, 1986]. In both areas, the dated plagiogranites are clearly part of the ophiolite because they are cut by massive dikes.

Pelagic/hemipelagic rocks conformably overlie the Josephine ophiolite (Fig. 10) and grade upward into the Galice flysch (Fig. 2). These rocks consist of chert, tuffaceous chert, and radiolarian argillite. Many of these rocks have high contents of terrigenous or tuffaceous detritus. Metalliferous horizons locally occur 8-23 m above the ophiolite and formed from low-T off-axis hydrothermal

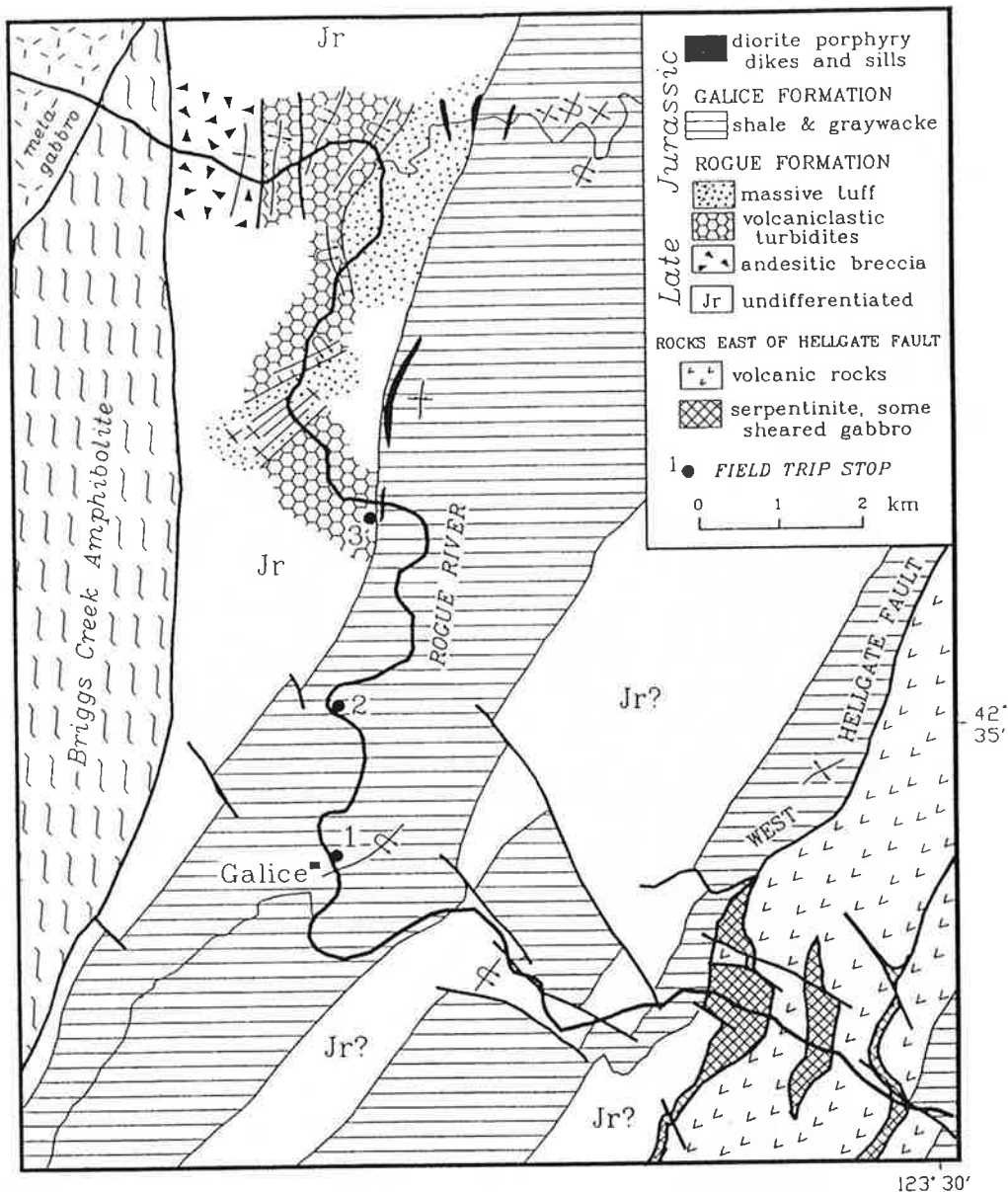


FIGURE 3 Geologic map of the Rogue River area modified from Wells and Walker [1953], Garcia [1982], Riley [1987], and Park-Jones [1988]. Fold hinges show locations of Nevadan folds in the Rogue Formation [Riley, 1987] and Galice Formation [Park-Jones, 1988].

springs [Pinto-Auso and Harper, 1985]. Well-preserved radiolaria preserved in limestone nodules at Stop 2 indicate an age of middle-upper Oxfordian [Pessagno and Mizutani, 1988]. *Buchia concentrica* (a bivalve) occurs in the lower part of the flysch (Fig. 2), and has a range of middle Oxfordian to upper Kimmeridgian [Imlay, 1980].

The pelagic/hemipelagic rocks grade upwards into flysch with the appearance of thick turbidites interbedded with radiolarian argillites (see Stop 2). Several hundred meters of massive and thick-bedded graywacke and rare conglomerate overlie this transition, whereas most of the remaining Galice consists of slate with some packets of

medium bedded graywacke.

Although the Josephine ophiolite and overlying Galice Formation were regionally metamorphosed to low grade, the ophiolite shows little penetrative deformation except where the metamorphic grade reaches lower greenschist facies in the southern part of the area shown in Figure 4. A strong, typically bedding-parallel cleavage is present in the Galice Formation. Isoclinal folds are locally well developed in the Galice. Calc-alkaline dikes, sills, and stocks were intruded during metamorphism; they are regionally metamorphosed and commonly deformed (Fig. 11). U/Pb zircon and Ar/Ar ages on these intrusives range from 148-151 Ma [Saleeby

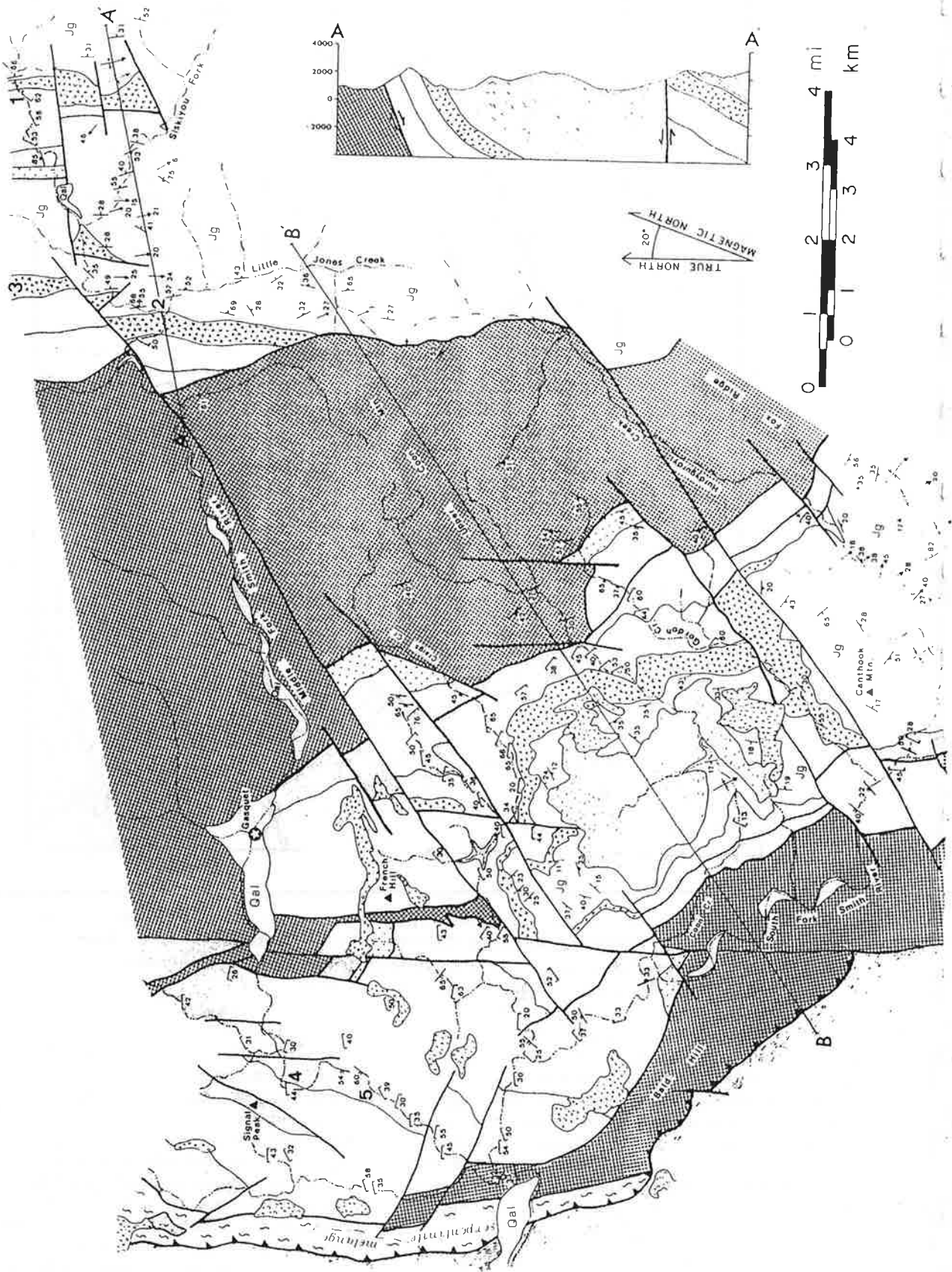


FIGURE 4 (caption and key on next page.)

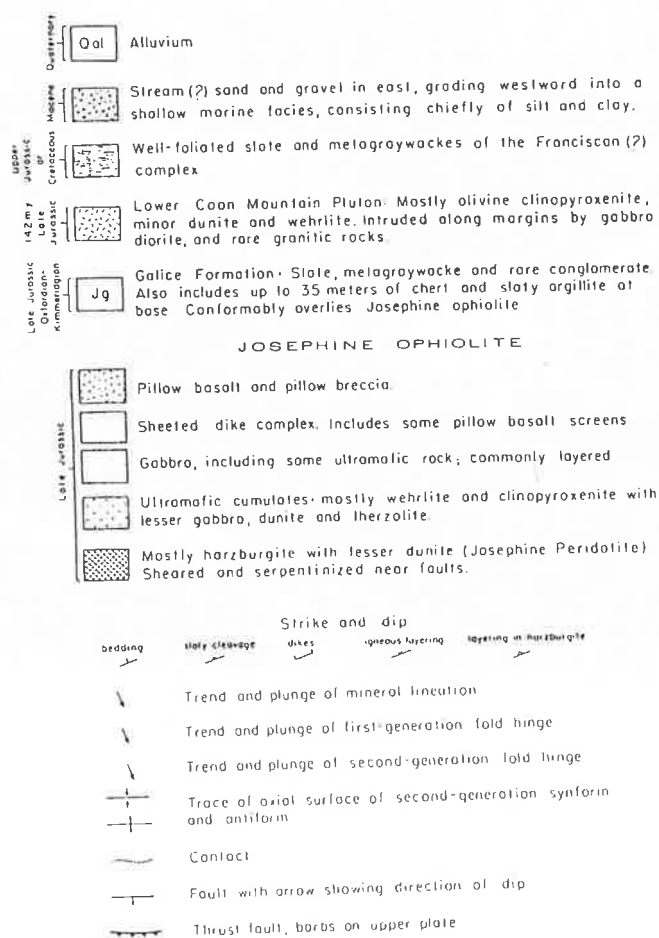


FIGURE 4 Geologic map of the Josephine ophiolite and overlying Galice Formation [Harper, 1984]. The ophiolite is broadly folded into an F_2 anticline and syncline, and the upper part of the ophiolite is repeated by three reverse faults in the northeastern part of the area. Numbers refer to field trip stops.

et al., 1982; Harper et al., 1986]. Dikes both intrude and are cut by small Nevadan faults; northwestward thrusting is indicated by fibrous slickensides and offset dikes and beds [G. Harper, in prep.]. Thrust directions inferred from the basal amphibolite sole of the Josephine ophiolite (Fig. 1) are north-northeast [Cannat and Boudier, 1985; K. Grady and G. Harper, in prep.].

Continued deformation after peak metamorphism is indicated by extensive folding of slaty cleavage, numerous reverse faults, and the local presence of a crenulation cleavage and lineation. The entire ophiolite was also folded



FIGURE 5 Layered gabbroic and ultramafic cumulates from near the base of the cumulate sequence, Josephine ophiolite.

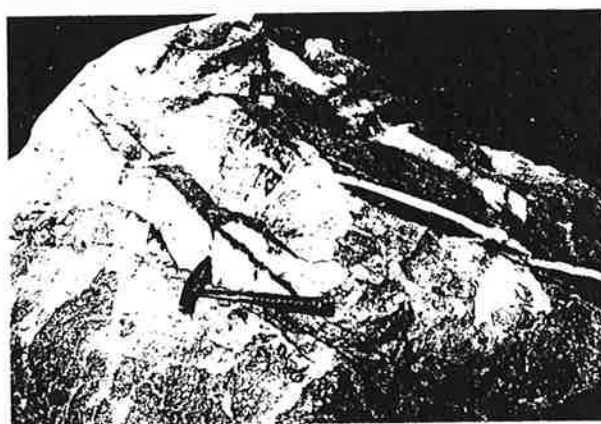


FIGURE 6 Complex intrusive breccia in high-level gabbro cut by a mafic dike and a thin plagiogranite dike (near Stop 5), Josephine ophiolite.

during this later phase of deformation (Figs. 1, 4).

Igneous Geochemistry

Dikes and lavas of the Josephine ophiolite show a wide range in composition because of extreme fractionation and multiple types of parental magmas. The great majority of dikes and lavas have "immobile" trace element concentrations that indicate magmatic affinities transitional between island-arc tholeiites and mid-ocean ridge basalt (Figs. 12 and 13) [Harper, 1984, 1988]. Highly

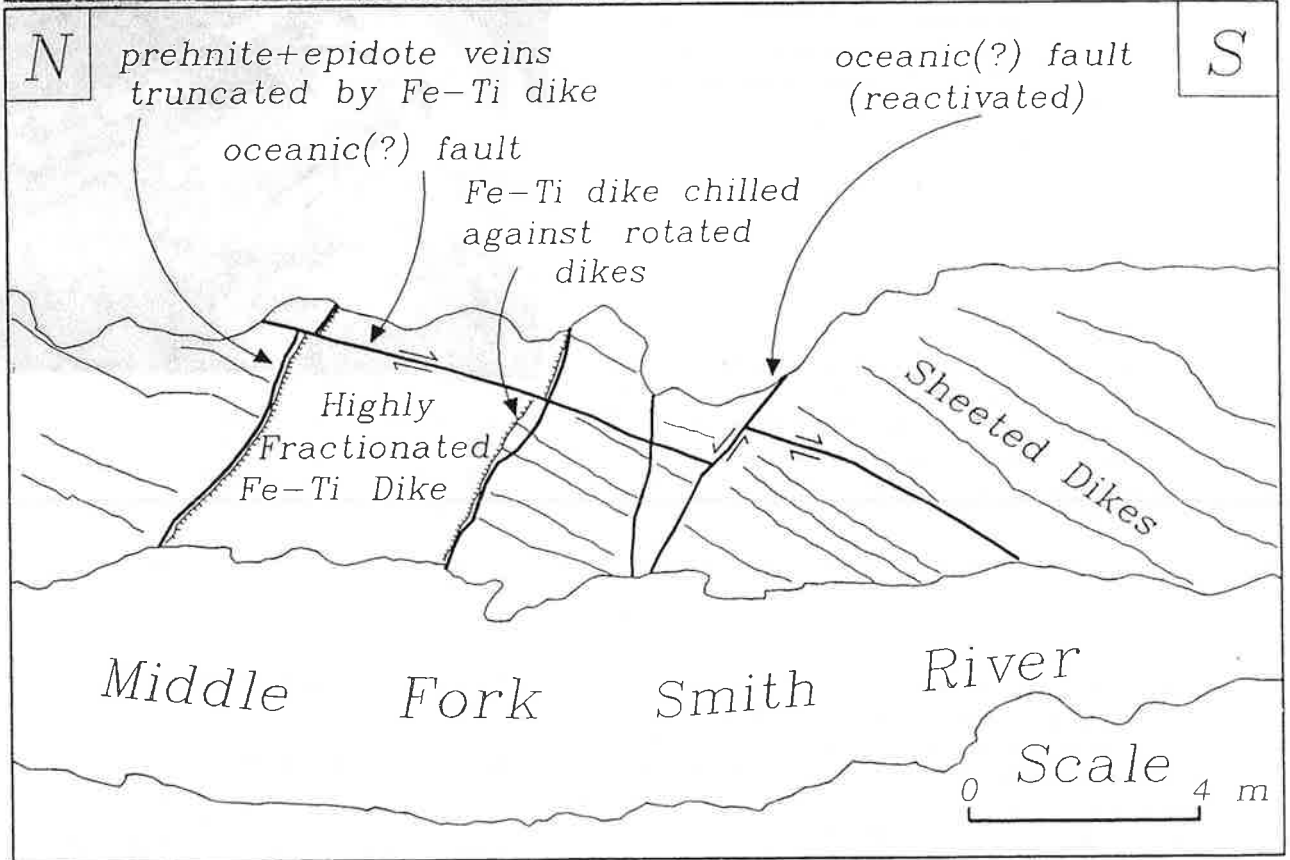
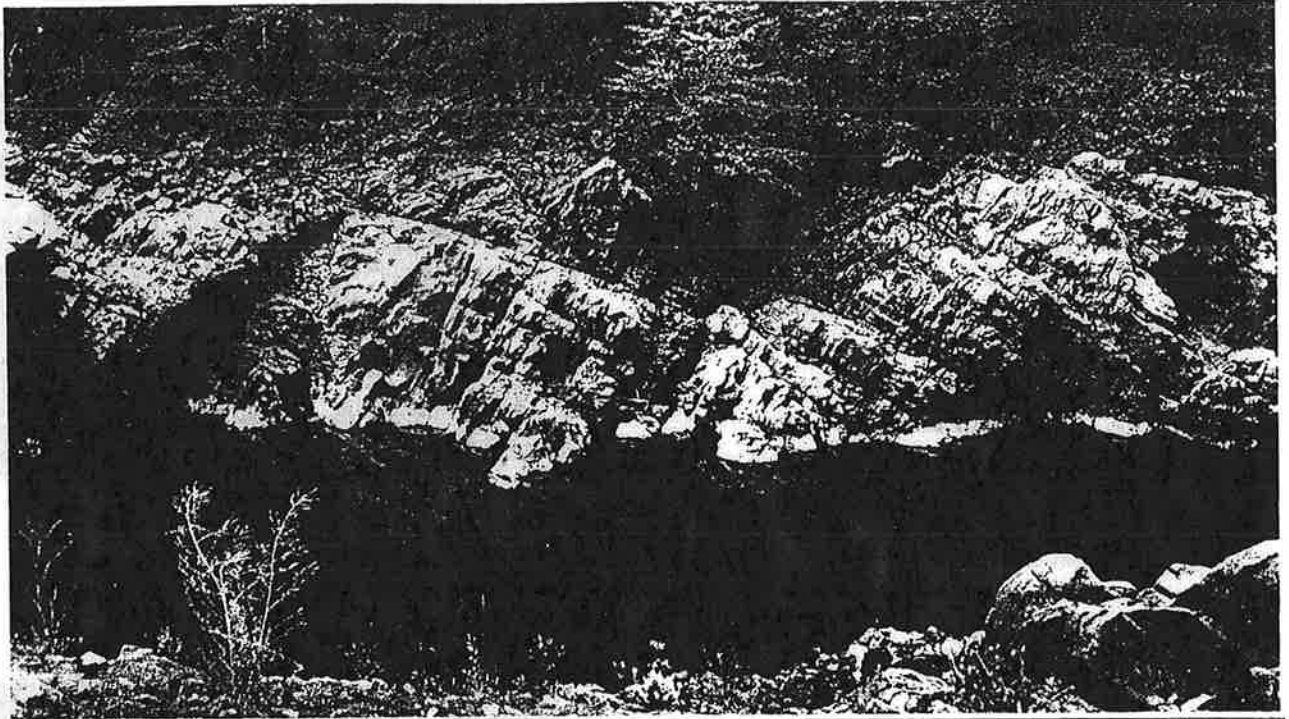


FIGURE 7 Sheeted dikes at Stop 5 dipping towards the south, viewed from Highway U.S. 199. This outcrop is in the hinge of a gently plunging syncline and thus the sheeted dikes are orientated essentially the same as when they were part of the oceanic crust (prior to ophiolite emplacement). The dip of the sheeted dikes reflects tilting at the spreading axis [Harper, 1982], probably by rotational faulting. The sketch shows the location of several probable oceanic faults, some of which are the locus of abundant prehnite veins. A late highly fractionated dike was intruded along one of these faults and much of its margins were subsequently sheared and veined with prehnite.



FIGURE 8 Sheeted dikes and gabbro screens (gb) at Stop 5. The center dike is ~0.4 m wide. In the right foreground is a probable oceanic normal fault; the lowermost gabbro screen is displaced 30 cm as shown by arrows. Prehnite veins (white), some with small offsets, occur on either side of the fault.

fractionated Fe-Ti basalts occur in the uppermost pillow lavas (Stop 2), and a Fe-Ti late dike (Fig. 7) and plagiogranite dikes and screens occur at the sheeted-dike/gabbro transition (Stop 4).

Very primitive lavas and dikes are widespread in Josephine ophiolite, and are highly variable in composition, ranging from primitive island-arc tholeiites to boninites (Fig. 12). We will look at a primitive pillow lava at Stop 1; black porphyritic primitive dikes also occur within high-level gabbro at Stop 4). The pillow lavas have thick chilled rims, distinctive variolitic textures, and abundant vesicles. Some of the lavas and dikes plot near melting curves, suggesting that they are primary mantle melts.

The geochemistry of the dikes and lavas clearly indicates a suprasubduction zone setting. Most of the lavas and dikes appear to have been generated by melting of a MORB-like source, but apparently involved higher degrees of partial melting than MORB (Fig. 12; or less melting of a depleted source). The high Th contents of the Josephine rocks compared to MORB (Fig. 13) reflects a "subduction-zone component" added to the source. The depleted primitive lavas (low Y, high Cr samples) apparently formed by hydrous partial melting of a depleted mantle source (Fig. 12).

These inferred variations in conditions and source rocks during partial melting is consistent with studies of the residual Josephine Peridotite which suggest two stages of partial melting [Dick and Bullen, 1984].

Subseafloor Hydrothermal Metamorphism

A study of the subseafloor metamorphism of the Josephine ophiolite has recently been published by Harper et al. [1988]. The ophiolite shows an overall downward increase in metamorphic grade and decrease in ^{18}O , similar to other ophiolites and resulting from metamorphism under a steep thermal gradient. Most rocks in the extrusives and sheeted dike complex have lost Ca and gained Mg and Na (Fig. 14), but relict igneous textures are well preserved. These chemical changes and pervasive metamorphism have been interpreted as the alteration by downwelling seawater (recharge, Fig. 15).

Alteration during upwelling (discharge) is much more localized at an outcrop scale. Mineral zonation resulting from discharging fluids is shown in Figure 15. One of the most significant recent discoveries in ophiolites is that the path of discharging fluids is represented by granoblastic

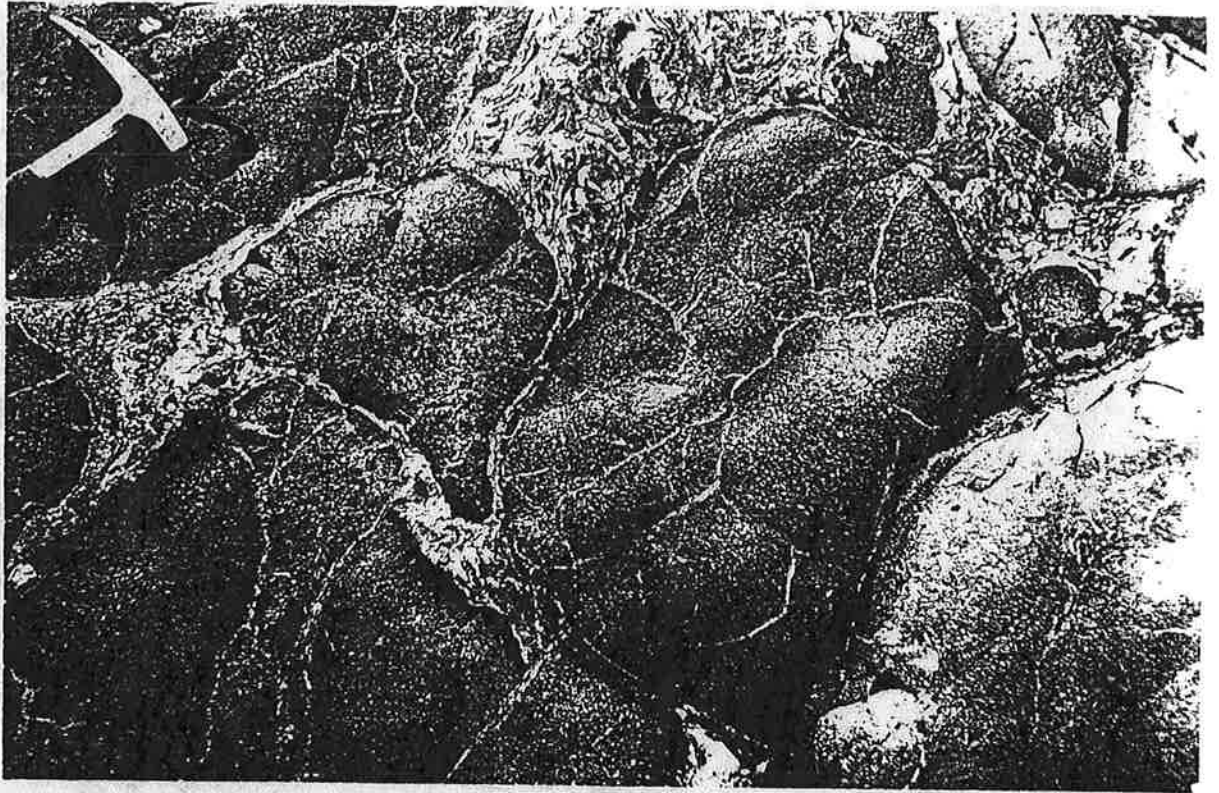


FIGURE 9 Pillow lavas ~50 m below the contact between the Josephine ophiolite and overlying sediments shown in Figure 10.

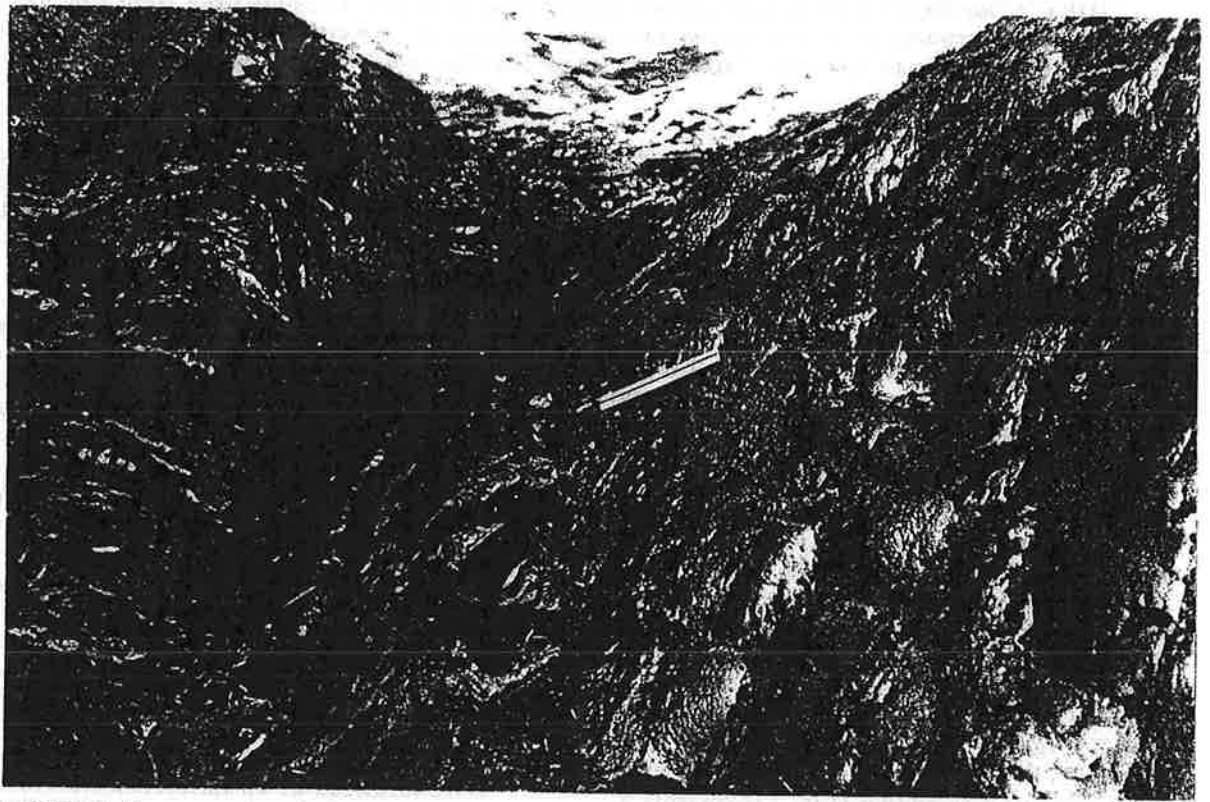


FIGURE 10 Depositional contact (15 cm scale rests on contact) between the uppermost pillow lavas of the Josephine ophiolite (left) and overlying thinly bedded chert and siliceous argillite (Stop 2). The contact dips 60° toward the left (east).



FIGURE 11 Boudinage in a sill within the pelagic/hemipelagic sequence overlying the Josephine ophiolite, near the mouth of Little Jones Creek (near Stop 1). Such calc-alkaline dikes and sills were intruded, deformed and regionally metamorphosed during the Nevadan orogeny at 145-150 Ma.

epidote + quartz \pm chlorite rocks called epidosites (Fig. 16) [Harper et al., 1988; Schiffman and Smith, 1988; Seyfried et al., 1988]. The epidosites are metasomatized and strongly enriched in Ca and depleted in Na and Mg (Fig. 14), as well as Cu and Zn. Chemical, isotopic, and experimental work indicates that the epidosites represent pathways for huge volumes of fluids discharging at high velocities (meters/sec); the discharging fluids were probably similar to 350°C fluids exiting from "black smokers" at modern mid-ocean ridges [Seyfried et al., 1988].

We will see abundant dike-parallel epidosites in the sheeted dike complex at Stop 1, respectively. The lowermost pillow lavas at Stop 1 are largely silicified and rich in sulfides. The silicification is almost certainly due to cooling of discharging fluids as they flow upwards into the more permeable pillow lavas. Above the lowermost pillows throughout the Josephine extrusives, bulbous "albite" epidosites and abundant hematite are evident in outcrop, and muscovite and K-

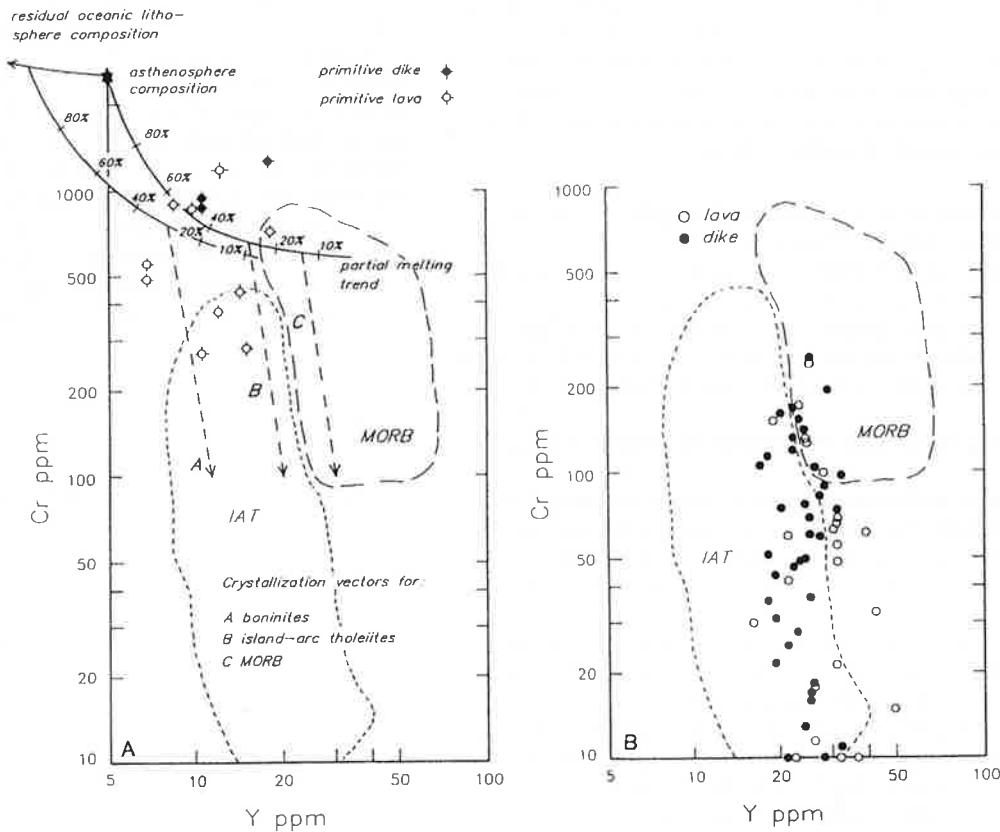


FIGURE 12 A. Y vs. Cr plot for primitive dikes and lavas from the Josephine ophiolite [Harper, 1988]. Note that several of the Josephine rocks plot near partial melting trends, indicating that they are essentially primary mantle partial melts. It is likely that the more depleted samples (lower Y) were derived by melting of a depleted mantle source because unrealistically high degrees of partial melting would be required for an undepleted source. B. Y vs. Cr plot for typical dikes and lavas of the Josephine ophiolite. This plot and other trace element data [Harper, 1984] indicate magmatic affinities transitional between IAT and MORB. Extrapolation upwards along fractionation trends suggests that these rocks were derived from partial melting of a relatively undepleted mantle source.

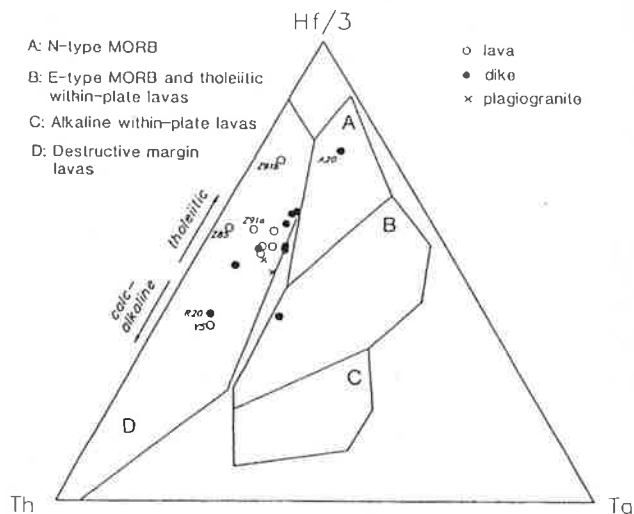


FIGURE 13 Hf/3-Ta-Th diagram showing affinities of Josephine ophiolite dikes and lavas to island-arc tholeiites [Harper, unpublished data]. The linear trend extending away from the Th apex may be the result of a variable "subduction component" present during melting or mixing of MORB magmas with depleted primitive lavas. Numbered samples are very primitive and show a wide variation in composition.

feldspar commonly occur in amygdules and in interpillow matrix (Fig. 15).

Locally in the Josephine ophiolite, hot fluids discharged directly onto the seafloor to form massive sulfide deposits. The Turner-Albright deposit, which occurs southwest of Obrien, Oregon (Fig. 15) is gold-rich [Koski and Derkey, 1981].

Spreading Rate and Magmatic/Tectonic Cycles

Modern mid-ocean ridges vary dramatically in morphology, intensity of faulting, and average depth and size of earthquakes. One of the most important differences appears to be the presence of long-lived magma chambers at fast spreading ridges, although they are much smaller (<4 km wide) than previously proposed, whereas magma chambers at slow spreading centers (<5 cm/yr) are almost certainly episodic as indicated, for example, by the presence of deep microearthquakes beneath the Mid-Atlantic Ridge (MAR) [Harper, 1985]. Although high-T springs (black smokers) have recently been discovered on the Mid-Atlantic Ridge, hydrothermal activity at slow spreading centers appears to be episodic and multistage [Sempere and Macdonald, 1987].

The widespread occurrence of very primitive Cr-spinel bearing lavas in the basal pillow lavas of the Josephine ophiolite requires that magma chambers periodically solidified because these mantle-derived melts would have otherwise mixed into an existing magma chamber [Harper, 1988]. Solidifying magma chambers would also produce

highly fractionated magmas such as Fe-Ti basalts that occur at Stops 1 and the late Fe-Ti dike and plagiogranite that occurs at Stop 4 (Fig. 7). The small size and episodic nature of magma chambers would also account for features of the cumulate sequence including a generally fine-grain size, poorly developed and discontinuous igneous layering (Stop 5), and the occurrence of ultramafic cumulates throughout the sequence [Harper, 1984].

During periods when no magma chamber is present, extension will be taken up entirely by structural processes such as fissuring and faulting [Harper, 1985, 1988]. Normal faulting often takes place by rotation of fault blocks. Rotated fault blocks have been observed at the MAR, but the amount of rotation is controversial [Sempere and Macdonald, 1987] and much be obscured by eruption of lava flows during rotation (growth faulting).

In the Josephine ophiolite the sheeted dikes and cumulate sequence are inclined with respect to conformably overlying sediments (Fig. 2) [Harper, 1982]. Assuming the dikes were intruded vertically and igneous layering was subhorizontal, >50° tilting prior to deposition of overlying pelagic rocks (i.e. at the spreading axis) is required. This tilting is especially evident at Stop 4 where the basal sheeted-dike complex occurs in the hinge of a large gently plunging syncline (Fig. 7). In this outcrop, the dikes have a dip of ~40° S and commonly show evidence of faulting in two directions: (1) along dike margins (Fig. 7), (2) along steep normal faults (Figs. 7, 8) which are similar in strike to the dikes. Both of these sets of

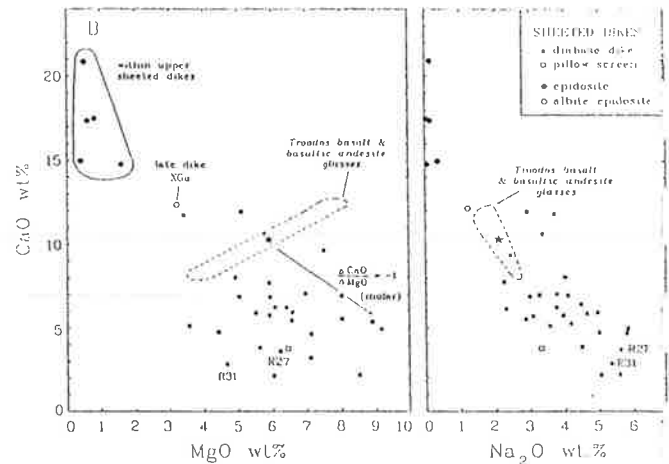
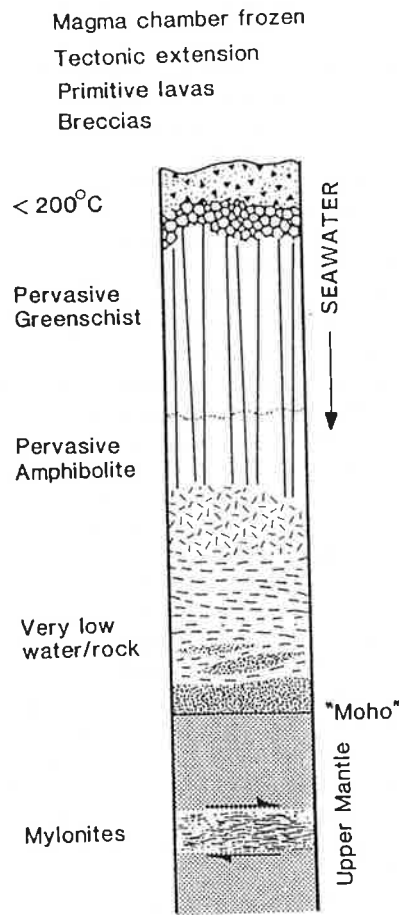


FIGURE 14 Plots of CaO versus MgO and Na₂O for sheeted dikes from the Josephine ophiolite [Harper et al., 1988]. The fields for Troodos illustrate variation due to igneous fractionation. Most of the dikes show the effects of seawater alteration during discharge which results in Ca loss and a gain in Mg and Na; these rocks typically have well-preserved relict textures. In contrast, epidiosites altered during discharge are strongly enriched in Ca and depleted in Mg and Na..

A Recharge Cycle



B Discharge Cycle

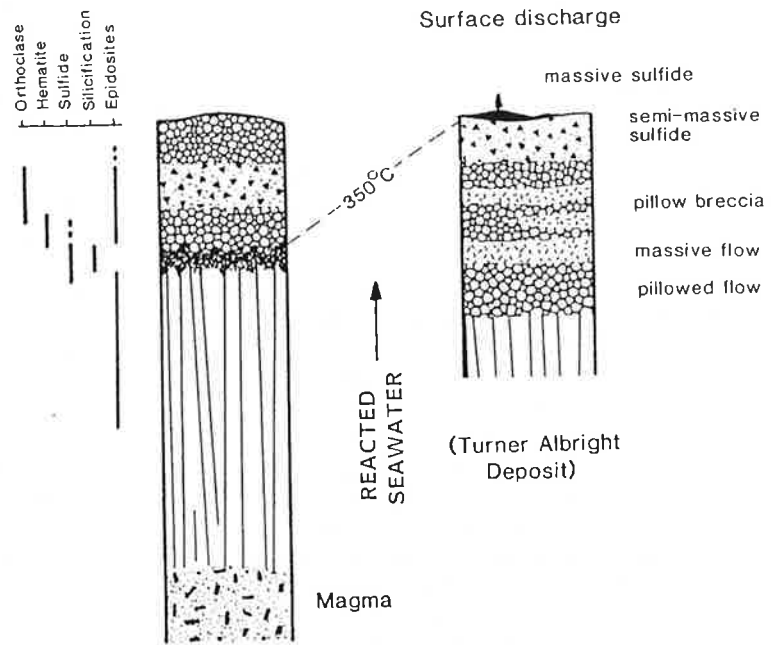


FIGURE 15 Summary diagram showing subseafloor metamorphism during recharge and discharge cycles [Harper et al., 1988]. Discharging fluids typically cooled as they flowed upward through the extrusives producing a distinctive mineral zonation. At the Turner-Albright deposit, however, high-T fluids vented onto the seafloor to form massive sulfide deposits [Zierenberg et al., 1988].

faults are probably oceanic because they have subseafloor hydrothermal alteration along including prehnite veins (Fig. 8), epidosite veins and epidosites. In addition, the late Fe-Ti at Stop 4 (Fig. 7) was intruded parallel to the steep faults, and much of its margins are sheared and contain abundant prehnite veins; this indicates that this dike was intruded during the faulting.

A likely mechanism for tilting is rotational normal faulting. In this case, both the fault blocks and the faults rotate. As the faults rotate, they become unfavorably oriented, and new steeper faults map form; the steep faults at Stop 4 (Fig. 7) may represent such new faults.

Because the entire crustal sequence of the Josephine ophiolite is tilted, oceanic faults would be expected to have extended into the upper mantle. Such faults could have died out into a zone of uniform ductile flow, or perhaps into a discrete subhorizontal horizon [Harper, 1985].

A regionally extensive flat shear zone in the upper mantle peridotite of the Josephine ophiolite has recently been mapped and consists of unusual antigorite mylonites and peridotite mylonites [Norrell et al., 1988]. This shear zone is interpreted to represent an oceanic detachment above which the crustal sequence was rotated by block faulting [Norrell and Harper, 1988]. If we assume that the >50° tilting above this fault took place by rotational faulting, then the ophiolite must have been stretched by ~100%. This would indicate the the crustal sequence, which is now ~3 km thick (Fig. 2), was originally ~6 km thick, similar to modern oceanic and back-arc basin crust.

These aspects of the Josephine ophiolite imply that it formed at a spreading center where the magma supply was low relative to the amount of extension. Slow spreading mid-ocean ridges appear to have a low magma supply as indicated by the absence of magma chambers along much of the

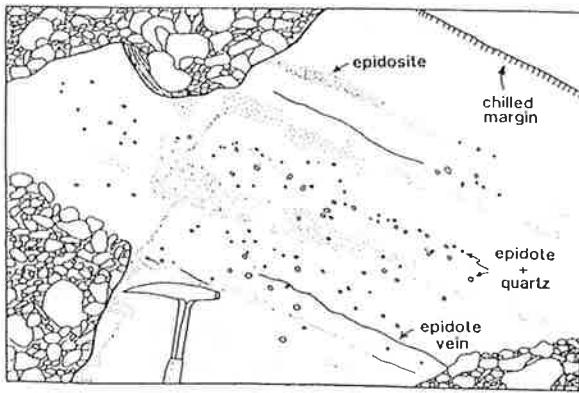


FIGURE 16 Sketch of epidiosites in the upper-sheeted dike complex at Stop 1. These probably represent pathways for discharging, $\sim 350^{\circ}\text{C}$ fluids similar to those at modern "hot smokers" at mid-ocean ridges [Harper et al., 1988].

Mid-Atlantic Ridge [Sempere and Macdonald, 1987]. By analogy, the Josephine probably formed at a slow spreading center to account for the apparent episodic nature of magma chambers [Harper, 1988] and the extreme tilting of the crustal sequence [Harper, 1985; Norrell and Harper, 1988]. It is possible, however, that the spreading rate was intermediate or even fast if the spreading segments were short and bounded by transforms (i.e., cold edge effect). In any case, the Josephine is different from the Oman or Bay of Islands ophiolites which have thick, well layered cumulate sequence, little evidence for large-scale tilting, and which probably formed by fast spreading with steady-state magma chambers.

TECTONIC EVOLUTION

The similarities in age and overlying flysch of the Galice Formation (Fig. 2) suggests that the Rogue island-arc complex and Josephine ophiolite suggest that they were formed in a single magmatic arc. Because the Rogue arc is thrust beneath the Josephine ophiolite, which is in turn thrust beneath older rocks of the Klamath Mountains, it is likely that the arc was west-facing with the Josephine ophiolite forming in a back-arc basin between the

arc and western North America [Harper and Wright, 1984]. The remains of an extensive Middle Jurassic magmatic arc occur east and structurally above the Josephine ophiolite, and is in the appropriate position to represent a remnant arc left behind as the Josephine back-arc basin opened. If this model is correct, the active arc (Rogue Formation and Chetco intrusive complex) migrated away from North America as spreading occurred in the back-arc basin.

Although it is difficult to directly tie the Rogue-Chetco arc and Josephine ophiolite to the western Klamath Mountains (i.e. rule out that they

are exotic to North America), there are several strong arguments. Recently, it has been recognized that several areas within the western Klamath terrane contain fragments of what appear to be the Late Triassic and Early Jurassic Rattlesnake Creek terrane. This terrane consists of a suite of disrupted ophiolitic and metasedimentary rocks, much of which forms a distinctive serpentinite melange, and which currently is thrust over the Josephine ophiolite and Galice Formation (Fig. 1). These fragments may have been rifted off western North America during Late Jurassic extension [Wyld and Wright, 1988]. Possible Rattlesnake Creek fragments include the Lems Ridge olistostrome (Fig. 4), serpentinite melange along the western edge of the ophiolite in the area of Figure 4 and in the southern Klamath Mountains, and ophiolitic rocks containing Triassic chert [Roure and DeWever, 1983] west of Cave Junction, Oregon (Fig. 1) which appear to lie beneath the Rogue Formation (these workers mistakenly assigned these cherts to the Josephine ophiolite). The presence of older Klamath basement is required by the occurrence of xenocrystic Precambrian zircon in a southern remnant of the Josephine ophiolite in the southern Klamath Mountains [Wright and Wyld, 1986]; the dated plagiogranites are clearly part of the ophiolite and the xenocrystic zircon is probably from epiblastic rocks in Klamath basement. The lower part of this ophiolite remnant is not exposed, but it must have been built on the edge of the Josephine basin during extension but just prior to sea-floor spreading.

New data suggests that the back-arc basin model needs to be modified or replaced by a more complex tectonic scenario. Harper et al. [1985] noted that the orientation of spreading centers inferred from the strike of sheeted dikes, however,

are approximately east-west [Harper et al., 1985; Norrell and Harper, 1988], suggesting that the back-arc basin may have had a geometry like the Gulf of California where long transforms separate short spreading segments. This geometry may result from intra-arc strike-slip faulting in response to oblique subduction as in the modern modern Anadaman Sea [Harper et al., 1985; Wyld and Wright, 1988]. In addition, preliminary dating suggested that the Middle Jurassic arc shut off just as the Josephine ophiolite formed, consistent with rifting to form a back-arc basin and remnant arc [Harper and Wright, 1984]. Recent Pb/U dating, however, has shown that the ophiolite is slightly older (164-162 Ma), and that the "Middle Jurassic" arc was active until 160 Ma [Saleeby, 1987; Wright and Fahan, 1988]. Thus, if the Rogue arc and Josephine ophiolite formed by rifting of the western Klamath Mountains, then the ophiolite must have been an intra-arc basin with active volcanism on both sides.

Radiolaria extracted from the pelagic/hemipelagic sequence overlying the Josephine ophiolite at Stop 2 indicates northward

migration of the ophiolite prior to deposition of the overlying flysch. Radiolaria indicative of the Central to Northern Tethyan Province occur in the lower 45 m, above which the first graywackes appear and radiolaria from interbedded argillites are indicative of the Southern Boreal Province [Pessagno and Blome, 1988]. *Buchia concentrica* and plant fossils in the Galice flysch are also indicative of Boreal Realm [E. Pessagno, personal communication, 1988]. The amount of relative motion with respect to the North American plate is uncertain, however, because paleomagnetic studies indicate that the North American plate was also moving northward during this time [Debiche et al., 1987].

The Galice flysch may represent the earliest sign of the Nevadan orogeny which culminated with thrusting and regional metamorphism of the Josephine and Rogue-Chetco terranes. The Galice sandstones contain clasts of volcanic rock fragments, plagioclase, chert, shale, and minor monocrystalline quartz and metamorphic rock fragments. The basal graywackes that we will see at Stop 2 are much richer in volcanic rock fragments and plagioclase than those higher in the sequence; they also have abundant clinopyroxene and hornblende, but pebbles at the base are mostly radiolarian chert. Other minerals in Galice graywackes include zircon, tourmaline, apatite, chromian spinel, and muscovite; less common minerals include biotite, garnet, and glaucophane. The detrital zircons are highly variable in color and morphology and have yielded Pb/U zircon isotopic data that indicate sources which are ~1500-1600 Ma and early Mesozoic [Miller and Saleeby, 1987]. The graywacke petrography, zircon ages, and sparse paleocurrent indicators [Harper, 1980; Park-Jones, 1988], indicate derivation of the flysch from older rocks of the Klamath Mountains to the east. The volcanic component of the wackes is probably derived from a Middle Jurassic arc complex built on older rocks of the Klamath Mountains [Harper and Wright, 1984; Wright and Fahan, 1988]. The absolute age range for flysch deposition is constrained by the age of basement rocks ($157-162 \pm 1$ Ma, Fig. 2) and by the age of cross-cutting sills, dikes, and plutons ($139-150 \pm 1$ Ma) [Saleeby et al., 1982; Harper et al., 1986; Saleeby, 1987]. Thus the Galice flysch was deposited and thrust beneath western North America within approximately 7 Ma. The cause of uplift and erosion to the east of the Josephine ophiolite may have been from underthrusting which eventually involved the Josephine and Rogue-Chetco terranes. If this is true, then the Galice is syntectonic and heralds the change from extensional to compressional tectonics.

The Rogue arc and Josephine back-arc basin underwent compression during the latest Jurassic Nevadan orogeny and were thrust beneath the Klamath Mountains. During and following thrusting, the Josephine ophiolite and overlying

Galice Formation became the locus of arc magmatism as indicated by the presence of abundant calc-alkaline dikes, sills (Fig. 11), and plutons (Fig. 1) ranging in age from 139-151 Ma [Saleeby et al., 1982; Saleeby, 1984; Harper et al., 1986]. The amount of underthrusting on the roof thrust overlying the Josephine ophiolite and Galice Formation (Fig. 1) is approximately 110 km [Jachens et al., 1986]. This thrust is cut by plutons as old as 150 ± 1 Ma [Harper et al., 1986]. Uplift to the surface occurred by ~130 Ma because the Galice Formation is overlain with angular unconformity by a small remnant of Early Cretaceous (Hauterivian-Barremian) sedimentary rocks near the Oregon-California border (Fig. 1) [Nilsen, 1984].

The change from back-arc extension to compression (Nevadan orogeny) correlates with an abrupt change in the polar wander path of cratonic North America and with plate reorganization in the Atlantic recorded by marine magnetic anomalies [Steiner, 1983; May and Butler, 1986]. Thus the Nevadan orogeny in the Klamath Mountains may have resulted from compression due to a major change in plate motions.

DAY 1

Drive from Grants Pass, Oregon, northwest on Interstate 5; the light-colored road exposures consist of the 139 Ma Grants Pass pluton (Fig. 1). Take the exit to Merlin, a few km north of Grants Pass. Follow the road west, through Merlin, and on to the small village of Galice. Exposures of sheared serpentinite, greenstones, and gabbro will be evident as we drive into the area shown on Figure 3; these may be the northward continuation of the Josephine ophiolite (Fig. 1). As we are waiting for rafts to be loaded, notice the picture on the wall of the Galice store which shows the water level during the great 1964 flood.

We will board the rafts and float downstream for approximately 13 km, with three stops (Fig. 3). We will go through numerous rapids, and you should see large birds called Great Blue Herrons.

Stop 1

Paddle across the Rogue River, directly opposite where the rafts are launched. This outcrop shows excellent turbidites with flute casts (Late Jurassic Galice Formation). The beds are overturned and the shales have a slaty cleavage formed during the Nevadan orogeny. Cleavage cuts bedding at a moderate angle. Faulting and associated veining is also present and may be related to the Nevadan folding.

Stop 2

Thin-bedded graywacke and slate are evident in

this exposure. The bedding is folded and there is an axial planar slaty cleavage. The folds and cleavage are Nevadan age. As we continue downstream, we will be approaching the Rogue Formation which is volcanoclastic and underlies the Galice Formation.

Stop 3

We will stop on the right side, just above the rapids and impressive iron staining. The staining is from weathering of a Kuroko-type massive sulfide (Almeda Mine) which is located just below the contact with the Galice Formation. The ore body was mined for gold, silver, copper, and lead. We will hike up to the mine shaft on the north side of the river. At the entrance to the mine shaft a contact between a massive sulfide and fine-grained bedded tuff is exposed. On the left side of the shaft, the massive sulfide locally contains barite. The tuff is exposed on the roof of the shaft, and on the right side of the shaft is a diorite dike [Wood, 1987].

Walk on up the road (east) to the black slate outcrops. This is the basal Galice Formation and the bivalve *Buchia concentrica* can be found. This is also an ammonite locality [Imlay, 1980]. The contact between the Rogue Formation and Galice Formation is not exposed here, but appears to be depositional as reported by [Wood, 1987].

Stop 3 to End of River Trip

As we continue down the river, we will enter a narrow, quiet part of the canyon with high walls. Notice the steeply dipping tuffs. Most of the tuffs are green and andesitic, but a few white silicic tuffs are evident. Upon careful observation, you may see overturned graded bedding and isoclinal fold hinges along the banks of the river. Many of the tuffs are turbidites.

Travel

We will drive back through Grants Pass and south on Highway U.S. 199 (Fig. 1), where we will stay overnight. Tomorrow we will visit the Josephine ophiolite.

DAY 2

We will leave Cave Junction and drive south on Highway U.S. 199. We are now situated on flysch of the Galice Formation which overlies the Josephine ophiolite. As we drive south, you will see the Josephine peridotite which forms the poorly vegetated mountains to the west; in this area, the entire crustal sequence of the ophiolite has been cut out by a large north-striking normal fault. As we cross into California, we will drive through a

long tunnel. As we exit the tunnel, the topography will be much steeper. We have entered the drainage area of the Smith River which is rapidly down-cutting. The erosion is the result of late Cenozoic uplift, which is probably the result of subduction of young, hot oceanic lithosphere of the Juan de Fuca plate. Relicts of an extensive Miocene erosion surface (Klamath peneplain) can be seen forming relatively flat mountain tops.

Stop 1

Continue southwest on highway U.S. 199 to a highway maintenance station (Idlewild) on the right side of the road. Walk several hundred meters further down the highway to where the trees begin on the left side of the road. Walk down the embankment and cross the stream to the other side. The ophiolite is exposed as a homocline in this area which dips approximately 60° east.

We are now in the upper part of the sheeted dike complex and will walk up-stream to the contact with pillow lavas. Notice chilled margins on sheeted dikes, epidiosites (Fig. 16), and disseminated sulfides. A screen (septa of country rock) of pillow lava will be pointed out. Notice the peculiar texture (variolitic) and thick chilled margin. This is a very primitive, depleted basalt (~1000 ppm Cr, 10 ppm Y) which contains Cr-spinel [sample R20, Harper et al., 1988].

Continue walking up-section to the contact of the sheeted-dike complex with the overlying pillow lavas (where trees begin on left). Notice the presence of a quartz-rich and sulfide-rich breccia near the contact; it was formed by discharging fluids and is very similar to "stockwork-like" rocks drilled from the sheeted-dike/pillow basalt transition zone in Deep-Sea Drilling Project Hole 504b, south of the Galapagos spreading center [J. Alt, personal communication, 1987].

The basal pillow lavas are sulfide-rich and strongly silicified, and the interpillow matrix is locally completely replaced by pyrite and chalcopyrite. This type of mineralization is typical along this contact in the Josephine ophiolite, although the intensity is highly variable. As noted above, this contact is apparently where discharging fluids cooled and possibly mixed with seawater.

Continue walking up-stream and observe red hematite-bearing lavas and light-green "albite epidiosites" within the red lavas. Muscovite and/or K-feldspar typically occurs in the hematitic lavas, particularly in amygdules and interpillow matrix.

Travel Between Stops 1 and 2

Return to vehicles and continue to drive southwest along U.S. 199 for ~10 km. We will be driving through sheeted dikes, gabbros, and cumulate ultramafics. This sequence is faulted at the base (Fig. 4) and as a result we will drive back into the Galice Formation overlying the ophiolite.

We will cross several more N-S reverse faults that repeat the upper part of the ophiolite (Fig. 4); these faults were probably formed during late-stage Nevadan thrusting.

Stop at large pull-out on left, just before the place where the road narrows abruptly and passes through very tight curves.

Stop 2

A depositional contact is clearly exposed on the Smith River between the uppermost pillow lavas of the ophiolite and the basal pelagic/hemipelagic sediments (Fig. 10). The pillows below the contact are large and best observed on the lower, downstream part of the outcrop. They are highly fractionated Fe-Ti basalts containing abundant microphenocrysts of plagioclase and clinopyroxene. 400 m of pillow lava (Fig. 9), massive lava, and pillow breccias are well exposed along the river below the contact (see Fig. 10 of Harper [1984] for stratigraphic section), but we will not be able to observe them because rafts and much time are needed to travel the deep canyon.

The basal 45 meters of sediments overlying the ophiolite consist of chert, tuffaceous chert, siliceous argillite (black), and rare nodules and layers of limestone (gray), and several sills. The siliceous argillites are slaty and have high Al contents indicative of a large component of terrigenous sediment [Pinto-Auso and Harper, 1985]. Surprisingly, the limestones have yielded abundant perfectly preserved radiolarians which indicate an Oxfordian age; furthermore the radiolarians indicate that the ophiolite moved northward from the Central Tethyan to Southern Boreal Realms during deposition of the basal 45 meters of the pelagic/hemipelagic sequence [Pessagno and Blome, 1984; Pessagno and Mizutani, 1988].

At 45 meters stratigraphically above the contact, two thick bedded graywackes are present and mark the beginning of flysch deposition. These are overlain by silty radiolarian argillites and a few graywacke beds exposed continuously to a sharp bend in the river (100 m above the ophiolite). Slates with abundant limestone nodules occur at the bend. Massive graywackes and some pebble conglomerate is exposed further upsection (upstream).

Many sills and dikes are present at this locality. They are regionally metamorphosed, and the sills have been extended to form boudinage (Fig. 11). The sills are mafic, calc-alkaline, and usually contain hornblende. Recent $^{40}\text{Ar}/^{39}\text{Ar}$ step heating ages on two of these sills have yielded ages of 147 ± 1 and 150 ± 1 Ma (the ophiolite is 162 ± 1 Ma) and thus tightly constrain the timing of sediment deposition and subsequent deformation and associated prehnite-pumpellyite facies metamorphism.

Nevadan structures evident in this section

include a bedding-parallel slaty cleavage, boudinage, extension veins, flattened pebbles, and bedding-parallel faults. The latter are preferentially eroded, have thin sheared calcite, and are especially evident ~25-30 m above the contact. A highly disrupted zone is evident for several meters below the first graywacke; small thrusts and ramps are evident on close examination, and some thrust surfaces have extension veins beneath them with fibers up to 25 cm long. Deformation in this zone is apparently due to bedding-parallel thrusting during the Nevadan deformation.

Travel Between Stops 3 and 4

Drive 1.5 km further south and west on U.S. 199 and take a right at the road just before the bridge (Patrick Creek Road). Drive 2.5 kilometers north and turn right. We are now at the base of the cumulates and will be driving all the way through the cumulates, sheeted dike complex and into the lower pillow lavas (Fig. 4). There are only weathered outcrops until we reach the pillow lavas, so this is a good time to enjoy the scenery.

Stop 3

Pillow lavas are exposed in a quarry on the east side of the road. Pillow lavas are best viewed on huge blocks on the quarry floor. Hydrothermal metamorphism during discharge is evident from epidote \pm hematite between pillows. Hematitic veins are also present in some of the outcrop. Volcanic breccias are exposed on the far end (south) of the quarry.

Travel Between Stops 3 and 4

Drive back to U.S. 199, turn right and drive 12 km toward the village of Gasquet (pronounced Gas-Key). We will be driving through the Josephine Peridotite; most of what is exposed is sheared and serpentinized along a northeast-striking fault zone (Fig. 4). Many landslides are evident, some of which are active.

Continue driving on U.S. 199 for ~20 km to locality 4 on Figure 4. Stop ~1 km past the second bridge (over Hardscrabble Creek) where the road becomes very wide, and rock outcrops are clearly evident along the river.

Stop 4

Park on the left side of the highway and walk down to the river. Exposed on the opposite side of the river and upstream on the highway side are sheeted dikes (Figs. 7, 8) that grade down-stream into high-level gabbro. Subparallel dikes with chilled margins are clearly evident, and gabbro screens are locally present (Fig. 8). A plagiogranite screen intruded by dikes which has been dated by

Pb/U occurs on the side opposite the highway. As the contact with the gabbro is approached (downstream), dikes become less abundant, and intrusive breccias such as those in Figure 6 become abundant. A late, highly fractionated Fe-Ti dike intrudes the sheeted dikes at a high angle (Fig. 7). A few very primitive dikes intrude the high-level gabbro and are recognized by their blue-black color and porphyritic texture.

Tilting of the crustal sequence is clearly apparent in this outcrop. Because it is situated in the core of a gently plunging syncline, the ophiolite is essentially horizontal and the ~40° dip of the dikes is due to tilting at the spreading axis. Probable oceanic faults are present in these outcrops (Fig. 7); an oceanic origin is indicated by the presence of hydrothermal veins (Fig. 8) or by the presence of an ophiolitic dike along the fault (Fig. 7).

The sheeted dikes and gabbros have amphibolite-facies assemblages resulting from high-temperature subseafloor hydrothermal metamorphism, but many are partially retrograded to greenschist facies. Epidote veins and abundant white prehnite veins occur throughout this exposure (Fig. 8), and quartz veins or quartz-matrix breccias are locally present. The prehnite veins are clearly oceanic in origin because some are cut by dikes.

Travel Between Stops 4 and 5

Return to vehicles and continue southwest on U.S. 199 to a large pullout on the left side of the road. Walk down the road and descend to the river before reaching guardrail.

Stop 5

The exposures along the river consist of gabbroic and ultramafic cumulates intruded by mafic dikes. We are still in the hinge area of a syncline so that the structures are essentially in their oceanic orientation. Igneous layering is present and dips steeply northwest. Most dikes are similar in orientation to the last stop, but many sills parallel to igneous layering are also present.

The igneous layering is discontinuous, often faint, and irregular. High-T hydrothermal alteration has resulted in mm-wide black hornblende veins and amphibolite-facies assemblages. Coarse-grained pegmatites are also common and may also be the result of high-T interaction with seawater.

Travel from Stop 5 to Crescent City, California

As we drive west on U.S. 199 toward Crescent City we will enter the small village of Hiouchi which is situated on the basal thrust which separates the Josephine ophiolite from the Franciscan Complex. This change in rock type is

reflected in a dramatic change in vegetation from Douglas Fir to Redwoods. Many of the Redwoods are more than 1000 years old and some are over 100 meters high. We will drive through several groves of giant Redwoods starting just west of Hiouchi, and we will make a stop for taking photographs. The redwoods and associated ferns once covered much of North America in the Cretaceous as indicated by fossils in coals of the western U.S. and Canada. Thus, the Redwoods are "living fossils". You may be able to imagine dinosaurs roaming through the Redwoods as often depicted in museums.

As we continue to drive west, we will drive down onto a large marine terrace which was uplifted in the Pleistocene. Crescent City is situated along the coast, at edge of the terrace. This town was largely destroyed by a tsunami resulting from the great 1964 Alaskan earthquake, and a huge "tetrapod" washed in from the breakwater sits along the side of U.S. 101. In a rare case of thoughtful urban planning, the coastal area of the town was turned into a park. Later in 1964 there was a gigantic flood that further damaged the town as well as much of coastal northern California and southwestern Oregon. This was the same flood that inundated the Galice resort on the Rogue River.

Acknowledgments

Field work and preparation was funded by NSF EAR-8518974. I thank G. Norrell and R. Alexander for their assistance.

REFERENCES

- Cannat, M., and R. Boudier, Structural study of intra-oceanic thrusting in the Klamath Mountains, northern California: Implications on accretion geometry, *Tectonics*, **4**, 435-452, 1985.
- Coleman, R.G., M.O. Garcia, and C. Anglin, The amphibolite of Briggs Creek: A tectonic slice of metamorphosed oceanic crust in southwestern Oregon?, *Geol. Soc. Am. Abs. Prog.*, **9**, 363, 1976.
- Debiche, M.G., A. Cox, and D. Engebretson, The motion of allochthonous terranes across the North Pacific basin, *Spec. Pap., Geol. Soc. Am.*, **207**, 49pp., 1987.
- Dick, H.J.B., The origin and emplacement of the Josephine Peridotite of southwestern Oregon, Ph.D. thesis, 409 pp., Yale Univ., New Haven, Conn., 1976.
- Dick, H.J.B., and T. Bullen, Chromian spinel as a petrogenetic indicator in abyssal and alpine-type peridotites and spatially associated lavas, *Contributions to Mineralogy and Petrology*, **86**, 54-76, 1984.
- Garcia, M.O., Petrology of the Rogue and Galice Formations, Klamath Mountains, Oregon: Identification of a Jurassic island arc sequence,

- J. Geol., 86, 29-41, 1979.
- Garcia, M.O., Petrology of the Rogue River island-arc complex, southwest Oregon, Am. J. Sci., 282, 783-807, 1982.
- Harper, G.D., Evidence for large-scale rotations at spreading centers from the Josephine ophiolite, Tectonophysics, 82, 25-44, 1982.
- Harper, G.D., The Josephine ophiolite, Geol. Soc. Am. Bull., 95, 1009-1026, 1984.
- Harper, G.D., Tectonics of slow-spreading mid-ocean ridges and consequences of a variable depth to the brittle/ductile transition, Tectonics, 4, 395-409, 1985.
- Harper, G.D., Freezing magma chambers and amagmatic extension in the Josephine ophiolite, Geology, 16, 831-834, 1988.
- Harper, G.D., and J.E. Wright, Middle to Late Jurassic tectonic evolution of the Klamath Mountains, California-Oregon, Tectonics, 3, 759-772, 1984.
- Harper, G.D., J.B. Bowman, and R. Kuhns, A field, chemical, and stable isotope study of subseafloor metamorphism of the Josephine ophiolite, California-Oregon, J. Geophys. Res., 93, 4625-4656, 1988.
- Harper, G.D., and R. Park, Comment on "Paleomagnetism of the Upper Jurassic Galice Formation, southwestern Oregon: Evidence for differential rotation of the eastern and western Klamath Mountains", Geology, 14, 1049-1050, 1986.
- Harper, G.D., J.B. Saleeby, and E. Norman, Geometry and tectonic setting of sea-floor spreading for the Josephine ophiolite, and implications for Jurassic accretionary events along the California margin, in Tectonostratigraphic Terranes of the Circum-Pacific Region, Earth Sci. Ser. vol. 1, edited by D. Howell, pp. 239-257, Circum-Pacific Council for Energy and Mineral Resources, Houston, Tex., 1985.
- Harper, G.D., J.B. Saleeby, S. Cashman, and E. Norman, Isotopic age of the Nevadan orogeny in the western Klamath Mountains, California-Oregon, Geol. Soc. Am. Abs. Prog., 18, 114, 1986.
- Hotz, P.E., Plutonic rocks of the Klamath Mountains, California and Oregon, U.S. Geol. Surv. Bull., 1290, 91 pp., 1971.
- Imlay, R.W., Jurassic paleobiogeography of conterminous United States in its continental setting, U.S. Geol. Surv. Prof. Pap. 1062, 134 pp., 1980.
- Irwin, W.P., Tectonic accretion of the Klamath Mountains, The Geotectonic Development of California, edited by W.G. Ernst, pp. 29-49, Rubey Series 1, Prentice-Hall, Englewood Cliffs, N.J., 1981.
- Jachens, R.C., C.G. Barnes, and M.M. Donato, Subsurface configuration of the Orleans fault: Implications for deformation in the western Klamath Mountains, California, Geol. Soc. Am. Bull. 97, 388-395, 1986.
- Kays, A., Zones of alpine tectonism and metamorphism Klamath Mountains, southwestern Oregon, J. Geol., 76, 17-36, 1968.
- Koski, R.A., and R.E. Derkey, Massive sulfide deposits in oceanic-crust and island-arc terranes of southwestern Oregon, Oregon Geology, 43, 119-125, 1981.
- May, S.R., and R.R. Butler, North American Jurassic apparent polar wander: Implications for plate motion, paleogeography and Cordilleran tectonics, J. Geophys. Res., 91, 1986.
- Miller, M. M., and J.B. Saleeby, Detrital zircon studies of the Galice formation: common provenance of strata overlying the Josephine ophiolite and Rogue island arc -- western Klamath Mountains (abstract), Geol. Soc. Am. Abs. Prog., 19, 772-773, 1987.
- Nilsen, T.H., Stratigraphy, sedimentology, and tectonic framework of the upper Cretaceous Hornbrook Formation, Oregon and California, Geology of the Upper Cretaceous Hornbrook Formation, Oregon and California, edited by T.H. Nilsen, Pacific Section S.E.P.M. 42, 51-88, 1984.
- Norrell, G.T., and G.D. Harper, Detachment faulting and amagmatic extension at mid-ocean ridges: The Josephine ophiolite as an example, Geology, 16, 827-830, 1988.
- Norrell, G.T., A. Teixell, and G.D. Harper, Microstructure of serpentinite mylonites from the Josephine ophiolite and serpentinization in retrogressive shear zones, Geol. Soc. Am. Bull., in press, 1988.
- Park-Jones, R., Sedimentology, structure, and geochemistry of the Galice Formation: Sediment fill of a back-arc basin and island arc in the western Klamath Mountains, M.S. thesis, 165 pp., State Univ. New York, 1988.
- Pessagno, E.A., Jr., and C.D. Blome, Biostratigraphic, chronostratigraphic, and U/Pb geochronometric data from the Rogue and Galice Formations, western Klamath Terrane (Oregon and California): -- Their bearing on the age of the Oxfordian-Kimmeridgian boundary and the *Mirifusus* first occurrence event, Proc. 2nd International Symposium on Jurassic Stratigraphy, Lisbon, Portugal, 14 pp., 1988.
- Pessagno, E.A., Jr., and S. Mizutani, Correlation of radiolarian biozones of the eastern and western Pacific (North America and Japan), in Jurassic of the Circum-Pacific Region, edited by G.E.G. Westermann, in press, 1988.
- Pinto-Auso, M., and G.D. Harper, Sedimentation, metallogenesis, and tectonic origin of the basal Galice Formation overlying the Josephine ophiolite, northwestern California, J. Geol., 93, 713-725, 1985.
- Riley, T.A., The petrogenetic evolution of a Late Jurassic island arc: the Rogue Formation, Klamath Mountains, Oregon, M.S. thesis, 40 pp., Stanford Univ., 1987.

- Roure, F., and P. DeWever, Triassic cherts discovered in the western Jurassic belt of the Klamath Mountains, southwestern Oregon, U.S.A.: Implications for the age of the Josephine ophiolite, C. R. Acad. Sci. Paris, 297, 161-164, 1983.
- Saleeby, J.B., Pb/U zircon ages from the Rogue River area, western Jurassic belt, Klamath Mountains, Oregon, Geol. Soc. Am. Abs. Prog., 16, 331, 1984.
- Saleeby, J.B., Discordance patterns in Pb/U zircon ages of the Sierra Nevada and Klamath Mountains (abstract), Eos Trans. AGU, 68, 1514-1515, 1987.
- Saleeby, J.B., G.D. Harper, A.W. Snoke, and W. Sharp, Time relations and structural-stratigraphic patterns in ophiolite accretion, west-central Klamath Mountains, California, J. Geophys. Res., 87, 3831-3848, 1982.
- Schiffman, P., and B.M. Smith, Petrology and oxygen-isotope geochemistry of a fossil seawater hydrothermal system within the Solca graben, northern Troodos Ophiolite, Cyprus, J. Geophys. Res., 93, 4612-4624, 1988.
- Sempere, J.-C., and Macdonald, K.C., Marine tectonics: Processes at mid-ocean ridges, Rev. Geophys., 25, 1313-1347, 1987.
- Seyfried, W.E., Jr., M.E. Berndt, and J.S. Seewald, Hydrothermal alteration processes at mid-ocean ridges: Constraints from diabase alteration experiments, hot spring fluids and composition of the oceanic crust, Can. Mineral., in press, 1988.
- Smith, J.G., N.J. Page, M.G. Johnson, B.C. Moring, and F. Gray, Preliminary geologic map of the Medford 1°x2° quadrangle, Oregon and California, U.S. Geol. Surv. Open File Rep., 82-955, 1982.
- Wagner, D., and G.J. Saucedo, Geologic map of the Weed quadrangle, scale 1:250,000, California, Calif. Div. of Mines Geol., Sacramento, 1987.
- Wood, R.A., Geology and geochemistry of the Almeda mine, Josephine County, Oregon, M.S. thesis, California State University, Los Angeles, 237 pp., 1987.
- Wright, J.E., and S.J. Wyld, Significance of xenocrystic Precambrian zircon contained within the southern continuation of the Josephine ophiolite: Devils Elbow ophiolite remnant, Klamath Mountains, northern California, Geology, 14, 671-674, 1986.
- Wright, J.E., and M.R. Fahan, An expanded view of Jurassic orogenesis in the western United States Cordillera: Middle Jurassic (pre-Nevadan) regional metamorphism and thrust faulting within an active arc environment, Klamath Mountains, California, Geol. Soc. Am. Bull., 100, 859-876, 1988.
- Wyld, S.J., and J.E. Wright, The Devils Elbow ophiolite remnant and overlying Galice Formation: New constraints on the Middle to Late Jurassic evolution of the Klamath Mountains, California, Geol. Soc. Am. Bull., 100, 29-44, 1988.

A rift-edge facies of the Late Jurassic Rogue–Chetco arc and Josephine ophiolite, Klamath Mountains, Oregon

J. Douglas Yule*

Jason B. Saleeby

*Division of Geological and Planetary Sciences, California Institute of Technology,
Pasadena, California 91125, USA*

Calvin G. Barnes

Department of Geosciences, Texas Tech University, Lubbock, Texas 79409, USA

ABSTRACT

The western Jurassic belt of the Klamath Mountains represents one of the Earth's best-preserved exposures of ancient marginal ocean basin lithosphere and chiefly consists of the coeval Rogue–Chetco volcanic-plutonic oceanic arc and Josephine ophiolite. This Late Jurassic ocean basin is hypothesized to have formed in response to rifting that initiated at ca. 165 Ma along the western margin of North America, disrupting a Middle Jurassic arc that had been constructed on older Klamath terranes and forming a marginal ocean basin with an active arc, inter-arc basin, and remnant arc. Previous workers characterized a “rift-edge” facies in the remnant-arc region. This chapter describes field, age, and geochemical data that suggest that a similar rift-edge facies exists in the vicinity of the active arc, on the opposite side of the marginal basin.

The rift-edge facies in the active arc setting consists of two main lithotectonic units, herein named informally as the Onion Camp complex and Fiddler Mountain olistostrome. The Onion Camp complex is partly composed of a characteristic metabasalt and red chert association. Red chert yielded scarce radiolarians of Triassic(?) and Early Jurassic age. A distinct chert-pebble conglomerate occurs at scarce localities within metasedimentary rocks. Concordant, composite bodies of amphibolite and serpentinitized peridotite represent another distinctive feature of the Onion Camp complex. The metamorphic and lithologic features of the Onion Camp complex are similar to the lower *mélange* unit of the Rattlesnake Creek terrane, and the units are interpreted to be correlative. The Fiddler Mountain olistostrome is composed of Late Jurassic (Kimmeridgian?) pelagic and hemipelagic rocks interlayered with ophiolite-clast breccia and megabreccia, similar in character to olistostromal deposits associated with the rift-edge facies of the remnant arc. The occurrence of the Rattlesnake Creek terrane and an associated olistostromal deposit within the western Jurassic belt of southwestern Oregon may therefore represent the rift-edge facies in the active arc setting, at the transition between the Rogue–Chetco arc and Josephine ophiolite,

*Present address: California State University, Department of Geological Sciences, Northridge, California 91330-8266, USA; j.d.yule@csun.edu.

Yule, J.D., Saleeby, J.B., and Barnes, C.G., 2006, A rift-edge facies of the Late Jurassic Rogue–Chetco arc and Josephine ophiolite, Klamath Mountains, Oregon, in Snoke, A.W., and Barnes, C.G., eds., Geological studies in the Klamath Mountains province, California and Oregon: A volume in honor of William P. Irwin: Geological Society of America Special Paper 410, p. 53–76, doi: 10.1130/2006.2410(03). For permission to copy, contact editing@geosociety.org. ©2006 Geological Society of America. All rights reserved.

further corroborating previous models for the Late Jurassic tectonic evolution of the Klamath Mountains.

Keywords: ancient marginal ocean basin, rifting, Rogue–Chetco volcanic-plutonic arc, Josephine ophiolite, olistostromal deposits, radiolarians, Rattlesnake Creek terrane, Late Jurassic, Klamath Mountains, Oregon

INTRODUCTION

Marginal ocean basins of the western Pacific commonly form in extension-dominated tectonic settings above subduction zones where subduction of relatively old oceanic lithosphere occurs (e.g., Curray et al., 1979; Stern and Bloomer, 1992; Lagabriele et al., 1997). They consist of oceanic lithosphere that is composite in nature and may record multiple magmatic and/or deformational episodes (Pearce et al., 1984; Parson and Wright, 1996; Lagabriele et al., 1997; Hawkins, 2003). Primary petrotectonic elements of these ocean basins include active arcs, remnant arcs, and spreading centers that can occur in fore-arc, inter-arc, and/or back-arc settings (Karig, 1971; Uyeda, 1977). Lithosphere generated at marginal ocean basin spreading centers therefore can separate “matching” rifted fragments of older oceanic lithosphere that typically occurs beneath the remnant and active magmatic arcs (Fig. 1).

Ancient marginal ocean basin lithosphere exposed in the western Jurassic belt of the Klamath Mountains (Fig. 1) chiefly consists of the accreted Rogue–Chetco arc and Josephine ophiolite (Garcia, 1979, 1982; Harper, 1980, 1984) that apparently formed in the Late Jurassic when a Middle Jurassic arc system rifted apart, leaving a remnant arc along the western edge of North America (e.g., Snoke, 1977; Saleeby et al., 1982; Harper and Wright, 1984). Snoke (1977) described a Late Jurassic mafic complex near Preston Peak that intruded the Rattlesnake Creek terrane, a basement unit of the Middle Jurassic arc, and interpreted the Preston Peak region to represent a rift-edge facies of the Josephine ophiolite. The identification of a rift-edge facies in the remnant arc setting implies that a similar facies may exist on the opposite side of the marginal ocean basin—perhaps in the active arc setting.

A clue that a rift-edge facies might exist in the active arc setting was provided by Roure and DeWever (1983), who reported a Late Triassic age from red chert collected to the west of Kerby, Oregon (Fig. 1). Paradoxically, Late Triassic to Early Jurassic chert occurs commonly in the Rattlesnake Creek terrane and related terranes exposed in the remnant arc setting to the east of, and structurally above, the western Jurassic belt (e.g., Irwin et al., 1982). The primary objective of this chapter, therefore, is to describe the rocks associated with the Triassic chert reported by Roure and DeWever (1983) and to explore the stratigraphic and structural relationships between these uncharacteristic rocks of the western Jurassic belt and rocks of the Rogue–Chetco arc and Josephine ophiolite. The occurrence of

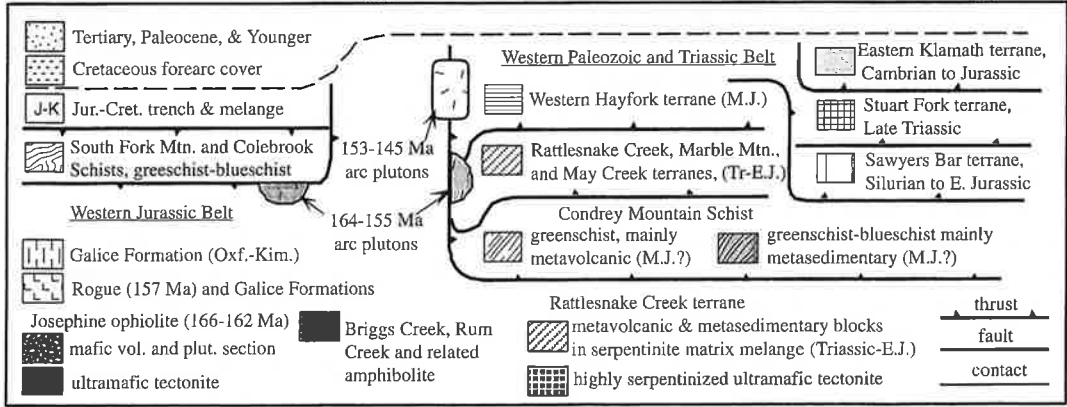
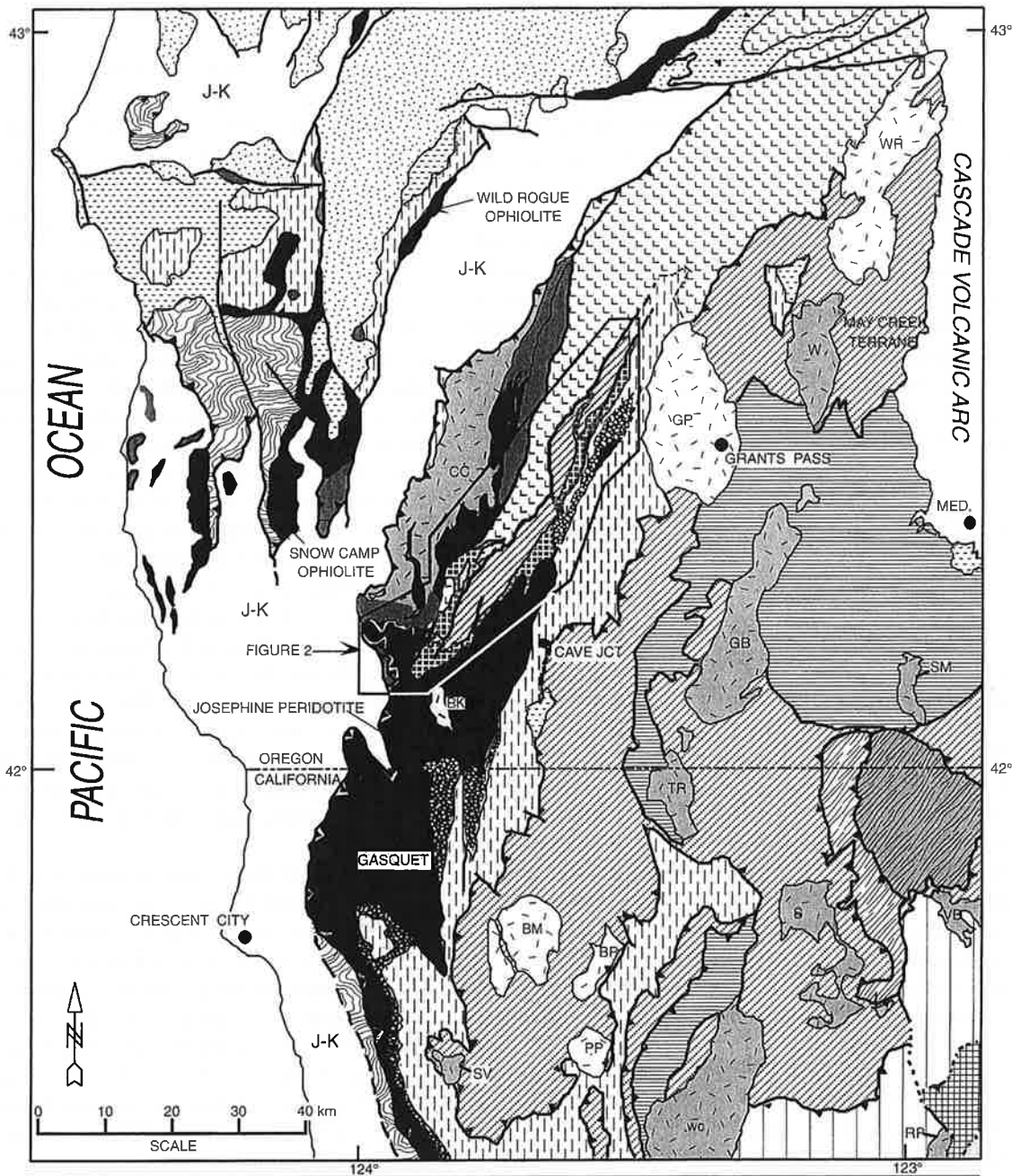
rocks similar to the Rattlesnake Creek terrane within the western Jurassic belt supports previous tectonic models that interpret the Rogue–Chetco arc and Josephine ophiolite as integral parts of a Late Jurassic marginal ocean basin that formed in response to rifting of older Klamath Mountains terranes (Snoke, 1977; Saleeby et al., 1982; Harper and Wright, 1984; Harper, 2003).

GEOLOGIC AND TECTONIC FRAMEWORK

Regional, east-dipping thrust faults bound the western Jurassic belt of southwestern Oregon. To the east, the Orleans/Preston Peak thrust forms an upper tectonic boundary where rocks of the western Paleozoic and Triassic belt form a hanging-wall sheet above the western Jurassic belt (e.g., Irwin, 1960, 1966, 1972; Davis, 1969; Snoke, 1977; Hamilton, 1978; Burchfiel and Davis, 1981). To the west, rocks of the Franciscan Complex are underthrust beneath the Valen Lake thrust, the western tectonic boundary of the western Jurassic belt (Ramp, 1977; Page et al., 1981; Blake et al., 1985; Fig. 1). Numerous northeast–southwest-striking faults and folds deform rocks of the western Jurassic belt, probably as a result of imbrication and emplacement of the large thrust sheets emplaced between ca. 155 and 150 Ma, the interpreted age of the Nevadan orogeny at this latitude (Saleeby et al., 1982; Harper and Wright, 1984; Harper et al., 1994).

The western Jurassic belt can be subdivided into three Late Jurassic petrotectonic units: the Josephine ophiolite (Harper, 1984, 2003); Rogue–Chetco volcano-plutonic arc complex and related metamorphic wall rocks (Jorgenson, 1970; Hotz, 1971; Dick, 1976; Loney and Himmelberg, 1977; Garcia, 1979, 1982; Saleeby, 1984; Coleman and Lanphere, 1991; Yule, 1996); and the Upper Jurassic Galice Formation, a flysch sequence, which overlaps both the ophiolite and arc-volcanic rocks (Harper, 1980; Miller and Saleeby, 1995). These units are part of a Late

Figure 1. Regional geologic map of the northern Klamath Mountains province and Oregon Coast Ranges. Outline shows area of Figure 2. Pluton names are: BK—Buckskin Peak, BM—Bear Mountain, BP—Bear Peak, CC—Chetco complex, GB—Grayback, GP—Grants Pass, PP—Pony Peak, RP—Russian Peak, S—Slinkard, SM—Squaw Mountain, SV—Summit Valley, TR—Thompson Ridge, VB—Vesa Bluffs, W—Wimer, WC—Wooley Creek, and WR—White Rock. Jurassic stages are: Kim.—Kimmeridgian, Oxf.—Oxfordian. Modified from Ramp (1977), Ramp and Peterson (1979), Coleman and Lanphere (1991), Irwin (1994), and Hacker et al. (1995).



Jurassic marginal ocean basin assemblage that is constructed of oceanic-arc plutonic and intra-arc ophiolitic crust and mantle rocks, and subsequently was overlapped by laterally equivalent arc-volcanic rocks and flysch deposits (Saleeby et al., 1982; Harper and Wright, 1984; Harper et al., 1994; Harper, 2003).

This study identifies two additional petrotectonic units, the Onion Camp complex and Fiddler Mountain olistostrome, which were previously mapped as part of the Rogue–Chetco arc complex. These new units share a striking resemblance with rocks of the Rattlesnake Creek terrane (e.g., Irwin, 1972; Snoke, 1977; Wright and Wyld, 1994) and Lems Ridge olistostrome (Ohr, 1987), respectively. Both the Rattlesnake Creek terrane and olistostromal deposits appear to be correlative with components of the western Paleozoic and Triassic belt in the hanging wall of the Orleans/Preston Peak thrust to the east of the study area (Snoke, 1977; Wright and Fahan, 1988; Hacker et al., 1995; Fig. 1).

ONION CAMP COMPLEX

Overview

The Onion Camp complex is named for an association of rocks at Onion Camp, northwest of Fiddler Mountain, that occur along a 3- to 5-km-wide, ~40-km-long, northeast–southwest-striking belt, extending from near Canyon Peak on the southwest to the Rogue River on the northeast (Fig. 2). In addition, isolated patches of the Onion Camp complex occur ~4 km to the southeast of Oak Flats, along the western margin of the Chetco plutonic complex (Fig. 2). Hill slopes underlain by the complex are very steep and densely vegetated, so exposure is limited to weathered roadcuts and ridgelines. The best exposures occur along the Illinois and Rogue Rivers, where up to 500-m-long outcrops can be studied. Other excellent exposures of Onion Camp complex rocks occur in road gravel quarries near Onion Camp and Onion Mountain and in cirque exposures surrounding Babyfoot Lake (Fig. 2).

Rocks of the Onion Camp complex were previously included as part of the Rogue Formation by Wells and Walker (1953). Subsequent workers noted differences between the type Rogue Formation and rocks near Onion Camp but did not subdivide the unit (Wise, 1969; Dick, 1976; Ramp, 1977, 1984; Ramp and Peterson, 1979; Page et al., 1981). Roure and DeWever (1983) collected red chert from near Onion Camp (F. Roure, personal commun., 1993) that yielded a Triassic age, an unusually old age for rocks of the western Jurassic belt, suggesting that rocks here may have experienced a more complex geologic history than previously recognized.

The Onion Camp complex consists primarily of mafic metavolcanic rocks, metachert, argillaceous metasedimentary rocks, a heterogeneous mafic intrusive complex, amphibolite and amphibolite gneiss, and serpentized harzburgite and dunite. Less common rock types include hornblende schist, garnet-mica quartzite, and lenses of variably sheared serpentinite.

Rock Units

Metavolcanic Rocks. Metavolcanic rocks compose most of the Onion Camp complex. Fresh samples exhibit a light green to dark gray-green hue, a manifestation of the abundant ferromagnesian, greenschist-facies minerals that characterize these rocks. Lithotypes can be classified into four main groups: (1) metamorphosed mafic lavas, locally amygdaloidal and pillowed (Fig. 3); (2) lava breccias (plagioclase > clinopyroxene-phyric clasts); (3) metamorphosed mafic volcanoclastic rocks (mainly pyroclastic deposits) consisting of fine-grained mafic tuffs and tuff breccias with highly flattened and altered lithic clasts and lapilli; and (4) metamorphosed, shallow-level mafic intrusive bodies and dikes (chilled dike and sill margins are present at a few localities). Massive lavas are the most common rocks, with subordinate amounts of fragmental volcanic rocks; shallow mafic intrusions and dikes are least common, comprising <10% of the metavolcanic rocks of the Onion Camp complex. The average chemical composition of the Onion Camp complex metavolcanic rocks is basaltic andesite (Yule, 1996).

The metavolcanic rocks of the Onion Camp complex consist chiefly of lower greenschist-facies minerals. Original igneous phases are commonly altered, partly or wholly, to various hydrous phases, but relict plagioclase (>An₅₀) and/or augite are present in many samples. The typical greenschist-facies assemblage is albite, quartz, actinolite, epidote, chlorite, white mica, and calcite. Pyrite and sphene are common accessory phases. Pumpellyite is present in some mafic lava samples. Abundant prehnite, quartz-prehnite, and quartz-calcite veins cut all exposures.

Layering in fine-grained fragmental volcanic rocks is discontinuous, probably due to shearing that transposed layering into parallelism with the regional northeast-striking, southeast-dipping foliation. Elongate pillow lobes (Fig. 3) may record paleohorizontal; however, like the fragmental rocks, the elongation orientation is parallel to the regional foliation. Non-clastic rocks are typically massive, but break along a cleavage that is parallel to the regional foliation. Tuffaceous rocks vary texturally and are ubiquitously metamorphosed; protoliths include crystal tuff, lithic lapilli tuff, and crystal-lithic tuff. Some of these rocks have been converted to chlorite schist.

Red Chert. Red chert blocks and lenses up to 10-m across crop out near metamorphosed pillowed and massive lavas, and are most common near Onion Camp, ~2 km to the west of Fiddler Mountain and Onion Mountain (Fig. 2). Red and whitish-red chert blocks commonly show transposed compositional layering and a sugary texture indicative of complete recrystallization. Interlayers of maroon chert 2- to 5-cm thick show original compositional layering that is oblique to the regional foliation. The maroon layers commonly contain clear, sub-mm-scale ovoids, which probably represent slightly recrystallized radiolarians.

Metasedimentary Rocks. Northeast–southwest-striking belts of metasedimentary rocks are most common along the eastern

margin of the Onion Camp complex. The most common rock type is siliceous argillite with lesser amounts of impure red, white, and gray chert; tuffaceous siltstone; and rare polymictic sandstone, conglomerate, and conglomeratic sandstone. Colors range from white to greenish gray, with local red to reddish-brown interlayers. All metasedimentary rocks break along an imperfect slaty cleavage.

Within the larger metasedimentary belts, distinctive but scarce polymictic conglomeratic sandstone layers occur as m to several-m-thick interbeds in predominantly wacke, siltstone, and siliceous argillite. Poorly to moderately sorted sand- and pebble- to cobble-sized rock clasts are subangular to subrounded. The coarse-grained conglomerates are generally matrix supported. Clasts in the sandstones and conglomerates are diverse and include wacke, siltstone, siliceous argillite, recrystallized chert (with relict radiolarians), sugary quartzite, monocrystalline quartz, mafic volcanic rocks (with porphyritic, intergranular, and spherulitic textures), and recrystallized limestone. Siliceous argillite and chert are by far the most abundant clast types. Volcanic clasts, though present, are subordinate in volume to sedimentary clasts. The conglomeratic sandstone is therefore distinct from other polymict deposits in the region that primarily consist of mafic volcanic and/or shallow-level intrusive clasts; for example, see the description of Fiddler Mountain olistostrome later in this chapter.

The metasedimentary rocks of the Onion Camp complex consist primarily of quartz, phyllosilicates, and opaque oxides. Secondary minerals are calcite, albite, and pyrite; accessory minerals include zircon, apatite, and sphene. Tuffaceous layers contain chlorite, albite porphyroclasts, and minor epidote.

Original stratification is rarely preserved, but when present, it is generally parallel or nearly parallel to the regional foliation and rock cleavage. Lithologic layering tends to pinch out along strike, probably reflecting a high degree of bedding transposition. Boudinage of chert and silicic argillite layers is common. The rocks are well indurated, intensely strained, and structurally interlayered.

Amphibolite and Amphibolite Gneiss. Discontinuous belts of foliated-to-massive amphibolite and amphibolite gneiss with subordinate impure quartzite occur throughout the Onion Camp complex (Fig. 2). Quartzose layers are most abundant in the amphibolite masses near Squaw Mountain, where they occur as infolded layers within outcrops consisting mostly of hornblende schist and amphibolite gneiss. In hand samples and in thin sections, the quartzites consist of sugary-textured, fine- to medium-grained, banded, well-foliated and lineated rocks. Previous researchers have described these rocks as gneissic migmatite (Wells et al., 1949), metagabbro (Ramp, 1977), and gabbroic rocks and dike complexes (Page et al., 1981) and have interpreted their origin as small intrusions into the Rogue Formation or its metamorphosed equivalent. However, the findings of this study suggest that the protolith materials were greenschist-facies, mafic metavolcanic, and subordinate metasedimentary rocks of the Onion Camp complex.

All occurrences of amphibolite within the Onion Camp complex are at least partially bounded by variably sheared and serpentized peridotite (Fig. 2). Local slivers of sheared serpentinite are contained entirely within the amphibolite. Small, isolated bodies of amphibolite have highly sheared and discordant contacts with serpentized peridotite and show ubiquitous, retrograde greenschist-facies and lower-grade alterations. In contrast, contacts between the larger amphibolitic belts and serpentized peridotite are weakly sheared, and rocks on either side of the contact have subparallel foliations. This finding suggests that these amphibolite and peridotite units comprise coherent, composite blocks.

The amphibolite consists of hornblende and plagioclase with subordinate epidote, sphene, and Fe-Ti opaque oxides (mostly ilmenite). Common alteration minerals include chlorite, epidote, clinozoisite, prehnite, green amphibole, white mica, and quartz. Hornblende usually comprises 60–80% of the rock. Plagioclase is generally untwinned and ranges in composition from albite to intermediate oligoclase in epidote-absent amphibolites. Impure quartzite consists of 60–90% quartz with metamorphic cumingtonite, almandine, biotite, white mica, and opaque oxides.

At Squaw Mountain, a distinct change from greenschist-facies to epidote-amphibolite-facies assemblages occurs across a narrow (<2-m-wide) zone (Fig. 2). In this zone, actinolite-chlorite schist, metabasalt, and impure chert abruptly change to hornblende schist, gneissic amphibolite, and impure meta-quartzite. This is coincident with a change in metamorphic assemblage from actinolite + chlorite + epidote + albite to hornblende + epidote + albite. In addition, the rocks become more coarsely crystalline across this boundary. A few exposures show plagiogranite dikelets and segregations cutting the highest-grade amphibolites.

Structural features include a faint to well-developed foliation that shows a faint to well-developed intersection lineation parallel to the hinge lines of tight to isoclinal folds. These folds are probably synmetamorphic and developed during amphibolite-facies metamorphism. Postmetamorphic, close to isoclinal folds deform the foliation and earlier folds.

Serpentinized Peridotite. Ultrabasic rocks of the Onion Camp complex occur as blocks, small lenses, and smears of sheared serpentinite (slickenite) and serpentized peridotite that show a sharp to gradational contact with, but are distinct from, the Josephine peridotite (Fig. 2). This gradation is typically marked in the field by a distinct change in hill slope vegetation that is conspicuous on air photos and is easily visible in the field (Fig. 4A). The Onion Camp complex serpentinite forms smooth, subdued topography with sparse to grassy vegetation that is subject to landslides and other downslope movements, whereas the Josephine peridotite forms blocky, resistant outcrops and rugged topography. Distinctions between the Onion Camp complex and Josephine peridotite can also be made on the basis of different crosscutting relations, metamorphic mineral assemblages, and structural features. Contacts between

Explanation of Geologic Map and Cross Section

CROSS-STITCHING PLUTONIC ROCKS

Jh mafic to intermediate hornblende-phyric dikes and small intrusions; U-Pb, K-Ar, and Ar-Ar ages cluster at ca. 150 Ma (Yule, 1996; Dick, 1976; and Harper et al., 1994).

QUATERNARY

Q Unconsolidated silt, sand, and gravel deposits occupying modern stream and river channels, and associated low terraces and flood plains.

SURFICIAL DEPOSITS

Jg Galice Formation; basal hemipelagic section of Callovian age overlain by flysch sequence of Oxfordian-Kimmeridgian age (Pessango and Blome, 1990).

INTER-ARC BASIN VOLCANIC AND SEDIMENTARY ROCKS

Jr Rogue Formation; massive to well-bedded, basaltic to andesitic volcanogenic turbidites, volcanic breccias, and flows; 157 Ma (U-Pb zircon, Saleeby, 1984), 153 Ma (Ar/Ar hornblende, Yule, 1996).

Jf Fiddler Mountain olistostrome; polymictic conglomerate, breccia, and megabreccia - ophiolite-clast types dominate, with subordinate chert and serpentine-clast types - interlayered with well-bedded sequences of chert and argillite (thin dashed lines near Fiddler Mtn. (FM)). Chert yields poorly preserved Late Jurassic (Kimmeridgian?) radiolaria (Yule et al., 1992).

CHETCO PLUTONIC COMPLEX

Jt weakly foliated tonalite-trondhjemite sill-like complex occupying high structural levels of plutonic complex (157 Ma, U-Pb zircon, Yule, 1996).

Jpd main phase of complex; foliated to massive biotite-hornblende quartz diorite; hornblende gabbro-diorite, and norite (160 Ma, U-Pb zircon, Yule, 1996).

Jog layered olivine gabbro and two-pyroxene gabbro forming the core of the plutonic complex. marginal facies consisting of faser quartz diorite, diorite, and gabbro with shallowly plunging lineations and steeply dipping foliations.

METAMORPHIC WALLROCKS

b Briggs Creek amphibolite (e.g., Coleman and Lanphere, 1991); amphibolite gneiss, schist, and impure quartzite (156-158 Ma, Ar/Ar amphibole, Yule, 1996).

a amphibolite and amphibolite gneiss; biotite-hornblende schist; impure quartzite and metagabbro found in metamorphic sole of Madstone Cabin thrust (148-153 Ma, Ar/Ar muscovite and hornblende, and U-Pb zircon, Harper et al., 1994).

LATE MIDDLE AND LATE JURASSIC

ONION CAMP COMPLEX

Jm heterogeneous mafic intrusive complex, consisting of diabase, gabbro, and sheeted mafic dikes; most extensive outcrop belts occur in areas near Whetstone Butte (WB), with local, smaller belts (not shown) occurring throughout the metavolcanic and metasedimentary sequence (JTrvs); age unknown, but may be broadly correlative with Josephine ophiolite gabbro, mafic dikes.

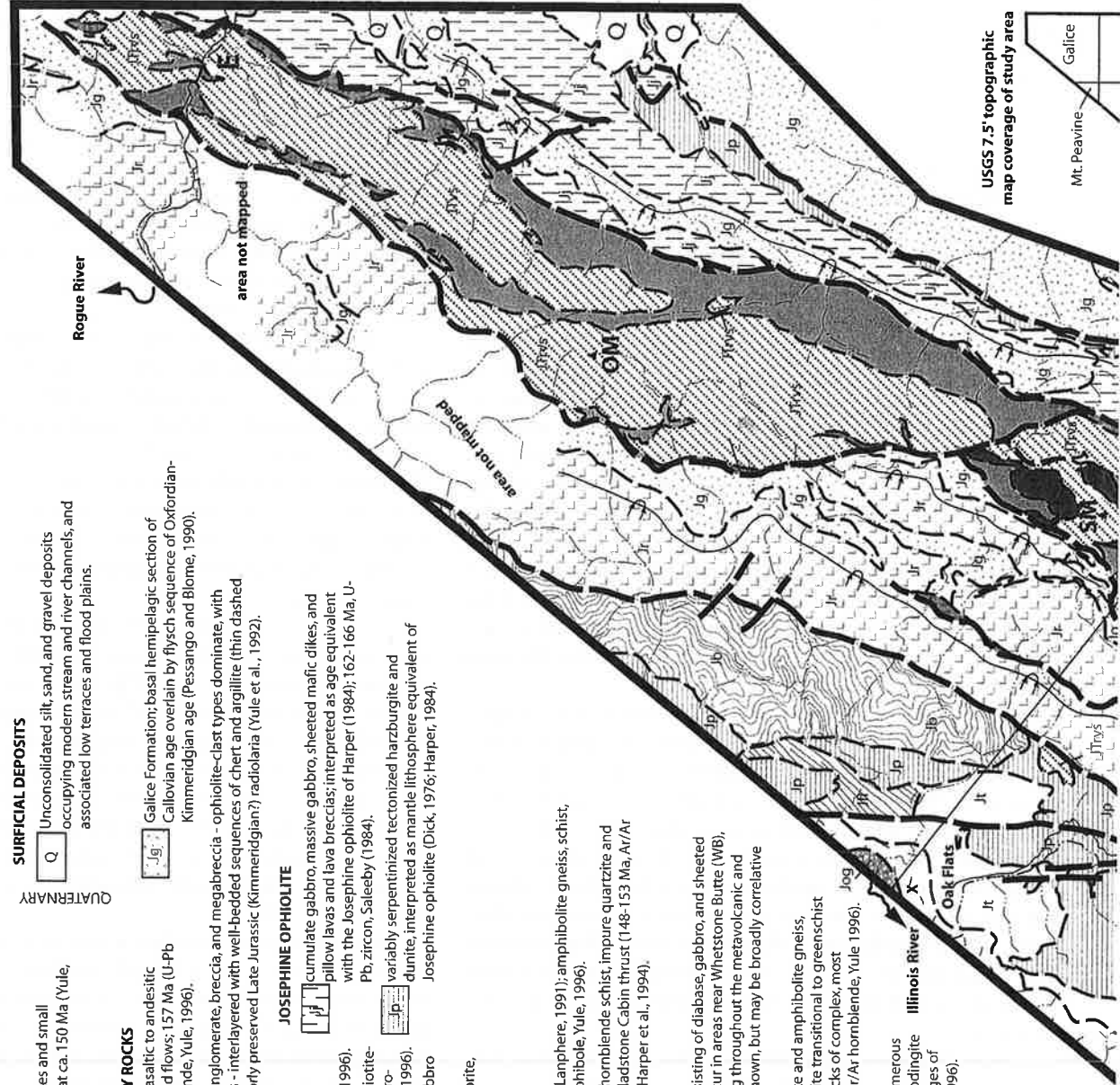
Jm complexly folded outcrop belts of amphibolite and amphibolite gneiss; biotite-hornblende schist, and impure quartzite transitional to greenschist facies metavolcanic and metasedimentary rocks of complex, most common near Squaw Mtn (SM); 170-173 Ma, Ar/Ar hornblende, Yule 1996).

Jm highly serpentinized and sheared dunite, harzburgite, and sparse websterite; cut by numerous intermediate to mafic dikes, and occasional rodingite dikes; plagiogranite dikes yield U-Pb zircon ages of 173 and 175 Ma (Table 2, this chapter; Yule, 1996).

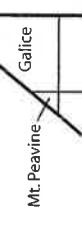
Jm greenschist facies metavolcanic and metasedimentary rocks, including massive greenstone, pillow lava, tuff and tuff-breccia, argillite and red chert; chert samples yield mostly amorphous radiolaria with scarce Triassic(?) and Jurassic forms (Yule et al., 1992; C. Blome, personal communication, 1992).

PRE-MIDDLE JURASSIC

TRIASSIC (?)



USGS 7.5' topographic map coverage of study area



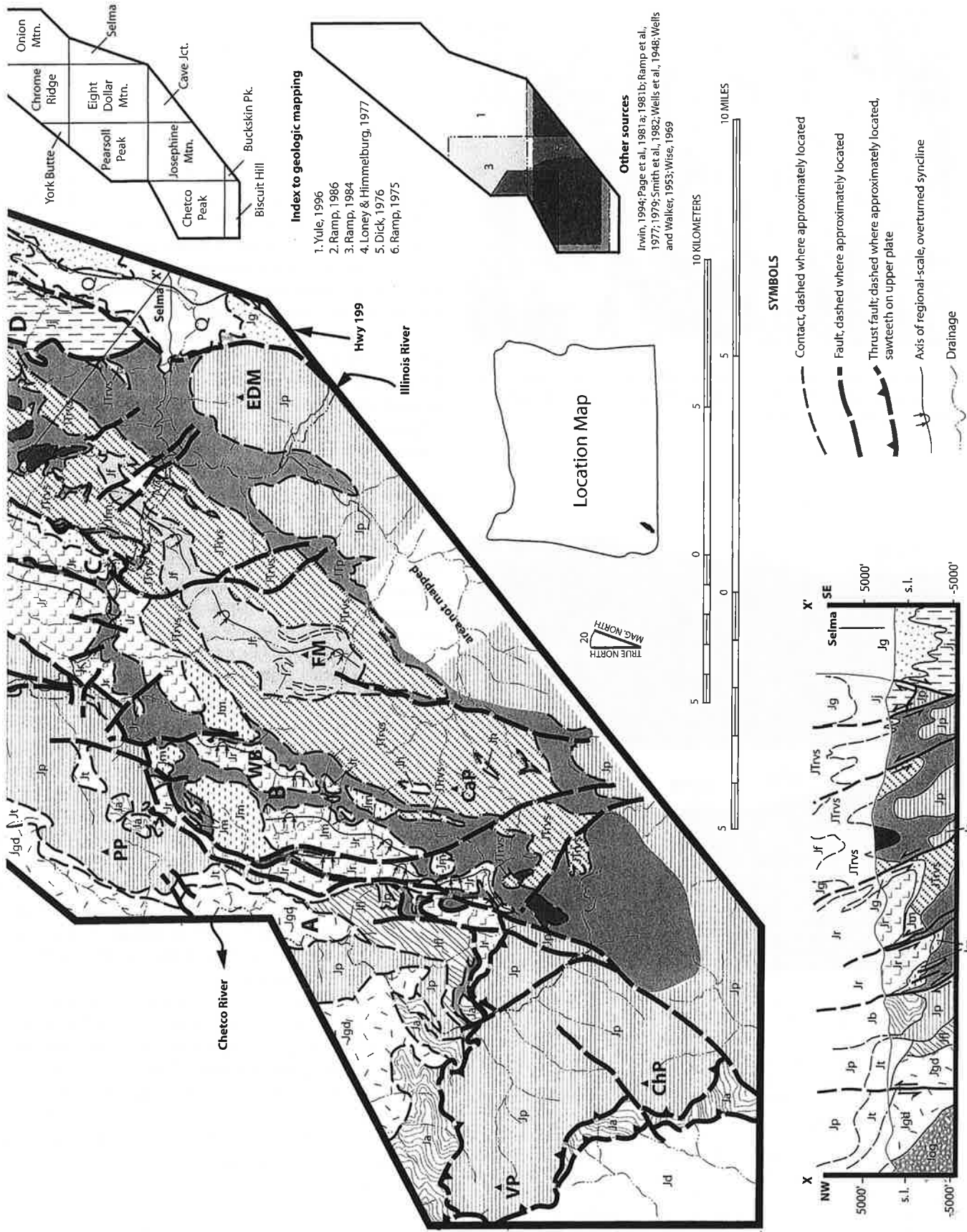


Figure 2. Geologic map, cross-section along X-X', and explanation of part of the western Jurassic belt, Klamath Mountains, Oregon. CaP—Canyon Peak, ChP—Chetco Peak, EDM—Eight Dollar Mountain, OM—Onion Mountain, PP—Pearsoll Peak, SM—Squaw Mountain, WB—Whetstone Butte, VP—Vulcan Peak. Bold-faced letters A-E refer to locations of columnar sections shown in Figure 15. This figure is also on the CD-ROM accompanying this volume as a continuous image.

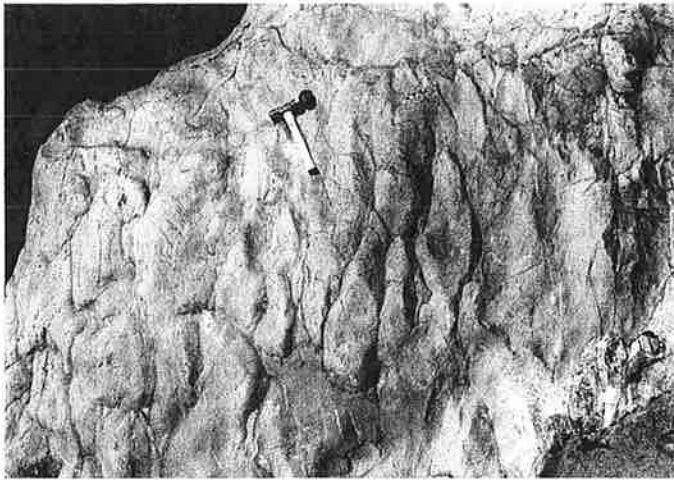


Figure 3. Photograph of river polished pillow lavas of the Onion Camp complex, locality EDM-83 (see Table 3A for latitude and longitude), north bank of the Illinois River.

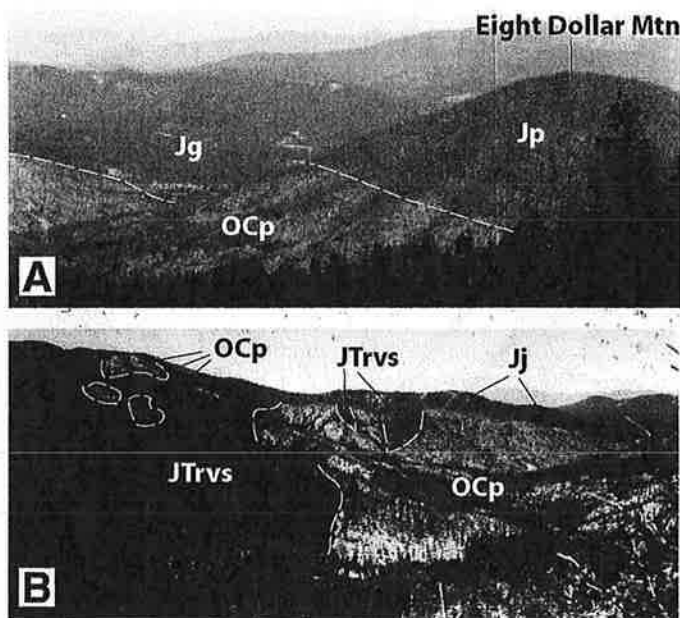


Figure 4. (A) Photograph of Eight Dollar Mountain, view toward the northeast. Vegetation change, indicated by dashed line on the west flank of Eight Dollar Mountain, marks the boundary between highly serpentinized peridotite of the Onion Camp complex (OCp) and relatively un-serpentinized Josephine peridotite (Jp). Valley to the northeast is underlain by Galice Formation (Jg). (B) Photograph looking upstream along the Illinois River, view to the northeast. Heavily vegetated slopes are underlain by metabasaltic and metasedimentary rocks of the Onion Camp complex (JTrvs) and Josephine ophiolite (Jj), and the relatively sparsely vegetated hillslopes are underlain by OCp. Small patches of barren slopes in the upper left are underlain by complexly folded serpentinite (OCp) near Squaw Mountain (Fig. 2). Small densely vegetated patches in the center are underlain by JTrvs and surrounded by OCp.

serpentinite and other units vary from a nonconformity beneath deposits of the Rogue Formation and Fiddler Mountain olistostrome to a variably sheared boundary with greenschist- to amphibolite-grade metamorphosed units of the Onion Camp complex (Figs. 2 and 4B).

Outcrops of Onion Camp complex serpentinite and serpentinized peridotite range from massive and blocky, unaffected by shearing, to incoherent, highly sheared, platy serpentinite. The massive outcrops generally weather brown to reddish orange, with weathered surfaces studded by aggregates of primary minerals, mostly to wholly pseudomorphosed by serpentine-group minerals. Some massive weathered exposures are blue-gray in color. Sheared serpentinite (slickenite) varies in appearance, depending on the degree of shearing, ranging from moderately sheared, dark green or blue-green slickenite to highly sheared, polished black or metallic blue slickenite. Shearing is most intense along faults, in axial-surface regions of folds, and near contacts with other units. The central portions of large blocks of serpentinized peridotite tend to be the least altered, but they still contain small lenses and smears of slickenite.

Harzburgite, dunite, and scarce pyroxenite were the probable compositions of the original ultramafic protoliths of the Onion Camp complex. In many of these rocks, magnesian olivine probably formed ~75–95% of the pre-serpentinized ultramafic rocks. Kernels of orthopyroxene and clinopyroxene are occasionally seen in thin section, but are scarce because of the degree of alteration and deformation. Chromian spinel octahedra are visible on weathered surfaces of massive outcrops, but are largely pseudomorphosed by magnetite.

Alteration minerals comprise >80% of all Onion Camp complex ultramafic rocks. Relict olivine grains are scarce, being most common in the more massive serpentinized ultramafic rocks. Orthopyroxene is generally bastitic or uralitic. Low-temperature serpentine-group minerals (lizardite and chrysotile) generally comprise >75% of the rocks and occur as massive replacement minerals as well as in intricate vein networks indicative of multiple episodes of serpentinization and alteration. Higher temperature minerals (>300 °C), such as antigorite and tremolite, occur as fragmented, irregular patches in sheared serpentinite and occasionally border fragmented mafic dikes. Magnetite is ubiquitous and provides an indication of the degree of serpentinization, with the more highly serpentinized rocks being most strongly magnetic.

Onion Camp complex serpentinite and serpentinized peridotite record four distinct mineral and structural associations that formed as metamorphic temperature decreased. The earliest association is rare and is characterized by a mesoscopic mylonitic foliation defined by flattened and elongated aggregates of primary (now pseudomorphosed) minerals. Weathered rock faces that display the mylonitic fabric show multi-grain porphyroclastic augens of olivine and pyroxene in a fine-grained, xenoblastic matrix of mostly olivine. In thin section, the porphyroclasts invariably show pronounced strain effects, such as kink bands, deformed exsolution lamellae, and undulatory extinction.

The second association is defined by a serpentine foliation and lineation that is best developed in massive outcrops near the amphibolite-peridotite contact at Squaw Mountain (Fig. 2), but also occurs in scattered exposures throughout the unit. The foliation is defined by semi-continuous bands of light green serpentine spaced at ~1–3 mm intervals in an otherwise dark green, massively serpentinized peridotite. The alternating light green and dark green bands give the serpentinite a gneissose appearance (Fig. 5A). A poor to moderate cleavage spaced ~1 cm apart intersects the light green serpentine foliation at an angle of ~25°. The resulting intersection lineation and foliation are parallel to similar features in the adjoining amphibolite bodies.

The third association is characterized by ubiquitous, low-temperature static serpentinization, intricate vein networks, and cemented breccia zones. These features cut the mylonitic and serpentinite gneissic fabrics. Locally, some serpentinites exhibit an intricate patchwork of veins and fragmental textures (Fig. 5B). These textures, alterations, fragmentation, and veining relations are similar to those that occur in the mafic intrusive complex. Replacement minerals in massive serpentinite include lizardite and chrysotile, with secondary urallite, and magnetite. Secondary alteration products and vein minerals include lizardite; chrysotile; and local calcite, malachite, limonite, hematite, barite, and various sulfide-group minerals, including pyrrhotite, chalcopryrite, chalcocite, and sphalerite. Zones with high concentrations of sulfides ~4 km to the southeast of Pearsoll Peak (Fig. 2) have been prospected for Au and Cu (Ramp, 1984).

The latest structural and textural features of the serpentinite are sets of anastomosing shear bands that parallel the northeast-striking, southeast-dipping regional foliation, most commonly observed along faults and in axial surface regions of folds. Shear surfaces either display a black to dark green lustrous polish or contain linear, stepped serpentine fibers that indicate the shear direction. At outcrop scale, low-strain shear zones have a widely spaced, anastomosing schistosity (0.5–1.0 m wide) and equidimensional augens, whereas high-strain zones generally have a centimeter-scale, subparallel schistosity.

Mafic Intrusive Suite. A heterogeneous assemblage of hydrothermally altered, mafic intrusive rocks occurs in close association with the metavolcanic and metasedimentary rocks of the Onion Camp complex. Some of the larger bodies are mapped in Figure 2; numerous smaller outcrops are not shown but occur throughout the complex. The rocks are massive, nonschistose, and extremely tough, and the penetrative foliation that characterizes the metavolcanic and metasedimentary rocks is absent. The mafic intrusive suite is best observed along the roadcuts and cliff exposures in the Hellgate Canyon portion of the Rogue River; in the roadcut and ridgeline exposures to the west of Fiddler Mountain (Fig. 2); and along the trails, ridgelines, and drainages south of Canyon Peak.

The mafic intrusive suite consists predominantly of meta-diorite and aphanitic greenstone with subordinate altered gabbro, diorite, and rare plagiogranite. Chilled dike-on-dike margins are common in some outcrops. Metamorphism of these

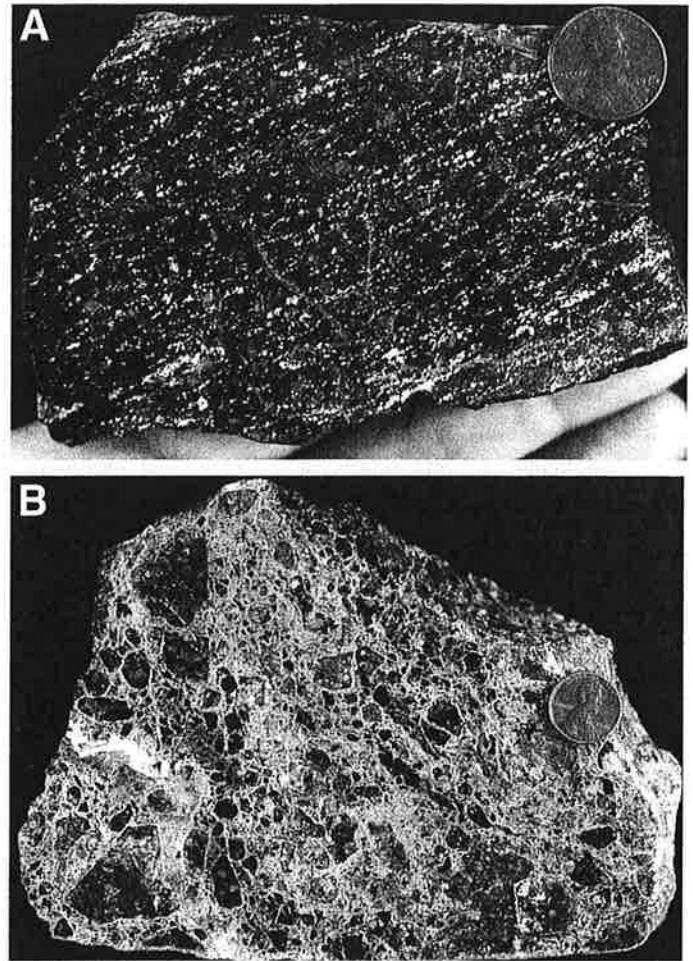


Figure 5. (A) Photograph of a cut slab of serpentinitized peridotite of the Onion Camp complex showing the metamorphic foliation that parallels foliation in gneissic amphibolite. The pale bands consist of light-green serpentine-group minerals (probably lizardite). The medium-gray bastite pseudomorphs of pyroxene grains in a dark-gray matrix of thoroughly serpentinized olivine. (B) Photograph of a cut slab of brecciated serpentinitized peridotite collected near Squaw Mountain. The sample was collected from a 1- to 2-m-wide outcrop of cemented breccia in otherwise intact serpentinized peridotite.

rocks is characterized by a static, ubiquitous greenschist-facies and sub-greenschist-facies hydrothermal alteration. The primary mineral constituents in mafic rocks are actinolitic amphibole, altered plagioclase, epidote, chlorite, sulfide minerals, and partially to wholly altered ilmenite (leucosene). Relict cores of clinopyroxene and hornblende are locally preserved in gabbro and diorite. Plagiogranite contains extensively altered plagioclase (saussurite), quartz, chlorite (replacing biotite), and minor Fe-Ti opaque oxides.

Distinctive features of the mafic intrusive suite include intricate networks of vein systems and patchworks of healed, fine- to coarse-grained breccia hosted in otherwise nondeformed, hy-

drothermally altered rock. Vein minerals are diverse and include epidote, epidote (and clinozoisite) + quartz, prehnite, prehnite + quartz, quartz + epidote + chlorite, and quartz + calcite. The breccia zones are locally sheared but typically lack penetrative deformation. Breccia clasts match the adjacent host rock type and are generally encased in vein materials and subordinate amounts of cataclastic matrix, probably the result of hydrofracturing. This distinctive hydrofracture texture is most commonly observed in the mafic intrusive suite but also occurs locally in other units of the Onion Camp complex and in the Josephine ophiolite.

Field relations support an intrusive relationship between the mafic intrusive suite and metavolcanic and metasedimentary sequences of the Onion Camp complex. In rare instances, the mafic intrusive suite shows chilled margins against metavolcanic and metasedimentary rocks. In addition, individual mafic dikes commonly intrude other units of the complex.

Dikes. A wide range of dikes cuts rocks of the Onion Camp complex, including pegmatitic websterite and gabbro, plagiogranite, diabase, aphanitic basalt, and acicular hornblende-phyric diorite. Rodingite dikes are scarce, suggesting that widespread serpentinization occurred prior to dike emplacement.

Dike orientations are random and probably reflect multiple episodes of intrusion and subsequent deformation. The dikes are rarely continuous for more than 10 m and essentially occur as megaboudins encased in serpentinite. Websterite and gabbro dikes contain clinopyroxene crystals as much as 50 cm in length but are now largely replaced by fibrous amphibole (uralite). Relatively unaltered mafic and intermediate dikes intrude the amphibolites. The mafic dikes display textures and mineralogy similar to rocks of the mafic intrusive suite, and the younger intermediate dikes are hornblende-phyric, typically with acicular crystals.

Crosscutting relations between dikes, though equivocal, suggest at least four episodes of dike intrusion: (1) highly altered and disrupted plagiogranite dikes; (2) diabasic and aphanitic basaltic dikes that resemble sheeted mafic dike complexes characteristic of some ophiolitic suites; (3) websterite and gabbro dikes that are similar in appearance to plutonic rocks of the Chetco plutonic complex; and (4) relatively unaltered, acicular hornblende-phyric dikes.

Metamorphic Conditions

The metavolcanic rocks of the Onion Camp complex contain mineral assemblages chiefly typical of greenschist-facies conditions (Liou et al., 1974; Apter and Liou, 1983). The absence of sodic amphibole or lawsonite precludes blueschist-facies metamorphic conditions. Pumpellyite occurs in a few samples and may indicate local pumpellyite-actinolite-facies conditions (Brown, 1977; Liou et al., 1987; Frey et al., 1991).

The metasedimentary rocks of the Onion Camp complex also contain mineral assemblages indicative of greenschist-facies conditions. The absence of biotite but the common oc-

currence of white mica + stilpnomelane \pm actinolite suggests temperatures below 400 °C (Brown, 1975; Yardley, 1989).

Amphibolite and amphibolite gneiss show the following parageneses: (1) brown hornblende + oligoclase + clinopyroxene + titanite, (2) green hornblende + oligoclase + titanite, and (3) green hornblende + epidote + albite + titanite. Quartzite shows the following parageneses: (4) quartz + cummingtonite + biotite + almandine, and (5) quartz + biotite + white mica + almandine. These assemblages indicate epidote-amphibolite- to upper-amphibolite-facies metamorphic conditions of >4 kb and ~550–650 °C (Thompson, 1976; Apter and Liou, 1983). Greenschist and lower-metamorphic-grade alteration and vein mineral assemblages are very similar to those noted for the mafic intrusive suite.

Lizardite and chrysotile dominate the metamorphic mineral assemblages associated with the serpentine gneiss and suggest lower greenschist-facies conditions. The close proximity of the serpentinite gneiss to amphibolitic rocks and their apparent shared structural features suggest that the serpentinite gneiss may have experienced higher-metamorphic-grade conditions that were completely retrograded to the current greenschist-facies mineral assemblages. Alternatively, the greenschist-facies conditions may be primary, with a tectonic contact between the amphibolites and serpentinite gneiss. Similar amphibolite-serpentinized peridotite relations are described from parts of the western Paleozoic and Triassic belt (Snoke, 1977; Donato, 1992; Kays, 1992).

Structural Fabric Elements

Structural and textural features of rocks in the Onion Camp complex distinguish four deformational episodes. The first episode, recorded only locally in the serpentinized peridotite, is defined by a pseudomorphed blastomylonitic texture interpreted as recording deformation during subsolidus plastic flow of mantle lithosphere beneath a spreading center. Presumably, this deformation accompanied the construction of an ophiolite or primitive-arc sequence represented by the metasedimentary and metavolcanic rocks.

The second episode is characterized by greenschist- to amphibolite-facies regional metamorphism. The primary structural feature is a well- to moderately developed gneissose to schistose foliation (S_1) defined by the alignment of metamorphic mineral grains; for example, mica, platy amphibole, and quartz ribbons (Figs. 6A and 7A). Tight to isoclinal intrafolial folds are locally preserved in outcrops comprised of mm-scale laminated, siliceous, and tuffaceous meta-argillite (Fig. 6B). Relatively inconspicuous linear elements were only locally observed in some amphibolites. However, a lineation ($L_{1 \times 2}$) is common in schistose rocks, produced by an intersection of S_1 and a second foliation/rock cleavage (S_2) formed during episode four (Figs. 7B and 8). At least two and possibly three generations of open to isoclinal folds are evident in some chert out-

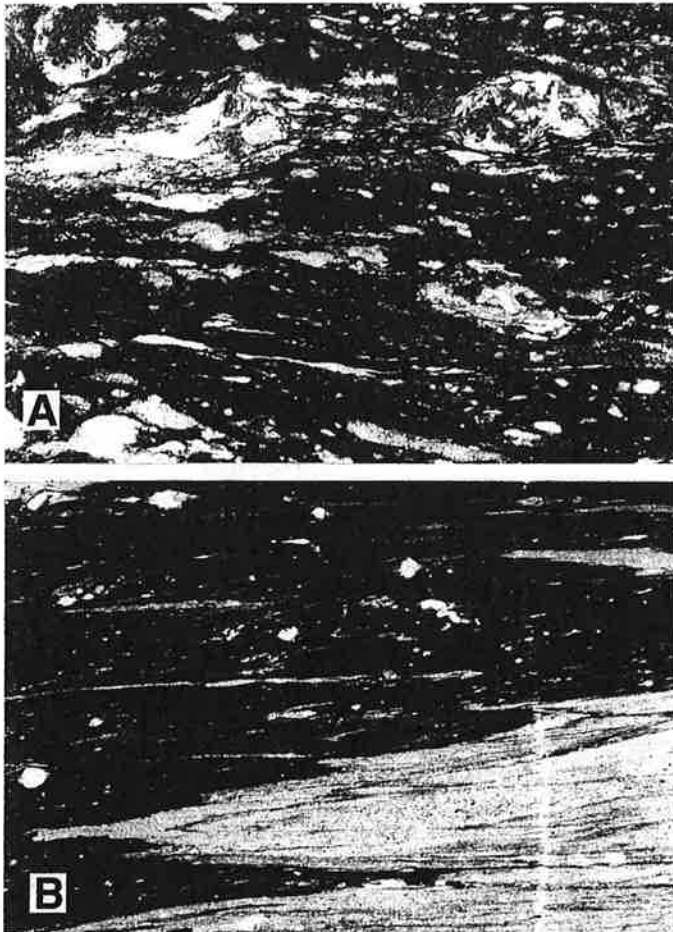


Figure 6. Photomicrographs of Onion Camp complex rocks, polarized light, horizontal field of view ~ 3 mm. (A) Strongly foliated, greenschist-facies metatuff with primary metamorphic minerals chlorite-actinolite-quartz-albite-oxide. (B) Highly strained silicic meta-argillite showing a tightly folded compositional boundary with axial surface foliation between quartz-rich and argillaceous layers.

crops, but it is unclear to which deformational episode these relate. Stereographic plots of S_1 and $L_{1 \times 2}$ (Fig. 7A and B) illustrate the apparent dispersal of amphibolite foliations and intersection lineations, probably the result of later deformational events.

The third episode is characterized by brittle fragmentation, cataclasis, and pervasive greenschist-facies and lower-grade alterations that affected all the rocks of the complex but are most common in the mafic intrusive suite. Zones of brecciation are commonly cemented by calcite and prehnite.

The fourth episode is characterized by regional to outcrop-scale, greenschist-facies folds, foliation, and faults. Structures include a northeast-striking, southeast-dipping foliation (S_2 ; Fig. 7C) defined by the alignment of metamorphic minerals,

such as chlorite, and by flattening of crystal and lithic fragments; a coplanar, locally developed syn-metamorphic foliation (S_3) defined by a weakly developed spaced cleavage; syn-metamorphic, shallowly northeast-southwest plunging, tight to near-isoclinal F_1 and F_2 folds (Fig. 7D, E, and F); and postmetamorphic, moderately east plunging, open F_3 folds, and kink bands (Fig. 7F). Foliations S_2 and S_3 are well developed to absent, depending on the rock type. The S_3 foliation is scarce and is restricted to the slaty rocks, where it occurs in the axial-surface regions of tight F_2 folds, which fold S_2 . The syn-metamorphic folds and linear structural features of the Onion Camp complex area are generally northeast-southwest-trending. F_1 folds commonly have attenuated and truncated limbs.

Fossil Ages

A sample of red chert (sample CP-5; Table 1) collected for radiolarians near Onion Camp yielded mostly amorphous forms, with the exception of a possible Late Triassic radiolarian form (*Canoptum* sp., M. Silk, written commun., 1991; Yule et al., 1992). Two additional samples collected from the same locality yielded scarce Jurassic, but no Triassic, forms (C. Blome, personal commun., 1993). These data support a Late Triassic to Jurassic age for chert near Onion Camp, consistent with chert ages from the Rattlesnake Creek terrane in the hanging wall of the Orleans/Preston Peak thrust (Irwin et al., 1982).

Radiometric Ages

Radiometric ages from Onion Camp complex rocks obtained for this study include two $^{40}\text{Ar}/^{39}\text{Ar}$ ages and two U-Pb zircon ages (Table 2). Brown pleochroic hornblende separated from two amphibolite gneiss samples collected near Squaw Mountain yield $^{40}\text{Ar}/^{39}\text{Ar}$ plateau cooling ages of 173 ± 0.6 Ma (EDM-10) and 169.6 ± 0.7 Ma (EDM-81A) (Hacker et al., 1995). These data suggest the amphibolites cooled below a temperature of ~ 500 °C at ca. 170 Ma.

U-Pb zircon ages were obtained from two plagiogranite dikes that intrude serpentinized peridotite near Whetsone Butte (JM-10 and JM-11; Fig. 2). Sample JM-11 yields a concordant age of 173 ± 1 Ma and sample JM-10 shows slight Pb loss with an intercept age of 175 ± 2 Ma (Fig. 9). Peridotite of the Onion Camp complex therefore predates ca. 173 Ma; in addition, the apparent lack of rodingitization of the plagiogranite dikes suggests that at least one serpentinization event occurred prior to ca. 173 Ma.

Geochemical Data

A wealth of geochemical data exists for metavolcanic rocks from the various lithotectonic units of the Klamath Mountains province (Barnes et al., 1995). The data set is complete enough

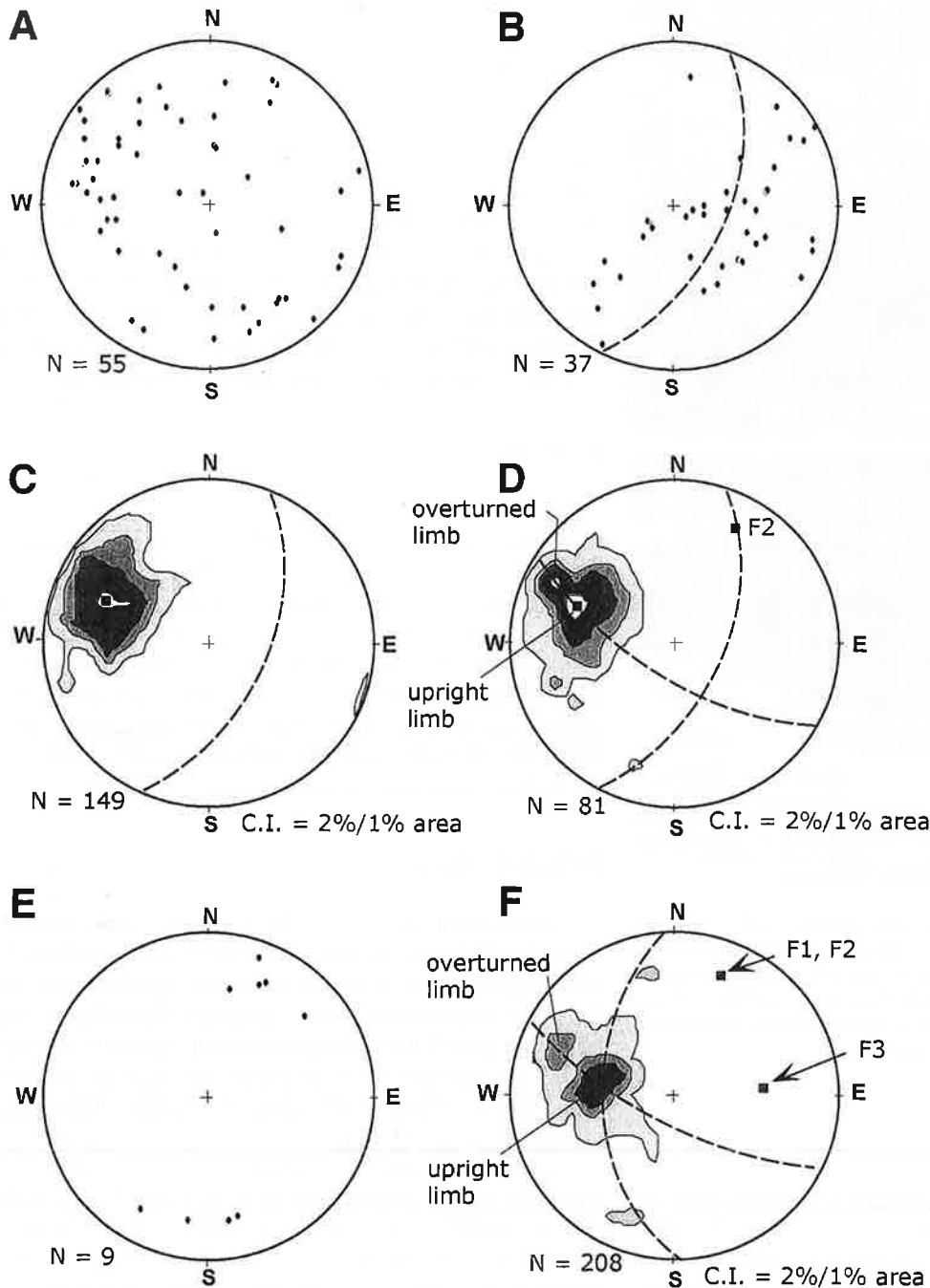


Figure 7. Lower hemisphere, equal-area stereographic plots of structural data. Onion Camp complex. (A) Poles to foliation in amphibolite (S_1); (B) intersection lineation ($L_{1 \times 2}$) measured on S_2 foliation planes (great circle = average S_2 orientation); (C) poles to regional foliation (S_2) and average S_2 orientation (great circle); (D) Rogue and Galice Formations and Fiddle Mountain olistostrome: poles to S_2 , average S_2 (north-east-striking great circle), and north-west-striking great circle whose pole defines average F_2 fold; (E) Galice Formation: gently plunging north-northeast and south-southwest F_1 and F_2 hinge lines; (F) Rogue Formation: poles to bedding with two primary maxima define limbs of northeast-plunging, northwest-vergent, tight F_1 and F_2 folds (pole to northwest-striking great circle); secondary maxima define limbs of east-plunging, upright, open F_3 folds (pole to north-striking great circle). C.I.—contour interval.

that the characteristic geochemical signatures of numerous lithotectonic units are well defined. Three rock associations—the crustal sequence of the Josephine ophiolite, the Rogue Formation, and the Rattlesnake Creek terrane—exhibit important differences in their diagnostic geochemical signatures.

Ten greenstone and pillow lava samples from the metavolcanic sequence were analyzed for major and trace element abundances (Table 3), with rare-earth element (REE) abundances

determined for two of these samples (Table 4). Though the major elements may be mobile during metamorphism, most trace and rare-earth elements are considered immobile at greenschist and lower metamorphic grades (e.g., Shervais, 1982).

The data in Barnes et al. (1995) provide criteria to evaluate the possible correlatives to the Onion Camp complex. In support of the age and lithologic similarities, the geochemical data in Tables 3 and 4 and Figure 10 exhibit trends that are quite similar

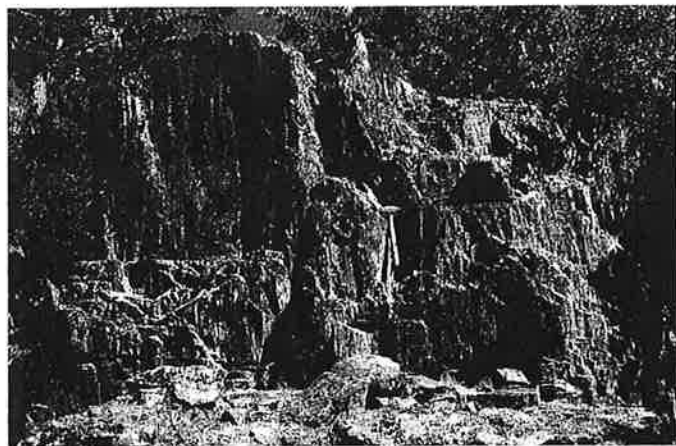


Figure 8. Photograph of steeply dipping metachert in the Onion Camp complex (rock hammer for scale). Note down-dip lineation, produced by an intersection of S_1 and a rock cleavage parallel to the later, regional foliation (S_2), typical of metavolcanic and metasedimentary rocks of the complex.

to those of the lower mélangé unit of the Rattlesnake Creek terrane (Wright and Wyld, 1994). The mafic rocks of the Rattlesnake Creek terrane and Onion Camp complex fall in the compositional range of 46–55% SiO_2 and display a wide range of FeO/MgO values and generally high TiO_2 concentrations (Wright and Wyld, 1994; Barnes et al., 1995). Also, the Onion Camp complex metavolcanic rocks plot within the same fields as the lower mélangé unit of the Rattlesnake Creek terrane on trace element discrimination diagram plots (Fig. 10). REE data (Fig. 11) from metavolcanic rocks of the Onion Camp complex show a strong enrichment in light REE typical of an alkalic, within-plate basalt (WPB) (pillow basalt sample EDM-83B), and a flat REE pattern typical of normal tholeiitic mid-ocean-ridge basalt (N-MORB) (greenstone sample OM-11); very similar to the red chert-basalt breccia and metabasalt association,

respectively, of the lower mélangé unit, Rattlesnake Creek terrane (Wright and Wyld, 1994).

Possible Broad Correlations

The rocks of the Onion Camp complex comprise a lithologically distinct petrotectonic unit that previously was unrecognized in the western Jurassic belt. Age relations show that the red chert-basalt association is Triassic(?) to Early Jurassic in age, and postmetamorphic dikes indicate that the serpentinized peridotite predates ca. 173 Ma. Distinctive lithotypes of the complex include the N-MORB and WPB metabasalts (usually associated with red chert), a scarce chert-clast conglomerate, and an amphibolite and serpentinized peridotite association. These features of the Onion Camp complex are also common to the Rattlesnake Creek terrane of the western Paleozoic and Triassic belt (Irwin, 1972), and are strikingly similar to the lower mélangé unit of the Rattlesnake Creek terrane (Wright and Wyld, 1994). Heterogeneous mafic complexes that intrude the Onion Camp complex (Yule, 1996; this study) and the Rattlesnake Creek terrane near Preston Peak (Snoko, 1977) further support a correlation between the Onion Camp complex and Rattlesnake Creek terrane.

FIDDLER MOUNTAIN OLISTOSTROME

Overview

The Fiddler Mountain olistostrome is named for natural exposures on the ridgelines and flanks of Fiddler Mountain. Additional exposures occur along the Babyfoot Lake–Onion Camp U.S. Forest Service access road (Fig. 2). The widest part of the outcrop belt coincides with Fiddler Mountain. Isolated patches of the olistostrome are not shown on Figure 2, but their locations are shown on maps in Yule (1996). The olistostrome occupies a position at the base of the interfingering and overlapping Rogue and Galice Formations, and is deposited on a variable substratum comprised of both the Onion Camp complex and northern outliers of the Josephine ophiolite.

TABLE 1. RADIOLARIAN FOSSIL SAMPLES AND LOCALITIES

Station	Description	Latitude (N) and longitude (W) (°/'/'')	Interpreted age	Species list
1. CP-37	Tightly folded white-gray chert; N46E, 31SE.	42/14/28.5 123/47/37.5	Late Jurassic (Upper Kimmeridgian– Lower Tithonian?)	<i>Lupherium</i> sp. <i>Praeconocaryomma magnimamma</i> Large spheres (unidentifiable)
2. CP-5	Locality of Roure and DeWever (1983). Isolated exposure of well-bedded red chert; N20E, 39SE.	42/14/19 123/46/52.5	Upper Triassic(?)– Bajocian	Probable <i>Conopturus</i>

TABLE 2A. URANIUM-LEAD ISOTOPIC DATA

Size (µm) [†]	Zircon fraction properties ^{††}	Wt. (mg) [Ⓢ]	U (ppm)	²⁰⁶ Pb* (ppm)	Atomic ratios					Apparent ages (m.y.) [§]		
					²⁰⁶ Pb/ ²⁰⁴ Pb	²⁰⁶ Pb*/ ²³⁸ U	²⁰⁷ Pb*/ ²³⁵ U	²⁰⁷ Pb*/ ²⁰⁶ Pb*	²⁰⁸ Pb*/ ²³⁸ U	²⁰⁷ Pb*/ ²³⁵ U	²⁰⁷ Pb*/ ²⁰⁶ Pb*	
93DY-JM-10: Plagiogranite dike cutting serpentinitized peridotite of the Onion Camp complex (123°48'35.5"W, 42°14'35.5"N).												
<45 ²	Clear, Eu > Fr, 2:1 to 5:1	2.3	379.8	8.37	13,361	0.02547(17)	0.17444	0.04970(12)	162.1	163.3	181 (6)	
45-64 ²	Clear, Eu > Fr, 2:1 to 5:1	1.4	726.6	16.69	12,111	0.02654(18)	0.18107	0.04950(55)	168.9	169.0	171 (26)	
64-80 ²	Clear, Eu > Fr, 2:1 to 5:1	0.8	562.3	13.21	8013	0.02760(17)	0.18817	0.04947(18)	175.5	175.1	170 (8)	
91DY-JM-11: Plagiogranite dike cutting serpentinitized peridotite of the Onion Camp complex (123°48'35"W, 42°14'45"N).												
45-64 ³	1:1 to 4:1 w/clear incl., Eu > Fr	2.3	198.3	4.67	9,855	0.02723(15)	0.18604	0.04957(19)	173.2	173.3	175 (6)	
64-100 ³	1:1 to 4:1 w/clear incl., Eu > Fr	1.3	215.2	5.08	8,002	0.02725(15)	0.18650	0.04965(15)	173.4	173.6	178 (7)	

[†] Fractions separated by grain size and magnetic properties. Magnetic properties are given as nonmagnetic split on Frantz Isodynamic Separator for 1.7 amps with side/front slopes of 10.5/20, 21/20, 32/20, or 45/20. Dissolution and chemical extraction technique modified from Krogh (1973).

^{††} All samples are hand-picked to 99.9% purity prior to dissolution. Abbreviations: Eu = euhedral grains; Fr = fragmented grains; ratios given are the respective length:width ratios of euhedral zircon grains; incl. = inclusion; Lt = light.

[Ⓢ] Due to uncertainties in weight of sample, U-Pb concentration may be in error, use of mixed ²⁰⁵Pb-²³⁰Th-²³⁵U spike ensures that age of sample is correct.

* Radiogenic/nonradiogenic correction based upon 40 picogram-blank Pb (1:18.78;15.61;38.50) and initial Pb approximations: 206/204 = 18.6; 207/204 = 15.6; 208/204 = 38.2.

[§] Decay constants used in age calculation: λ²³⁸U = 1.55125 × 10⁻¹⁰, ²³⁵U = 9.98465 × 10⁻¹⁰ (Jaffey and others, 1971); ²³⁸U/²³⁵U atom = 137.88. Uncertainties (±) in radiogenic ratios calculated by quadratic sum of total derivatives of ²³⁸U and ²⁰⁶Pb* concentration and ²⁰⁷Pb*/²⁰⁶Pb* equations with error differentials defined as follows: (1) isotope ratio determinations from standard errors (β/n) of mass spectrometer runs plus uncertainties in fractionation corrections based on multiple runs of NBS 981, 983, and U500 standards; (2) Spike concentrations from range of deviations in multiple calibrations with normal solutions; (3) Spike compositions from external precisions of multiple isotope ratio determinations; (4) Uncertainty in natural ²³⁸U/²³⁵U from Chen and Wasserburg (1981); and (5) Nonradiogenic Pb isotopic compositions from uncertainties in isotope ratio determinations of blank Pb and uncertainties in composition of initial Pb from estimates of regional variations based on references given above and consideration of rock type.

TABLE 2B. ⁴⁰Ar/³⁹Ar APPARENT AGES

Lithologic unit	Station	Latitude (N) and longitude (W) (°/')		Description	Mineral	Plateau age (Ma)
Onion Camp complex	91-EDM-81A	42/20/40N	123/39/40W	Squaw Mountain; amphibolite gneiss	Hornblende	169.6 ± 0.5
	90-EDM-10	42/18/58N	123/40/46W	Squaw Mountain; hornblende schist	Hornblende	173.1 ± 0.6

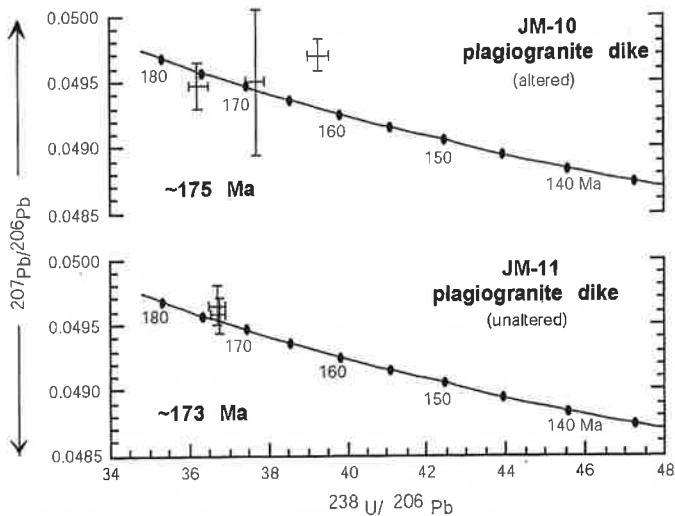


Figure 9. Tera-Wasserburg plots of U-Pb and Pb-Pb radiogenic age data (Tera and Wasserburg, 1972) for plagiogranite dikes cutting serpentinitized peridotite of the Onion Camp complex (JM-10 and JM-11).

Rock Units

Metasedimentary Polymictic Breccia and Conglomerate.

Poorly exposed breccia, conglomerate, and sandstone occur throughout the olistostromal unit (Fig. 12). The dominant clast types are aphyric to porphyritic green to gray metabasalt, fine- to medium-grained metadiabase, and medium- to coarse-grained gabbro. Secondary clast types include chert (red and gray), slaty argillite, serpentinite, and serpentinitized peridotite and scarce occurrences of quartzite, chlorite schist, phyllonite, and amphibolite. In cases where the olistostromal rocks are deposited upon serpentinitized peridotite, the breccias consist entirely of serpentinite and serpentinitized peridotite clasts (Fig. 13). A rare but distinctive ophicalcite breccia, exposed in a road-cut near locality "C" on Figure 2, consists of matrix-supported serpentine clasts in a hematitic and calcareous serpentine mud matrix. The matrix materials generally consist of clay- to angular sand-size and coarser grains derived from the same material as the clasts.

Grain size ranges from silt- to boulder-sized, with coarse pebble- and fine cobble-sized the most common. Matrix in the coarse pebble and fine cobble breccias consists of silt- to fine pebble-sized material, similar in composition to the larger clasts. Matrix:clast ratios are highly variable but are typically >1:10. Fine cobble and coarser breccias are typically massive, but layering is common in pebble breccias, conglomerates, and sands (Fig. 12).

Megabreccia. Decameter- and larger-sized ($\leq 100\text{-m}$) blocks of gabbro, diabase, and basalt are exposed along the south flank of Fiddler Mountain and comprise ~50% of the complex. Altered and fragmented gabbro and diabase are the most common

megabreccia clast lithology. The largest blocks often consist of sheeted mafic dikes, commonly with gabbro and/or basaltic screens. The size of these blocks gives the impression that the unit is a heterolithic intrusive complex or a tectonic mélange. However, zones of relatively nonresistant, polymictic-clast breccias occur between the large-scale blocks, and indicate that the large blocks are entirely part of a sedimentary breccia/megabreccia deposit.

Metachert and Slaty Argillite. Horizons of white to gray bedded chert and slaty argillite comprise <10% of the olistostrome and occur as 1- to 20-m-thick, chert-rich intervals that can be traced laterally for up to 100 m. The chert is mostly recrystallized, but oval to round vugs, mm-sized and finer, are evident in broken faces of gray chert. Samples processed for radiolarian yield a poorly constrained Late Jurassic (Kimmeridgian?) age for these deposits (Yule et al., 1992; Table 1).

Provenance and Depositional Environment

Clasts correlate with rock types found in the Onion Camp complex and the northern outliers of the Josephine ophiolite. The primary outcrop belt overlies the Onion Camp complex (Fig. 2), but isolated outcrops too small to be shown on Figure 2 overlie northern outliers of Josephine ophiolite. Both could be the source terrane for the olistostromal deposits. The Fiddler Mountain olistostrome, therefore, is interpreted to have originated as a talus breccia along a marine escarpment that exposed the Onion Camp complex and/or Josephine ophiolite, perhaps along a transform fault in the Josephine marginal basin. Pelagic sedimentary rocks would have accumulated between episodes of catastrophic deposition of the megabreccia and breccia deposits.

Metamorphic Conditions

The metasedimentary rocks of the Fiddler Mountain olistostrome consist chiefly of prehnite-pumpellyite to lowermost greenschist-facies mineral phases (Liou et al., 1974; Apter and Liou, 1983). Original igneous mineral phases in clasts are commonly altered, partly or wholly, to various hydrous phases, but relict calcic plagioclase and pyroxene (augite?) are present in some samples. The typical mineral assemblage for mafic clasts is albite + quartz + epidote + chlorite + white mica + calcite + prehnite + opaque minerals, and for argillaceous rocks is quartz + albite + white mica + clinozoisite + chlorite + opaque minerals. Pumpellyite is scarce, but was identified in some metabasaltic clasts. Pyrite is a common accessory mineral phase in gray, slaty argillite.

Ubiquitous lower greenschist-facies static alteration is present in all clast types and probably records hydrothermal alteration of the bedrock prior to incorporation of the clasts into the sedimentary breccia deposit. This interpretation is supported by the observation that regional foliation and shear planes cut veins and fractures associated with the static alteration.

TABLE 3A. GEOCHEMICAL SAMPLES AND LOCALITIES

Station	Lithology	Latitude (N) (°/'/'')	Longitude (W) (°/'/'')	Remarks
CP-3	Pillow lava	42/14/11	123/47/46	Collected from quarry near Onion Camp.
OM-8	Pillow lava	42/26/26	123/35/44	
EDM-83A	Pillow lava	42/17/20	123/37/33	River-polished exposure of pillow lavas adjacent the Illinois River.
EDM-83B	Pillow lava	42/17/20	123/37/33	River-polished exposure of pillow lavas adjacent the Illinois River.
EDM-87	Pillow lava	42/17/48	123/43/42	
G-14C	Pillow lava	42/32/37	123/30/40	Roadcut opposite highway overlook at Hellgate Canyon, Rogue River gorge.
OM-11	Massive greenstone	42/27/55	123/35/44	Collected from quarry near Onion Mountain.
OM-14	Massive greenstone	42/29/52	123/32/36	
G-14A	Massive greenstone	42/32/37	123/30/40	Roadcut opposite highway overlook at Hellgate Canyon, Rogue River gorge.
CP-45	Massive greenstone	42/13/12	123/48/22	Collected from cirque wall above Babyfoot Lake.
CR-22	Massive greenstone	42/25/38	123/37/33	
JM-11	Dike	42/14/45	123/48/35	Zircon sample (ca. 173–174 Ma). Plagiogranite dike cutting Onion Camp complex peridotite near Whetstone Butte.

TABLE 3B. MAJOR AND TRACE ELEMENT ANALYSES FROM THE ONION CAMP COMPLEX

Sample	Pillow lava						Massive Greenstone					Dike
	CP-3	OM-8	EDM-83A	EDM-83B [#]	EDM-87	G-14C	OM-11 [#]	OM-14	G-14A	CP-45	CR-22	JM-11 [†]
SiO ₂	48.51	48.54	46.31	45.68	52.12	52.49	54.06	53.98	49.02	50.14	49.52	76.63
TiO ₂	2.66	1.38	2.20	2.06	0.70	0.77	1.18	0.51	1.27	0.93	1.38	0.22
Al ₂ O ₃	14.45	14.57	15.36	15.39	16.33	15.45	13.47	14.79	15.89	16.19	12.12	13.33
Fe ₂ O ₃	13.10	12.24	10.75	9.65	10.26	8.38	7.82	7.99	9.25	8.89	13.70	1.12
MnO	0.20	0.21	0.16	0.15	0.15	0.13	0.17	0.14	0.15	0.15	0.22	0.02
MgO	4.47	5.93	6.70	5.00	6.61	9.12	7.70	8.23	6.46	6.63	7.17	0.53
CaO	8.86	10.05	9.73	11.42	5.44	7.42	8.57	8.45	9.69	13.14	8.86	2.27
Na ₂ O	4.58	3.68	4.03	4.44	4.77	4.14	4.09	3.23	3.68	2.21	2.83	4.68
K ₂ O	0.27	0.42	0.30	0.48	0.43	0.12	0.75	0.34	0.14	0.03	0.22	1.06
P ₂ O ₅	0.39	0.20	0.39	0.38	0.09	0.09	0.16	0.08	0.16	0.10	0.11	0.03
LOI	2.84	2.43	4.44	6.33	3.41	2.74	2.20	2.99	2.66	3.69	3.09	0.68
Total	100.33	99.66	100.37	100.97	100.31	100.85	100.16	100.75	98.37	102.11	99.22	100.57
Rb	7	9	6	8	7	3	13	8	4	2	7	22
Sr	225	245	361	419	145	137	90	156	256	56	100	121
Zr	197	81	156	146	44	57	99	36	104	65	68	105
Y	43.3	39.7	26.1	24.7	23.8	22.1	29.6	16.5	32.8	24.5	32.8	10.9
Nb	28	4	30	32	1	1	4	b.d.	2	b.d.	4	5
Ba	70	46	132	201	123	27	62	155	33	11	26	355
Sc	33.4	43.8	24.4	21.9	35.6	38.7	28.4	36.2	35.5	37.6	49.3	2.3
V	285	279	209	204	296	223	212	228	245	195	325	16
Cr	64	212	200	179	111	547	247	341	233	209	109	11
Ni	44	53	138	121	91	252	97	101	90	75	50	20
Cu	55	23	51	41	60	75	53	74	52	104	85	n.d.
Zn	115	83	78	74	87	57	55	51	63	46	103	9
Ti	15,947	8271	12,350	13,178	4180	4598	7070	3081	7641	5551	8273	1338

Notes: Major element data given in wt%; minor and trace element data in ppm. Analyses done at Texas Tech University, Lubbock, by inductively coupled plasma mass spectrometry, inductively coupled atomic emission mass spectrometry, and, for Rb, by flame emission spectroscopy. Some of the trace elements (Sr, Ba, Zr, and Y) were analyzed twice; once with dilute solutions used for major elements and again with concentrated solution used for the other trace elements. Values from the two runs were averaged with the following exceptions: (1) for high Sr values, the trace element run values were used; (2) for high Ba values, the major element run values were used; and (3) for Y, the trace element runs were used because of a better fit to standards. b.d.—below detection limits; Greenst.—greenstone; LOI—loss on ignition; n.d.—no data available.

*Total Fe content is given as Fe₂O₃.

†U/Pb geochronologic samples.

#Samples with rare-earth element analyses (see Tables 2–5).

TABLE 4. RARE-EARTH ELEMENT COMPOSITIONS OF SELECTED BASALTS

Sample	La	Ce	Nd	Sm	Eu	Tb	Yb	Lu
92-DY-EDM-83B	21.5	41.4	23	5.3	1.50	0.81	2.07	0.31
92DY-OM-11	4.2	11.1	8.9	2.9	1.00	0.67	2.51	0.40

Notes: Data in ppm. Samples are from Onion Camp complex.

The overall metamorphism of the Fiddler Mountain olistostrome may be best described as a low-pressure, low-temperature type regional metamorphism associated with strong penetrative deformation.

Structural Elements

Structures in the Fiddler Mountain olistostrome are similar in orientation and style to those observed in the Rogue and Galice Formations, units that interfinger and overlap the olistostromal units and suggests that the Fiddler Mountain, Rogue, and Galice units share the same deformational history. For example, S_2 foliations in the olistostrome strike northeast and dip southeast and are coplanar with those observed in the Rogue and Galice Formations (Fig. 7D). In addition, bedded chert exposed immediately to the north of Fiddler Mountain in the hinge region of the synclinoria (Fig. 2) contains F_1 and F_2 folds that trend north-northeast to south-southwest and plunge $<15^\circ$, similar to those observed in the Galice Formation (Fig. 7E). Chert and argillite layers near Fiddler Mountain define a synclinorium with an overturned, steeply southeast-dipping western limb and an upright, moderately southeast-dipping eastern limb similar to the F_1 and F_2 folds observed in the Rogue Formation (Fig. 7F). The chert and argillite are also deformed by east-west open (F_3) folds (Fig. 7F). Large-offset faults are difficult to recognize in the field, but numerous small-offset faults can be observed cutting sand, conglomerate, and pebble breccia layers (Fig. 12B).

Possible Regional Correlations

Deposits similar in description to the Fiddler Mountain olistostrome occur at various localities throughout the Klamath Mountains and California Coast Ranges; for example, the Lems Ridge olistostrome (Ohr, 1987); the Devils Elbow ophiolite (Wyld and Wright, 1988); and the Preston Peak ophiolite (Snoke, 1977). In these locations, and in this study area, coarse, polymict breccia/megabreccia deposits generally overlie Late Jurassic ophiolitic crust and underlie and interfinger with the basal section of the Galice flysch; in addition, the olistostromal deposits are spatially associated with the outcrop belts of the Rattlesnake Creek terrane and/or the Josephine ophiolite. These relations suggest that localized areas of considerable topographic relief occurred within the Late Jurassic Josephine basin, probably as a result of extensional and/or transform faulting.

DISCUSSION

The northeast-striking belt of Rattlesnake Creek terrane contained within the western Jurassic belt of Oregon corroborates previous models for the Late Jurassic tectonic evolution of the Rogue–Chetco/Josephine paired arc/ophiolite basin (Snoke, 1977; Saleeby et al., 1982; Harper and Wright, 1984). This model invokes rifting of preexisting Klamath terranes—primarily the western Paleozoic and Triassic belt—to produce an active arc, inter-arc basin, and remnant arc triad along the margin of western North America (Fig. 14A). This model predicts that fragment(s) of older oceanic crust may occur as rift-screens within ophiolitic crust and/or as constructs for the active arc. It is, therefore, not surprising to discover a fragment of the Rattlesnake Creek terrane within the western Jurassic belt, beneath and adjacent to the Rogue–Chetco arc forming the “active arc” rift-edge facies, perhaps a matching piece to the “remnant arc” rift-edge facies of Snoke (1977) exposed in the Preston Peak region. This finding illustrates the complexity of the stratigraphic and structural relations in the Rogue–Chetco/Josephine basin prior to their accretion along the western margin of North America in Late Jurassic time.

Basement-Level Exposures in the Rogue–Chetco/Josephine Basin

The structural features and framework of marginal ocean basins is known from studies in modern settings (e.g., Karig, 1971; Uyeda, 1977; Curray et al., 1979; Pearce et al., 1984; Stern and Bloomer, 1992; Parson and Wright, 1996; Lagabriele et al., 1997). However, modern marginal ocean basin lithosphere is concealed by water or buried beneath thick surficial deposits. Without direct observation, several questions regarding the tectonic framework and evolution of marginal ocean basin lithosphere remain unanswered. For example, relatively little is known regarding (1) the age of the mantle lithosphere relative to the overlying crustal sequences and the nature of the boundary between lithospheric and asthenospheric mantle; (2) the nature of the transition between arc and oceanic crust; (3) the character of the relatively thick crust and mantle lithosphere in oceanic arcs and remnant arcs; and (4) the relative similarities and/or differences between active and remnant arc basement lithotypes. The relatively deep-level exposures of the Rogue–Chetco/Josephine marginal ocean basin provide an opportunity to explore these relatively poorly understood relations through direct observation.

The lithotectonic elements of the Rogue–Chetco/Josephine ocean basin can be grouped into three levels (Figs. 14B and 15): (1) a basal, upper-mantle lithosphere level composed of two distinct types of variably serpentinized peridotite; (2) an intermediate lower- to mid-crustal level composed of a heterogeneous complex of arc-plutonic rocks and variably metamorphosed mafic volcanic and metasedimentary rocks; and (3) an upper-crustal level composed of arc-derived flysch and olis-

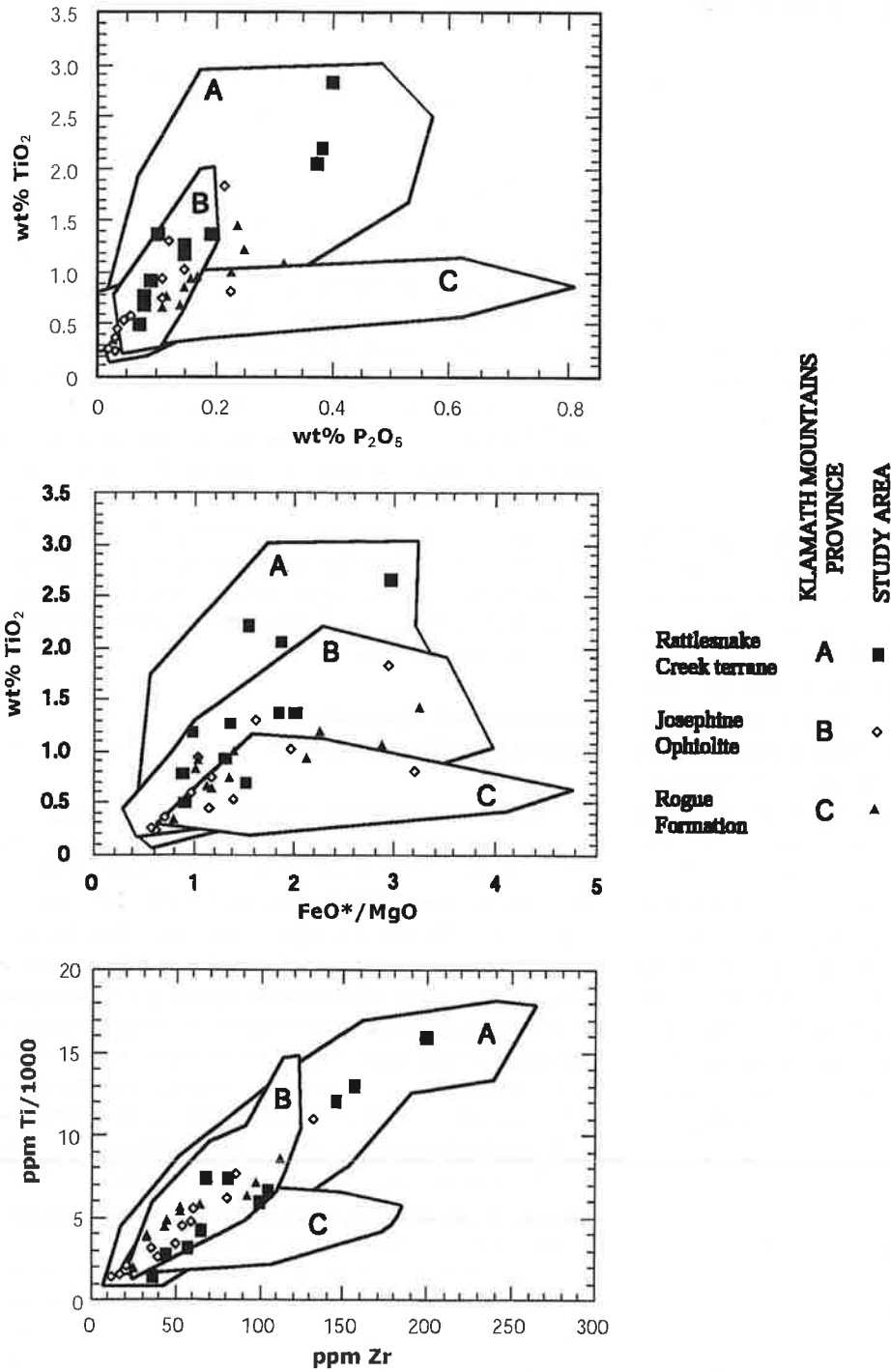


Figure 10. Plots of P₂O₅, FeO*/MgO, and Zr vs. Ti abundance/concentrations for basaltic rocks of the study area. Fields A, B, and C are fields for the entire Klamath Mountains province (Barnes et al., 1995) from rocks of the Rattlesnake Creek terrane, the Josephine ophiolite, and the Rogue Formation, respectively.

tostromal deposits. The basal level contains peridotite that is spatially and temporally linked to either the Josephine ophiolite (Harper, 1984) or Onion Camp complex (this study). The intermediate level consists of the Chetco plutonic complex and related metamorphic rocks (Jorgenson, 1970; Hotz, 1971; Dick, 1976; Loney and Himmelberg, 1977; Garcia, 1979, 1982; Saleeby, 1984; Coleman and Lanphere, 1991; Yule, 1996),

Onion Camp complex (this study), and mafic sequence of the Josephine ophiolite (Harper, 1984, 2003). The upper level consists of the Rogue Formation (Garcia, 1979, 1982), Galice Formation (Harper, 1980; Miller and Saleeby, 1995), and Fiddler Mountain olistostrome (this study). Therefore, at least eight lithotectonic elements comprise the Late Jurassic lithosphere of the western Jurassic terrane.

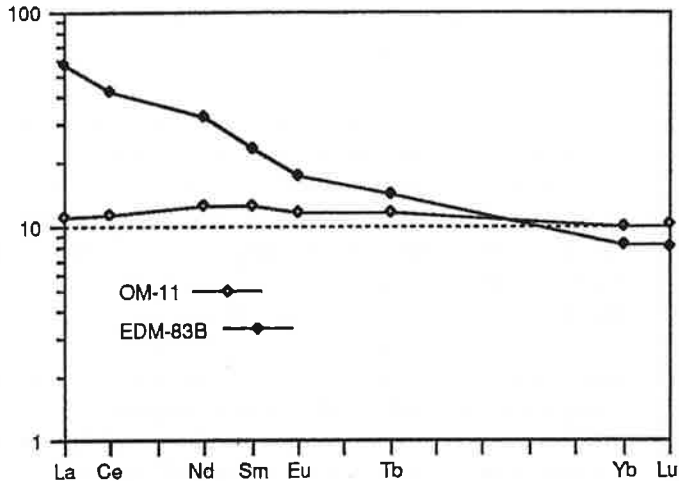


Figure 11. REE abundances of two Onion Camp complex basalts (in ppm), normalized to chondrite values, showing two distinctly different patterns. Sample OM-11 exhibits a flat, MORB-like pattern and sample EDM-83B exhibits a light REE-enriched pattern, typical of alkalic within-plate basalts.

Two Types of Peridotite

The Josephine peridotite is exposed over ~700 km² of the California-Oregon border region. The peridotite is thought to represent the residue of partial melting (Dick, 1976) and presumably formed during the genesis of the Late Jurassic Josephine ophiolite sequence (Harper, 1984). However, the northern and northeastern part of the Josephine peridotite sheet may consist of two distinct types of peridotite (Table 5; Figs. 1 and 2). Field relations and crosscutting ca. 173-Ma dikes (Yule, 1996; this chapter) in peridotite associated with the Onion Camp complex indicate that at least part of the peridotite massif is pre-Middle Jurassic in age. The fact that the ca. 173-Ma plagiogranite dikes are not rodingitized indicates that the Onion Camp complex peridotite experienced at least one episode of serpentinization prior to dike emplacement. The age of serpentinization is not constrained but may be as old as Late Triassic to Early Jurassic based on its association with metavolcanic rocks and chert of this age and on its tentative correlation with the lower mélangé unit of the Rattlesnake Creek terrane (Wright and Wyld, 1994).

The northern region of the Josephine peridotite sheet is bounded by, and, near Onion Mountain, appears to be infolded with, greenschist- and amphibolite-facies rocks of the Onion Camp complex (Figs. 2 and 4). Field relations show a relatively sharp “serpentinization front” ~0.5–2 km from the crustal rocks (Fig. 2) that in places appears to mark a transition between highly serpentinized peridotite, characteristic of the Onion Camp complex, and little to moderately serpentinized peridotite, characteristic of the Josephine peridotite. No noticeable shearing or structural discontinuity was recognized along this serpentinization boundary. South and east of this boundary, rel-

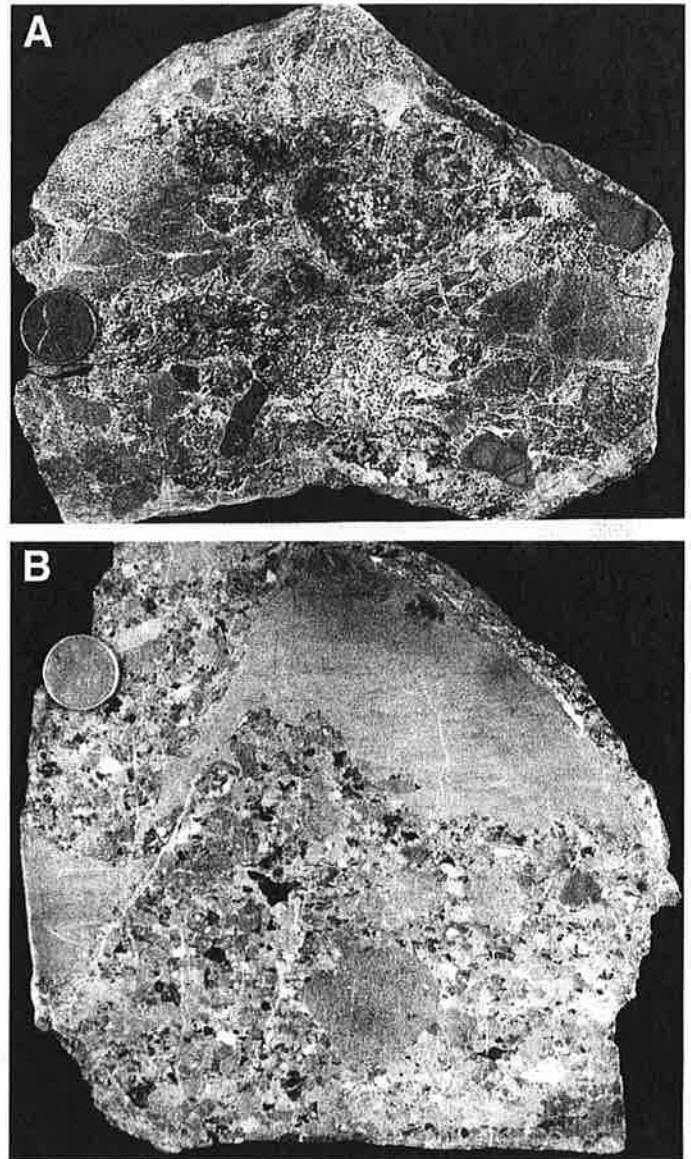


Figure 12. Photographs of slabs of Fiddler Mountain olistostrome rocks. (A) Ophiolite-clast conglomerate, common constituent of the Fiddler Mountain olistostrome, clasts consist entirely of gabbro, diabase, and greenstone. (B) Ophiolite-clast conglomerate with a medium-grained silty-sand interlayer, clast types are diabase, greenstone, chert, and secondary chert (small white clasts) and serpentinite (e.g., black clast near the center of the photo). Note the small fault offset of the silty sand layer.

atively fresh peridotite can be traced ~30 km to the Smith River region, where the type locality of the crustal sequence of the Josephine ophiolite is exposed (Harper, 1984). In the type area, radiometric ages constrain the age of the ophiolite to be 162–164 Ma (Saleeby et al., 1982; Harper, 2003). The boundary between Onion Camp complex and Josephine peridotite is therefore interpreted to be the serpentinization front, which separates

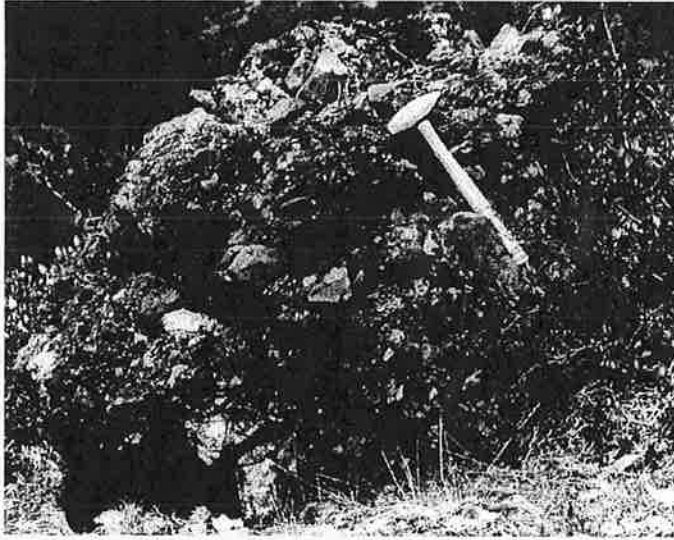


Figure 13. Photograph of monolithic, serpentinite-clast, and debris flow breccia located ~3 km to the northwest of Whetstone Butte (Fig. 2). Deposit occurs at the base of the overlapping Rogue Formation, which nonconformably overlies serpentinitized peridotite of the Onion Camp complex.

>173-Ma, highly serpentinized peridotite from ca. 164-Ma, weakly serpentinized peridotite.

There are at least two explanations for the difference in apparent ages of the Onion Camp complex and Josephine peridotites. One considers the two peridotites to represent a >9 m.y. continuum of formation, from >173 Ma to ca. 164 Ma, perhaps spanning the full history of ophiolite genesis at Josephine basin spreading centers. Interestingly, dikes of ca. 172 Ma in northern California have been attributed to the onset of Josephine ophiolite genesis (Saleeby and Harper, 1993). However, this hypothesis cannot explain the structural and apparent stratigraphic association of >173-Ma peridotite with other rocks of the Onion Camp complex as old as Early Jurassic and perhaps Triassic. In the alternative explanation, the two peridotites are interpreted as forming at two distinct times. The Onion Camp complex peridotite formed in Triassic and Early Jurassic times and is associated with the crust rocks of the Onion Camp complex. It represents a rifted fragment or screen of preexisting oceanic lithosphere within the Late Jurassic Rogue–Chetco/Josephine basin (Fig. 14). The close association of the upper mantle and crustal rocks of the Onion Camp complex is therefore interpreted to be a composite fragment of preexisting Klamath lithosphere (Rat-

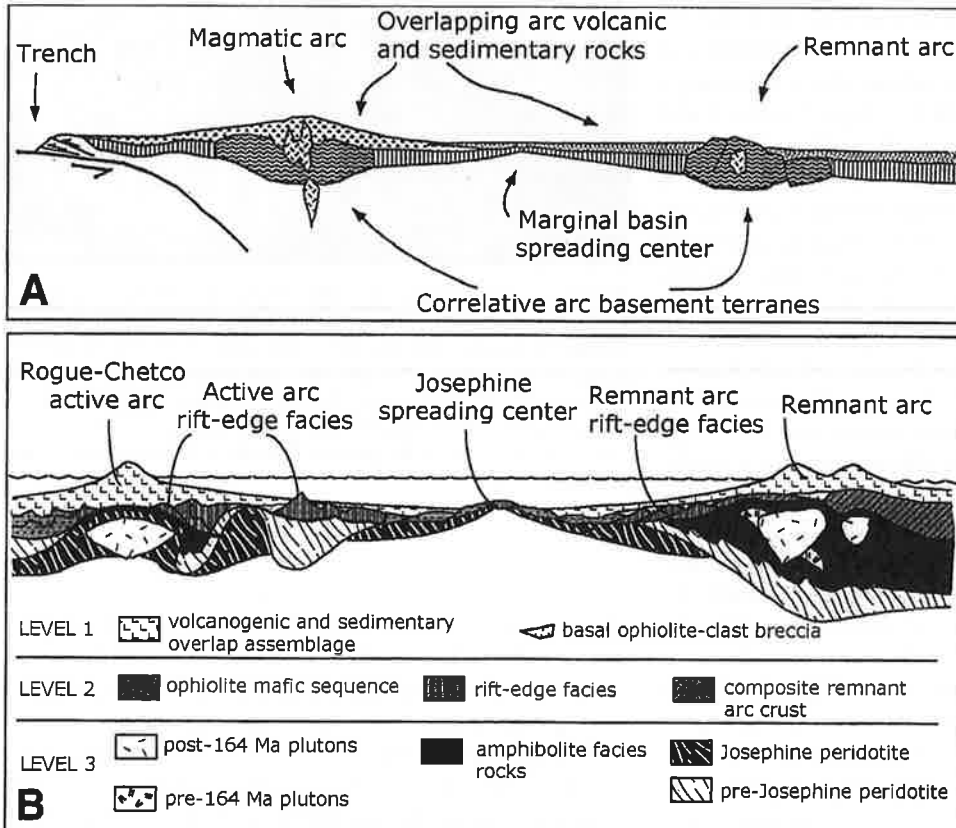


Figure 14. (A) Generalized cross-section through a marginal ocean basin (modified from Karig, 1971). (B) Simplified cross-section across the reconstructed (pre-accretion) Rogue–Chetco/Josephine marginal ocean basin system at ca. 155–160 Ma; vertical exaggeration ~3:1. The distance across the inter-arc basin is minimized to give equal emphasis to the three lithotectonic elements, the Rogue–Chetco active arc, Josephine inter-arc basin ophiolite, and remnant arc.

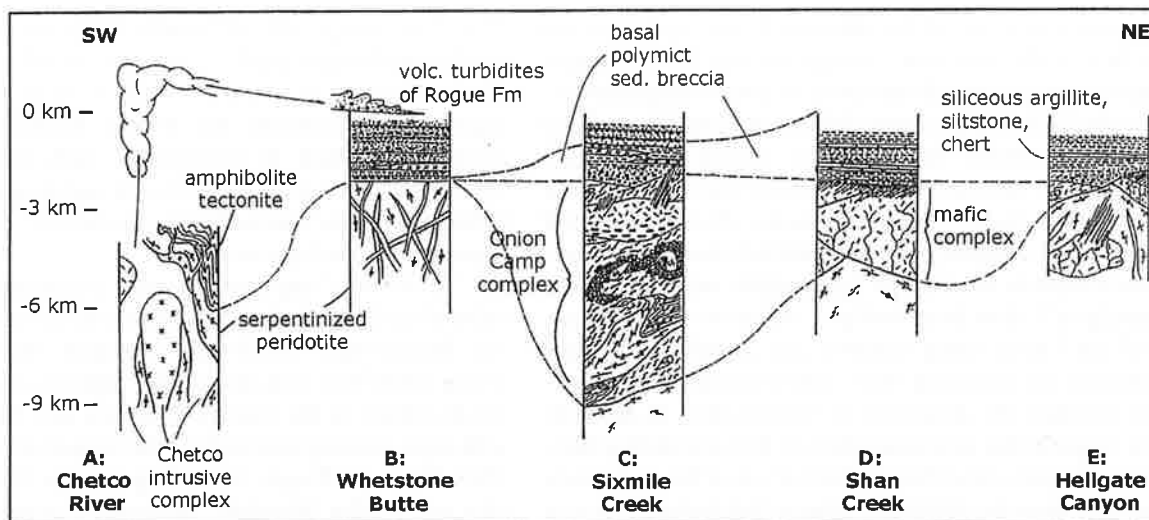


Figure 15. Diagrammatic columnar sections from five locations within the study area showing the three-tiered stratigraphy of the region (see Fig. 2 for locations of columns A–E). Upper layer is comprised of arc volcanogenic flysch (Rogue and Galice Formations) and Fiddler Mountain olistostrome. Intermediate layer of variable thickness is comprised of the Union Camp complex and Josephine ophiolite. Deep layer is comprised of variably serpentinized peridotite, locally intruded by dikes. The Chetco plutonic complex intrudes and metamorphoses the middle and deep layers. Fm—formation.

tlesnake Creek terrane) that rifted from the margin of the Klamath Mountain province as the Josephine basin opened. In this scenario, it is conceivable that the contact between the Josephine and Union Camp complex peridotites is the lithospheric/asthenospheric boundary prior to Josephine-age spreading.

Rift-Edge Facies

Most general cross-section views of modern marginal ocean basins (Fig. 14) show sharp boundaries that separate inter-

arc basin crust from active arc or remnant arc crust. However, Snoke (1977) described a more gradual transition or “rift-edge” facies for rocks in the remnant arc setting, specifically the “Preston Peak ophiolite” (see Ohr, 1987; Snoke and Barnes, this volume). The rift-edge concept applies in very similar ways to the Union Camp complex and Fiddler Mountain olistostrome of the western Jurassic belt described in this chapter. These units therefore are thought to represent the rift-edge facies for rocks in the active arc setting (Yule and Saleeby, 1993; Yule, 1996; Fig. 14).

TABLE 5. DISTINGUISHING FEATURES OF THE JOSEPHINE AND RATTLESNAKE CREEK TERRANE PERIDOTITE MASSES

Rattlesnake Creek terrane (RCT)	Josephine peridotite
1. Completely to moderately serpentinized (>50%).	1. Moderately to nonserpentinized, with pristine harzburgite and dunite locally common.
2. Amphibolite facies penetrative fabric, now mostly serpentinized; associated with Middle Jurassic (ca. 173 Ma) amphibolite tectonites.	2. Absence of amphibolite facies penetrative fabric.
3. Exposed on the seafloor, as evidenced by the nonconformable overlap of Rogue Formation strata.	3. No evidence of exposure on seafloor.
4. Anastomosing regional Nevadan (155–150 Ma) shear foliations common.	4. Anastomosing regional Nevadan (155–150 Ma) shear foliations rare.
5. At least Middle Jurassic in age, but may be Triassic in age by association with crustal rocks of the RCT. Cut by numerous generations of dikes ranging in age from ca. 175 to 150 Ma (Yule, 1996). Podiform chromite rarely present.	5. Probably Late Jurassic in age, the age of the crustal sequence of the Josephine ophiolite. Less commonly intruded by dikes whose ages range from ca. 160 to 150 Ma (Yule, 1996). Podiform chromite locally abundant.
6. Rodingite dikes rare.	6. Rodingite dikes common.

Distinctive features of the rift-edge facies in the western Jurassic belt, in the "active arc" setting include: (1) a heterogeneous mafic complex, chiefly consisting of gabbro and sheeted diabase and basalt dikes that intrude other units of the Onion Camp complex; (2) extensive vein and vein-cemented-breccia networks, and lower- and sub-greenschist-facies static alteration that affect rocks of the mafic complex and locally affect other units of the Onion Camp complex; and (3) ophiolite-clast megabreccia and breccia deposits interlayered with argillite and Late Jurassic (Kimmeridgian?) chert that overlap a basement mélange comprised of the Onion Camp complex and Josephine ophiolite. These features are consistent with a rift-dominated tectonic setting. For example, the abundance of sheeted dikes in the mafic complex suggests that extension played a key role during intrusion of the complex. Heat from shallow levels of the mafic complex probably drove hydrothermal systems that produced the vein networks and static alteration that occur throughout the Onion Camp complex. In addition, rifting could have produced ophiolite-cored escarpments that shed coarse olistostromal deposits.

Identifying a rift-edge facies beneath and/or adjacent to the active and remnant arcs, on either side of the Josephine basin (Fig. 14), should help constrain paleogeographic models for the Josephine ophiolite. The current position of the Onion Camp complex and Fiddler Mountain olistostrome, the active arc rift-edge facies, is ~50 km to the north of the Preston Peak ophiolite and Lems Ridge olistostrome, the remnant arc rift-edge facies (Fig. 13). Restoring a minimum of 40 km of east-west apparent shortening across the Preston Peak thrust (Harper et al., 1994) would place the two rift-edge facies at least 60 km to the northwest and southeast of each other, respectively (Fig. 13). Lateral displacement across the Preston Peak fault is not constrained; left- and right-oblique thrust motion across the fault would increase and decrease the apparent offset of these two belts, respectively. This model suggests that the Josephine basin may have opened during northwest-southeast-directed extension, a slight modification to the previous paleogeographic models (Pessagno and Blome, 1990; Alexander and Harper, 1992) that invoke north-south-directed spreading.

CONCLUSIONS

Two previously unrecognized lithotectonic units are present in the western Jurassic belt in the Oregon Klamath Mountains. These units, named the Onion Camp complex and Fiddler Mountain olistostrome, are elongate, lithosphere-scale blocks along the transition zone between the Late Jurassic Rogue-Chetco oceanic island arc and Josephine ophiolite. The Onion Camp complex is characterized by (1) N-MORB and WPB mafic metavolcanic rocks and associated Triassic(?) and Early Jurassic red chert; (2) scarce, but distinctive chert-clast conglomerate lenses in metasedimentary sequences; and (3) complexly folded regions of greenschist- to amphibolite-facies metavolcanic, metasedimentary, and serpentinized peridotite. The

$^{40}\text{Ar}/^{39}\text{Ar}$ cooling ages of hornblende in amphibolite suggest that the amphibolite-grade metamorphism ended by ca. 169 Ma. Plagiogranite dikes with ca. 173-Ma U-Pb zircon ages cut the serpentinized peridotite. The Fiddler Mountain olistostrome consists of pelagic to hemipelagic rocks interlayered with ophiolite-clast conglomerate, breccia, and megabreccia. Radiolarians from chert interbeds indicate that the olistostrome was deposited in Late Jurassic time.

The Onion Camp complex bears a striking resemblance to rocks of the Rattlesnake Creek terrane of the western Paleozoic and Triassic belt. The Fiddler Mountain olistostrome shares strong similarities with olistostrome deposits at Lems Ridge and Devils Elbow in the western Paleozoic and Triassic belt, and with other olistostromal units of the western Jurassic belt (Ohr, 1987; Wyld and Wright, 1988). Together the Onion Camp complex and Fiddler Mountain olistostrome comprise a rift-edge facies, formed when preexisting Klamath terranes rifted to form the Late Jurassic Rogue-Chetco/Josephine marginal ocean basin. This conclusion is consistent with previous models for the tectonic evolution of the western Jurassic belt put forth by Snoke (1977), Saleeby et al. (1982), and Harper and Wright (1984).

ACKNOWLEDGMENTS

We thank Robert B. Miller and Arthur W. Snoke for their helpful reviews. Many field visits and conversations with Greg Harper were invaluable. Conversations with W.P. Irwin were of great assistance for this study. A 1983 National Association of Geology Teachers summer internship working for W.P. Irwin served as JDY's introduction to the geology of the Klamath Mountains in California; an introduction that sparked interest in the Oregon Klamath Mountains and eventually led to this study. A field visit by L. Ramp in the earliest stages of this project was greatly appreciated. Much of the field mapping in the Kalmiopsis Wilderness could not have been completed without the assistance of B. Yule. We thank B.R. Hacker for obtaining $^{40}\text{Ar}/^{39}\text{Ar}$ age determinations and M.O. McWilliams for the use of his lab at Stanford University. We also thank C. Blome and M. Silk, who kindly made their unpublished radiolarian fossil age determinations available to us. This work was supported by a grant from the Oregon Department of Geology and Mineral Industries, Geological Society of America Research grants nos. 4596-90, 4842-91, and 5089-92 to JDY, by National Science Foundation grants EAR-9117103 and EAR-8720141 to CGB. Contribution 9132 of the Division of Geological and Planetary Sciences, California Institute of Technology, Pasadena, California.

REFERENCES CITED

- Alexander, R.J., and Harper, G.D., 1992, The Josephine ophiolite, an ancient analog for oceanic lithosphere formed at intermediate-spreading ridges, in Parsons, B., and Browning, P., eds., *Ophiolites and their modern oceanic analogues*: Oxford, Blackwell Scientific Publications, p. 3-38.

- Apted, M.J., and Liou, J.G., 1983, Phase relations among greenschist, epidote-amphibolite, and amphibolite in a basaltic system: *American Journal of Science*, v. 283-A, p. 328–354.
- Barnes, C.G., Donato, M.M., Barnes, M.A., Yule, J.D., Hacker, B.R., and Helper, M.A., 1995, Geochemical compositions of metavolcanic and metasedimentary rocks, western Jurassic and western Paleozoic and Triassic belts, Klamath Mountains, Oregon and California: Reston, Virginia, U.S. Geological Survey Open-File Report 95–227-A, 63 p.
- Blake, M.C., Jr., Engebretson, D.C., Jayko, A.S., and Jones, D.L., 1985, Tectonostratigraphic terranes in southwest Oregon, in Howell, D.G., ed., *Tectonostratigraphic terranes of the Circum-Pacific region*: Houston, Circum-Pacific Council for Energy and Mineral Resources, Earth Science Series 1, p. 147–157.
- Brown, E.H., 1975, A petrogenetic grid for reactions producing biotite and other Al-Fe-Mg silicates in the greenschist facies: *Journal of Petrology*, v. 16, p. 258–271.
- Brown, E.H., 1977, Phase equilibria among pumpellyite, lawsonite, epidote and associated minerals in low grade metamorphic rocks: *Contributions to Mineralogy and Petrology*, v. 64, p. 123–136, doi: 10.1007/BF00371507.
- Burchfiel, B.C., and Davis, G.A., 1981, Triassic and Jurassic tectonic evolution of the Klamath Mountains–Sierra Nevada geologic terrane, in Ernst, W.G., ed., *The geotectonic development of California—Rubey Volume 1*: Englewood Cliffs, New Jersey, Prentice-Hall, p. 50–70.
- Chen, J.H., and Wasserburg, G.J., 1981, Isotopic determination of uranium in picomole and subpicomole quantities: *Analytical Chemistry*, v. 53, p. 2060–2067, doi: 10.1021/ac00236a027.
- Coleman, R.G., and Lanphere, M.A., 1991, The Briggs Creek amphibolite, Klamath Mountains, Oregon: Its origin and dispersal: *New Zealand Journal of Geology and Geophysics*, v. 34, p. 271–284.
- Curry, J.R., Moore, D.G., Lawver, L.A., Raitt, R.W., and Henry, M., 1979, Tectonics of the Andaman Sea and Burma, in Watkins, J.S., et al., eds., *Geological and geophysical investigations of continental margins*: American Association of Petroleum Geologists Memoir 29, p. 189–198.
- Davis, G.A., 1969, Tectonic correlations, Klamath Mountains and western Sierra Nevada, California: *Geological Society of America Bulletin*, v. 80, p. 1095–1108.
- Dick, H.J.B., 1976, The origin and emplacement of the Josephine Peridotite of southwestern Oregon [Ph.D. dissertation]: New Haven, Connecticut, Yale University, 409 p.
- Donato, M.M., 1992, A newly recognized ductile shear zone in the northern Klamath Mountains, Oregon—Implications for Nevadan accretion: Reston, Virginia, U.S. Geological Survey Bulletin 2028, 10 p.
- Frey, M., de Capitani, C., and Liou, J., 1991, A new petrogenetic grid for low-grade metabasites: *Journal of Metamorphic Geology*, v. 9, p. 497–509.
- Garcia, M.O., 1979, Petrology of the Rogue and Galice Formations, Klamath Mountains, Oregon: Identification of a Jurassic island-arc sequence: *Journal of Geology*, v. 87, p. 29–41.
- Garcia, M.O., 1982, Petrology of the Rogue River island-arc complex, southwest Oregon: *American Journal of Science*, v. 282, p. 783–807.
- Hacker, B.R., Donato, M.M., Barnes, C.G., McWilliams, M.O., and Ernst, W.G., 1995, Timescales of orogeny: Jurassic construction of the Klamath Mountains: *Tectonics*, v. 14, p. 677–703, doi: 10.1029/94TC02454.
- Hamilton, W., 1978, Mesozoic tectonics of the western United States, in Howell, D.G., and McDougall, K.A., eds., *Mesozoic paleogeography of the western United States*, Pacific Coast Paleogeography Symposium 2: Los Angeles, Pacific Section, Society of Economic Paleontologists and Mineralogists, p. 33–70.
- Harper, G.D., 1980, The Josephine ophiolite—remains of a late Jurassic marginal basin in northwestern California: *Geology*, v. 8, p. 333–337, doi: 10.1130/0091-7613(1980)8<333:TJOOAL>2.0.CO;2.
- Harper, G.D., 1984, The Josephine ophiolite: *Geological Society of America Bulletin*, v. 95, p. 1009–1026, doi: 10.1130/0016-7606(1984)95<1009:TJONC>2.0.CO;2.
- Harper, G.D., 2003, Fe-Ti basalts and propagating rift tectonics in the Josephine ophiolite: *Geological Society of America Bulletin*, v. 115, p. 771–787, doi: 10.1130/0016-7606(2003)115<0771:FBAPTI>2.0.CO;2.
- Harper, G.D., and Wright, J.E., 1984, Middle to Late Jurassic tectonic evolution of the Klamath Mountains, California-Oregon: *Tectonics*, v. 3, p. 759–772.
- Harper, G.D., Saleeby, J.B., and Heizler, M., 1994, Formation and emplacement of the Josephine ophiolite, and the age of the Nevadan orogeny in the Klamath Mountains, California-Oregon: U/Pb zircon and $^{40}\text{Ar}/^{39}\text{Ar}$ geochronology: *Journal of Geophysical Research*, v. 99, p. 4293–4321, doi: 10.1029/93JB02061.
- Hawkins, J.W., 2003, Geology of suprasubduction zones; Implications for the origin of ophiolites, in Dilek, Y., and Newcomb, S., eds., *Ophiolite concept and the evolution of geologic thought*: Boulder, Colorado, Geological Society of America Special Paper 373, p. 227–268.
- Hotz, P.E., 1971, Geology of lode gold districts in the Klamath Mountains, California and Oregon: Washington, D.C., U.S. Geological Survey Bulletin 1290, 91 p.
- Irwin, W.P., 1960, Geologic reconnaissance of the northern Coast Ranges and Klamath Mountains, California, with a summary of the mineral resources: California Division of Mines Bulletin 179, 80 p.
- Irwin, W.P., 1966, Geology of the Klamath Mountains province, in Bailey, E.H., ed., *Geology of northern California*: California Division of Mines Bulletin 190, p. 19–38.
- Irwin, W.P., 1972, Terranes of the western Paleozoic and Triassic belt in the southern Klamath Mountains, California: Washington, D.C., U.S. Geological Survey Professional Paper 800-C, p. C103–C111.
- Irwin, W.P., 1994, Geologic map of the Klamath Mountains, California: Reston, Virginia, U.S. Geological Survey Miscellaneous Investigations Series Map I–2148, scale 1:500,000, 2 sheets.
- Irwin, W.P., Jones, D.L., and Blome, C.D., 1982, Map showing radiolarian localities in the western Paleozoic and Triassic belt, Klamath Mountains, California: Reston, Virginia, U.S. Geological Survey Miscellaneous Field Investigations MF-1399, 1 sheet.
- Jaffey, A.H., Flynn, K.F., Glendenin, L.E., Bentley, W.C., and Essling, A.M., 1971, Precision measurement of half-lives and specific activities of ^{235}U and ^{238}U : *Physical Review*, v. 4, p. 1889–1906.
- Jorgenson, D.B., 1970, Petrology and origin of the Illinois River gabbro, a part of the Josephine peridotite-gabbro complex, Klamath Mountains, southwestern Oregon [Ph.D. dissertation]: University of California, Santa Barbara, 195 p.
- Karig, D.E., 1971, Origin and development of marginal basins in the western Pacific: *Journal of Geophysical Research*, v. 76, p. 2542–2560.
- Kays, M.A., 1992, Geologic guide for the northern Klamath Mountains, 1, Cow Creek to Red Mountain: *Oregon Geology*, v. 54, no. 2, p. 27–33.
- Krogh, T.E., 1973, A low contamination method for the hydrothermal decomposition of zircon and extraction of U and Pb for isotopic age determinations: *Geochimica et Cosmochimica Acta*, v. 37, p. 485–494, doi: 10.1016/0016-7037(73)90213-5.
- Lagabrielle, Y., Goslin, J., Martin, H., Thiroit, J.-L., and Auzende, J.-M., 1997, Multiple active spreading centres in the hot North Fiji Basin (Southwest Pacific); A possible model for Archaean seafloor dynamics? *Earth and Planetary Science Letters*, v. 149, p. 1–13, doi: 10.1016/S0012-821X(97)00060-5.
- Liou, J.G., Kuniyoshi, S., and Ito, K., 1974, Experimental studies of the phase relationships between greenschist and amphibolite in a basaltic system: *American Journal of Science*, v. 274, p. 613–632.
- Liou, J.G., Maruyama, S., and Cho, M., 1987, Very low-grade metamorphism of volcanic and volcanoclastic rocks: Mineral assemblages and mineral facies, in Frey, M., ed., *Low temperature metamorphism*: Glasgow, Blackie and Son Limited, p. 57–113.
- Loney, R.A., and Himmelberg, G.R., 1977, The geology of the gabbroic complex along the northern border of the Josephine peridotite, Vulcan Peak area, southwestern Oregon: U.S. Geological Survey Journal of Research, v. 5, p. 761–781.
- Miller, M.M., and Saleeby, J.B., 1995, U-Pb geochronology of detrital zircon

- from Upper Jurassic synorogenic turbidites, Galice Formation, and related rocks, western Klamath Mountains: Correlation and Klamath Mountains provenance: *Journal of Geophysical Research*, v. 100, p. 18,045–18,058, doi: 10.1029/95JB00761.
- Ohr, M., 1987, Geology, geochemistry and geochronology of the Lems Ridge olistostrome, Klamath Mountains, California [M.S. thesis]: Albany, State University of New York, 278 p.
- Page, N.J., Gray, F., Cannon, J.K., Foose, M.P., Lipin, B., Moring, B.C., Nicholson, S.W., Sawline, M.G., Till, A., and Ziemianski, W.P., 1981, Geologic map of the Kalmiopsis Wilderness Area, Oregon: Reston, Virginia, U.S. Geological Survey Miscellaneous Field Studies Map MF-1240-A, 1 sheet.
- Parson, L.M., and Wright, I.C., 1996, The Lau-Hauvre-Taupo back-arc basin: A southward propagating, multi-stage evolution from rifting to spreading: *Tectonophysics*, v. 263, p. 1–22, doi: 10.1016/S0040-1951(96)00029-7.
- Pearce, J.A., Lippard, S.J., and Roberts, S., 1984, Characteristics and tectonic significance of suprasubduction zone ophiolites, in Kokelaar, B.P., and Howells, M.F., eds., *Marginal basin geology*: London, Blackwell Scientific Publications, Geological Society Special Publication 16, p. 77–94.
- Pessagno, E.A., Jr., and Blome, C.D., 1990, Implications of new Jurassic stratigraphic, geochronometric, and paleolatitudinal data from the western Klamath terrane (Smith River and Rogue Valley subterrains): *Geology*, v. 18, p. 665–668, doi: 10.1130/0091-7613(1990)018<0665:IONJSG>2.3.CO;2.
- Ramp, L., 1977, Geology, mineral resources, and rock material of Curry County, Oregon: Oregon Department of Geology and Mineral Industries Bulletin 88, 47 p.
- Ramp, L., 1984, Geologic map of the southeast quarter of the Pearsoll Peak quadrangle, Curry and Josephine counties, Oregon: Oregon Department of Geology and Mineral Industries Geologic Map Series GMS-30, scale 1:24,000.
- Ramp, L., 1986, Geologic map of the northwest quarter of the Cave Junction quadrangle, Josephine County, Oregon: Oregon Department of Geology and Mineral Industries Geologic Map Series GMS-38, scale 1:24,000, 1 sheet.
- Ramp, L., and Peterson, N.V., 1979, Geology and mineral resources of Josephine County, Oregon: Oregon Department of Geology and Mineral Industries Bulletin 100, 45 p.
- Roure, F., and DeWever, P., 1983, Découverte de radiolarites du Trias dans l'unité occidentale des Klamath, sud-ouest de l'Oregon, U.S.A.: Conséquences sur l'âge des péridotite de Josephine: *Comptes Rendus de l'Académie des Sciences (Paris)*, v. 297, p. 161–164.
- Saleeby, J.B., 1984, Pb/U zircon ages from the Rogue River area, western Jurassic belt, Klamath Mountains, Oregon: *Geological Society of America Abstracts with Programs*, v. 16, no. 5, p. 331.
- Saleeby, J.B., and Harper, G.D., 1993, Tectonic relations between the Galice Formation and the Condrey Mountain Schist, Klamath Mountains, northern California, in Dunn, G.C., and McDougall, K.A., eds., *Mesozoic paleogeography of the western United States—II*: Los Angeles, Pacific Section, Society of Economic Paleontologists and Mineralogists, v. 71, p. 61–80.
- Saleeby, J.B., Harper, G.D., Snoke, A.W., and Sharp, W.D., 1982, Time relations and structural-stratigraphic patterns in ophiolite accretion, west central Klamath Mountains, California: *Journal of Geophysical Research*, v. 87, p. 3831–3848.
- Shervais, J.W., 1982, Ti-V plots and the petrogenesis of modern and ophiolitic lavas: *Earth and Planetary Science Letters*, v. 59, p. 101–118, doi: 10.1016/0012-821X(82)90120-0.
- Snoke, A.W., 1977, A thrust plate of ophiolitic rocks in the Preston Peak area, Klamath Mountains, California: *Geological Society of America Bulletin*, v. 88, p. 1641–1659, doi: 10.1130/0016-7606(1977)88<1641:ATPOOR>2.0.CO;2.
- Snoke, A.W., and Barnes, C.G., 2006, this volume, The development of tectonic concepts for the Klamath Mountains province, California and Oregon, in Snoke, A.W., and Barnes, C.G., eds., *Geological studies in the Klamath Mountains Province, California and Oregon: A volume in honor of William P. Irwin*: Geological Society of America Special Paper 410, doi: 10.1130/2006.2410(01).
- Stern, R.J., and Bloomer, S.H., 1992, Subduction zone infancy; Examples from the Eocene Izu-Bonin-Mariana and Jurassic California arc: *Geological Society of America Bulletin*, v. 104, p. 1621–1636, doi: 10.1130/0016-7606(1992)104<1621:SZIEFT>2.3.CO;2.
- Tera, F., and Wasserburg, G.J., 1972, U-Th-Pb systematics in three Apollo 14 basalts and the problems of initial Pb in lunar rocks: *Earth and Planetary Science Letters*, v. 14, p. 281–304, doi: 10.1016/0012-821X(72)90128-8.
- Thompson, A.B., 1976, Mineral reactions in pelitic rocks: I. Prediction of P–T–X (Fe–Mg) phase relations: *American Journal of Science*, v. 276, p. 401–424.
- Uyeda, S., 1977, Some basic problems in the trench-arc-back arc system, in Talwani, M., and Pitman, W.C., III, eds., *Island arcs, deep trenches, and back-arc basins*: Washington, D.C., American Geophysical Union, Maurice Ewing Series v. 1, p. 1–14.
- Wells, F.G., Hotz, P.E., and Cater, F.W., Jr., 1949, Preliminary description of the geology of the Kerby quadrangle, Oregon: Oregon Department of Geology and Mineral Industries Bulletin 40, 23 p.
- Wells, F.G., and Walker, G.W., 1953, Geology of the Galice quadrangle, Oregon: Washington, D.C., U.S. Geological Survey Quadrangle Map GQ-25, scale 1:62,500, 1 sheet.
- Wise, J.P., 1969, Geology and petrography of a portion of the Jurassic Galice Formation, Babyfoot Lake area, southwestern Oregon [M.S. thesis]: Pocatello, Idaho State University, 108 p.
- Wright, J.E., and Fahan, M.R., 1988, An expanded view of Jurassic orogenesis in the western United States Cordillera: Middle Jurassic (pre-Nevadan) regional metamorphism and thrust faulting within an active arc environment, Klamath Mountains, California: *Geological Society of America Bulletin*, v. 100, p. 859–876, doi: 10.1130/0016-7606(1988)100<0859:AEVOJO>2.3.CO;2.
- Wright, J.E., and Wyld, S.J., 1994, The Rattlesnake Creek terrane, Klamath Mountains, California: An early Mesozoic volcanic arc and its basement of tectonically disrupted oceanic crust: *Geological Society of America Bulletin*, v. 106, p. 1033–1056, doi: 10.1130/0016-7606(1994)106<1033:TRCTKM>2.3.CO;2.
- Wyld, S.J., and Wright, J.E., 1988, The Devils Elbow ophiolite remnant and overlying Galice Formation: New constraints on the Middle to Late Jurassic evolution of the Klamath Mountains, California: *Geological Society of America Bulletin*, v. 100, p. 29–44, doi: 10.1130/0016-7606(1988)100<0029:TDEORA>2.3.CO;2.
- Yardley, B.W.D., 1989, An introduction to metamorphic petrology: Essex, England, Longman Scientific and Technical, 248 p.
- Yule, J.D., 1996, Geologic and tectonic evolution of Jurassic marginal ocean basin lithosphere, Klamath Mountains, Oregon [Ph.D. dissertation]: Pasadena, California Institute of Technology, 308 p.
- Yule, J.D., and Saleeby, J.B., 1993, Highly extended oceanic lithosphere: The basement and wallrocks for the Late Jurassic Rogue–Chetco oceanic arc, Oregon Klamath Mountains: *Geological Society of America Abstracts with Programs*, v. 25, p. 169.
- Yule, J.D., Saleeby, J.B., Jones, D.L., and Silk, M., 1992, Correlation of basement terranes across the Late Jurassic Josephine inter-arc basin, southwestern Oregon and northern California: *Geological Society of America Abstracts with Programs*, v. 24, p. 93.